



Hungarian University of Agriculture and Life Sciences

Institute of Landscape Architecture

Urban Planning and Garden Art

Optimization of carbon sink capacity in parks

——A case of China Green Expo

Student name: Jia Xiaoali

Neptun ID: F7OQX2

Supervisor: László Zoltán Nádasy

Landscape architecture and Garden art

2023 4 29

Contents

ABSTRACT:	3
1 INTRODUCTION:	5
1.1 RESEARCH BACKGROUND AND SIGNIFICANCE:	5
1.2 RELATED RESEARCH PROGRESS:	8
1.2.1 Research progress on carbon sinks in urban green areas.....	8
1.2.2 Methodology for estimating carbon storage in urban green spaces	11
1.3 RESEARCH CONTENT AND OBJECTIVES	14
1.3.1 Main research content	14
1.3.2 Main research objectives	16
1.4 SCIENTIFIC PROBLEMS TO BE SOLVED	16
1.5 TECHNOLOGY LINE	17
2 RESEARCH AREA AND METHODOLOGY.....	19
2.1 NATURE PROFILE	19
2.1.1 Geographic location.....	19
2.1.3 Topography.....	25
2.1.4 Hydrologic conditions.....	25
2.1.5 Vegetation profile	26
2.2 LANDSCAPE FUNCTION	26
2.2.1 The original design concept	26
2.2.2 Site transportation and functional analysis.....	27
2.3 MATERIALS AND METHODS	35
2.3.1 Field survey	35
2.3.2 Radar data	36
2.3.3 Remote sensing image data	39
2.3.4 Biodiversity Information.....	43
2.3.5 Data analysis	44
3 VEGETATION STATUS AND CARBON DENSITY DISTRIBUTION IN CHINA GREEN EXPO ...	47
3.1 STATUS OF VEGETATION IN CHINA GREEN EXPO.....	47
3.2 SPATIAL DISTRIBUTION OF VEGETATION CARBON DENSITY IN CHINA GREEN EXPO.....	51
4 GROWTH FACTORS AND CARBON SEQUESTRATION CAPACITY OF TREE SPECIES.....	53
4.1 GROWTH FACTOR ANALYSIS OF 169 TREE SPECIES	53
4.2 CARBON SEQUESTRATION CAPACITY OF 169 TREE SPECIES AND APPLICATION IN LANDSCAPE GARDEN PLANNING	53
5 MULTIPLE SCALE DRIVING FORCE ANALYSIS OF CARBON DENSITY	57
5.1 MULTISCALE VARIATION OF CARBON DENSITY AND INFLUENCING FACTORS	57
5.2 CORRELATION ANALYSIS OF CARBON DENSITY AND INFLUENCING FACTORS	59
5.3 ANALYSIS OF THE MULTI-DRIVER RELATIONSHIP BETWEEN CARBON DENSITY AND INFLUENCING FACTORS	62

6 DISCUSSION	65
6.1 COMPARISON WITH RELATED RESEARCHES	65
6.2 GROWTH FACTORS AND TREE PLANNING APPLICATION	67
6.3 SCALE DEPENDENCE OF CARBON DENSITY AND INFLUENCING FACTORS	73
6.4 DRIVING RELATIONSHIP OF CARBON DENSITY	74
7 CONCLUSION AND OUTLOOK	79
7.1 MAIN RESEARCH CONCLUSION	79
7.1.1 Carbon storage density and carbon sequestration density in China Green Expo	79
7.1.2 Growth factors and carbon sequestration capacity of tree species in China Green Expo	79
7.1.3 Multiple scale driving relationship of carbon density in urban park green space	80
7.2 RESEARCH INNOVATIONS	81
7.3 SHORTCOMINGS AND OUTLOOK	81
8 OPTIMIZATION DESIGN OF CHINA GREEN EXPO	83
9 REFERENCE	105
10 APPENDIX	117

Abstract:

A growing number of studies have demonstrated that urban green spaces play a crucial role in regulating the carbon cycle of terrestrial ecosystems and slowing down the increase of atmospheric CO₂ concentration. However, previous studies on carbon sequestration potential have mainly focused on natural or semi-natural ecosystems such as forests, grasslands, or farmlands, while research on the carbon sequestration capacity and carbon sequestration of urban green spaces is limited. The role of urban green space in promoting the construction of urban green space and serving the national "carbon-neutral" strategy will become more and more significant with the progress of urbanization, the increase of people's ecological awareness, the rise of demand for urban green space ecosystem services, and the development of theories such as low-carbon cities, forest cities, and park cities. Therefore, this study will concentrate on the urban green space, which needs to be researched and take the China Green Expo in Zhengzhou City as the research site. Based on the data from multiple sources, such as field surveys, LiDAR point clouds, remote sensing, and literature, we will use LiDAR scanning and point cloud data processing techniques, spatial data analysis, and processing techniques, as well as correlation analysis, full-subset regression, HP analysis, structural equation modeling, and cluster analysis. The spatial quantification and influence mechanisms of carbon storage and sequestration in urban green spaces at different scales are systematically studied in terms of vegetation configuration, green space structure, remote sensing information, and multiple scales. The main research results are as follows:

1) In 2021, the carbon storage and carbon sequestration in Zhengzhou-China Green Expo were 48.58 Gg and 3.26 Gg, while the carbon density and carbon sequestration density were 30.72 kg m⁻² and 2.06 kg m⁻² yr⁻¹, respectively. Among them, the carbon storage of trees, shrubs, and herbs were 43.17 Gg, 5.31 Gg, and 0.1 Gg, while the carbon sequestration was 2.57 Gg, 0.64 Gg, and 0.05 Gg, respectively.

2) The trees in Zhengzhou-China Green Expo Park consist of 108,241 trees of 54 families, 97 genera, and 169 species, with an average height and diameter at breast height of 6.3m and 0.32m.

3) For the first time, "DBH-age" relationships were established for 169 tree species during the rapid growth period. Then I calculated growth factors for landscape trees in the Zhengzhou area.

4) The carbon sequestration capacity of trees varies widely among different species. Based on the cluster analysis, 169 tree species were classified into nine categories.

Considering the planning and design scenarios and the characteristics of each type of species, this study proposed suitable planting recommendations. It offers a theoretical basis for planting design with the goal of carbon sink enhancement.

5) The optimal sample size for investigating carbon storage and sequestration in urban green space parks is 100 m. The traditional sample size for forest ecosystems is inaccurate when applied to urban green space.

6) Carbon sequestration is significantly influenced by biodiversity, while the stand structure mainly influences carbon stock. This driving relationship varies with scale, for example, the proportion of water bodies has a more significant effect on carbon density in large-scale samples. In urban green space planning, carbon density can be enhanced by increasing the area of water bodies in large green spaces; urban green spaces of all scales can get greater carbon density by optimizing Planting configuration.

7) Compared with the vegetation index, the texture characteristics can better explain the variation of vegetation carbon density. Meanwhile, RVI can replace NDVI better to predict carbon sequestration density in urban green space. Future studies on the carbon density of urban green space can improve the accuracy of the results by applying RVI and texture features. The above findings improved our systematic understanding of the carbon sink in the urban green area, provided an essential reference for the study of the carbon cycle in urban green space, and provided a theoretical basis for planning and designing urban green space with the goal of carbon sink enhancement.

Keywords: Urban green space; Carbon density; Growth factors; Planting configuration; Impact factors; Scale Dependence

1 Introduction:

1.1 Research Background and Significance:

According to China's National Bureau of Statistics and related studies, China's urbanization rate reached 17.29% in 1978 ^[1]. China's urbanization rate exceeded 50% for the first time by 2011 and has risen to 64.72% by 2021 ^[2]. With the increasing urbanization in China, the world population is also increasing in size. UN statistics show that in 1950, the urban population accounted for about 30% of the world's total population; by 2018 this figure had increased to 55%, and the growth rate continues to accelerate; it is expected that by 2050, 68% of the world's population will live in urban areas, and there is a 95% chance that the total world population will increase to 7.4-10 billion ^[3]. As a direct result of frequent and intense urbanization and the continuous increase in the total population, a large number of green spaces in urban spaces have been turned into impermeable surfaces, which is also one of the important factors contributing to climate change ^[4]. High-speed urbanization has brought immeasurable benefits to our society, facilitating inter- and intra-provincial population movement; the concentration of population and labor force has promoted mass production in various industries; high-density transportation systems have facilitated international trade and domestic economic development; advanced information technology has facilitated the development of industries such as education, technology, medical and public services, providing more job opportunities and industrial diversity, all of which have improved the overall standard of living of urban and rural residents ^[5]. Meanwhile, rapidly urbanization has also brought many problems to the environment and social management. Energy plays a crucial role in urban development, and energy consumption in urban areas accounts for 60-80% of the world's total energy consumption ^[6]. However, the burning of large amounts of fossil fuels produces large amounts of greenhouse gases, causing environmental problems such as global warming and acid rain. The IPCC survey reports that about 75% of global carbon emissions come from urban areas, which has a strong impact on urban climate and even global climate ^[7,8]. With the massive emission of carbon-based greenhouse gases in urban areas, the urban heat island problem has become an important environmental issue that has to be faced ^[9,10]. Rapid urbanization is often accompanied by a decline in drainage capacity and degradation of river ecosystems, with water bodies and wetlands disappearing as urban areas expand outwards ^[11]. In the face of urban environmental problems, a growing number of studies have confirmed that vegetation in urban environments can improve microclimates and thus mitigate the environmental degradation caused by urban expansion ^[12]. China has developed and implemented many policies and actions to address the ecological degradation caused by urbanization, adopting strategies such as low resource consumption and high economic growth. However, the task of improving the ecological environment remains daunting, and there is a great demand for finding methods to reconcile the problem of ecological degradation with economic development.

With the growing number of people worldwide, the high rate of urbanization on a global scale has put

great pressure on the urban environment. Rapid urbanization has resulted in the conversion of diverse urban land types into impervious surfaces, a process that has caused irreversible damage to natural ecosystems such as urban green spaces ^[13]. A study of 386 European cities found that urban sprawl is covering more and more green space ^[14]. The large amount of impermeable surfaces causes urban areas to tend to absorb more solar radiation, so the urban heat island effect also poses a great threat to the urban ecology ^[15]. Numerous studies have demonstrated that the urban heat island effect also increases energy use in urban areas, increases ozone emissions, and increases the risk of death among urban residents due to persistent high temperatures ^[16,17]. Also, it is not only urban residents who are affected by the persistent high temperatures in urban areas due to urbanization, but this phenomenon also causes irreversible damage to the ecosystems in urban areas. The urban heat island effect and changes in precipitation in urban areas have changed the climatic conditions in urban areas, with very serious effects on the net primary productivity of vegetation, functional diversity of ecosystems and biodiversity in urban ecosystems ^[18]. The increase in population also means more municipal waste generation, and solid waste in cities is often disposed of through recycling, incineration or landfills. The decomposition process of these wastes inevitably produces a large amount of CO₂, CH₄ and other gases, which again increases the greenhouse gas emissions in urban areas. Data show that CO₂ accounts for 30%-60% and CH₄ accounts for 40%-70% of the emitted gases ^[19]. A large number of studies on the relationship between urban green space and urban microclimate in cities have emerged from studies related to urbanization ^[20-22]. Achieving ecological sustainability and ecological resilience in urban areas must be a top priority for future urban development strategies. How to create a healthy and livable urban living space is one of the major challenges of our time.

The definition of the term "urban green space" in China has two meanings: one is the various areas for greening within the scope of urban construction land; and the other is the area with a better greening environment that has a positive effect on urban ecology, urban landscape and the life of residents ^[23]. In European studies, all areas with natural surfaces and vegetation growth within the city limits are urban green areas. As cities expand, the benefits that urban green spaces bring to urban areas are becoming more and more prominent, both in terms of improving the ecological environment in the city and providing a healthy living environment for residents and animals in the city. High green space ratio significantly increases the attention span and emotional stability of residents ^[24]; Significant reduction in mortality, cardiovascular disease and violence in urban areas ^[25-27]; Improves climate conditions, air quality and rainfall regulation in urban areas, and provides a natural solution for wastewater treatment in urban areas ^[28,29]; Provides a large number of jobs and the value of surrounding properties ^[30]. Urban residents rely on green spaces for their daily recreational needs and multiple ecosystem services.

Since the beginning of the 21st century, with the accelerated global urbanization, the total global carbon emissions have been rising, and the negative impact on the ecological environment has shown a gradually increasing tendency. The data show that China's per capita CO₂ emissions in 2018 were 8.4t, while the per capita CO₂ emissions in the United States were 17.74t, 13.04t in South Korea and 9.13t in

Japan in the same year. China's per capita carbon emissions are much lower than those of the United States and South Korea, and slightly lower than those of Japan. However, even so, China's total CO₂ emissions are still large. From the late 20th century onwards, our CO₂ emissions have risen significantly. According to 《Climate Watch》, the total global CO₂ emissions in 2018 were 36.43 billion tons. Among them, China's CO₂ emissions were 9.66 billion tons, accounting for 26.5% of global emissions, making it the world's largest greenhouse gas emitter, and there is still some room for CO₂ emission reduction compared to other countries^[31]. CO₂ is the second most important greenhouse gas in the Earth's atmosphere after water vapor. Large amounts of greenhouse gases can lead to a constant increase in the temperature of the Earth's surface and the risk of overheating. On the other hand, vegetation absorbs CO₂ from the atmosphere through photosynthesis, which produces organic matter and provides a food source for all microorganisms, animals and humans^[8]. The amount of CO₂ sequestration by vegetation in urban areas is influenced by factors such as climate, pollution levels and vegetation maintenance, while tree age also plays a role. A study of the United States shows that urban areas account for about 10% of carbon storage in U.S. ecosystems^[32]. This percentage is much smaller in China, at about 0.74%^[33]. Up to now, carbon emissions from urban fossil fuel combustion in China are much higher than the carbon storage of intra-urban vegetation, which also indicates that China's urban areas still maintain a large potential for carbon sequestration^[34,35]. With the transformation of urban development model, the study of urban development model in China has gradually changed from "incremental optimization" to "stock optimization". Emphasis is placed on the trade-offs and conflicts of interest between the internal development of cities and the preservation of urban green spaces^[36]. Faced with the same problem, European experts and scholars have also proposed the concept of "Compact City" to guide future urban development planning^[37]. The rapid increase in the share of room gases in the Earth's atmosphere is already leading to higher global temperatures and rapid climate change^[38,39]. These phenomena not only seriously affect human daily life and cause incalculable economic losses, but also have a serious impact on human health^[40]. The role of urban green spaces in the global carbon cycle is equally important compared to their importance in reducing surface temperatures, purifying air, protecting water resources and reducing water logging.

A report published by the IPCC shows that climate change will lead to irreparable degradation of natural ecosystems if governments do not quickly contain warming to less than 1.5°C^[41]. The impacts of climate change relate to development issues such as social well-being, economic development, and environmental protection. On September 21, 2021, China emphasized at the United Nations General Assembly that "China will strive to achieve carbon peaking by 2030 and carbon neutrality by 2060"^[42]. The 2015 《Paris Agreement》 identifies this climate crisis as a common problem that needs to be faced by all countries in the world and requires concerted efforts to address it.^[43] According to the statistics of China's "garden city" construction status, the green area of urban built-up areas nationwide reached 2.3 million hectares, an increase of 50% compared to 2012. There are 18,000 new urban parks and green areas, and 14.8m² of green space per urban resident^[44]. The construction of a balanced distribution of urban green

space system, and gradually realize the residents travel "300 meters to see the green, 500 meters to see the garden" goal.

In order to explore the issue of carbon enhancement in urban green areas, this study takes the China Green Expo in Zhengzhou City as the research object. This thesis collected radar point cloud data, remote sensing image data of Super View-1 and biodiversity data obtained from outdoor survey of China Green Expo Park in Zhengzhou City. This thesis conducted a parametric analysis of the driving relationships between forest stand structure, remote sensing image information and carbon storage and sequestration, as well as the scale dependence.

1.2 Related Research Progress:

1.2.1 Research progress on carbon sinks in urban green areas

Urbanization has dramatically changed the global biogeochemical cycle ^[45]. On the one hand, it is because urban ecosystem carbon emissions exceed 75% of global anthropogenic carbon emissions; On the other hand, it is attributed to the fact that urban ecosystems store a large amount of organic carbon and their carbon sequestration capacity far exceeds the natural ecosystem. For example, a study conducted in 48 U.S. states demonstrated that urban green spaces account for 10% of organic carbon storage in terrestrial ecosystems ^[32]. 在 The results of a study conducted in Seattle, USA, proved that the above-ground biomass of urban green spaces is much higher than the average above-ground biomass of natural forests ^[46]. With the growing urbanization, urban green space has an increasing capacity to sequester carbon. Compared to the large amount of carbon emissions from urban areas, the carbon sequestration effect of urban green spaces largely cuts down on the CO₂ emissions generated by high intensity human activities.

Current studies on carbon storage in urban green spaces have focused on regional assessments. Studies on carbon storage in urban vegetation were first conducted by the Nowak group in the United States. In 1993, the group estimated the carbon stocks of urban trees throughout the United States ^[47]; In 2002, Nowak used an optimized method to estimate urban vegetation carbon storage and sequestration for the entire U.S. based on vegetation cover data for ten cities in the U.S. ^[48]; In 2013, the group updated the estimation method based on the vegetation cover data of 6 states and 28 cities in the U.S., and obtained better information on the carbon storage and sequestration of urban vegetation across the U.S. ^[49]. A large number of vegetation carbon storage surveys and assessments have also been conducted in China. Compared to the findings of other countries, the urban green space carbon density in China (19.8 t C/hm²) is much lower than that of the United States (76.9 ± 13.6 t C/hm²).

The carbon storage of urban green space is very important in future research. The analysis of carbon sequestration services in urban green space ecosystem services is crucial to the implementation of future global carbon cycle strategies and provides important theoretical support for sustainable urban development.

1.2.1.1 Research Progress on Species Diversity and Carbon Sink Capacity

A large number of existing studies on biodiversity and carbon stocks are focused on grasslands and natural forests ^[50–52]. There are many research gaps on the relationship between biodiversity and carbon storage in urban green spaces. Since urban green spaces are often disturbed by a large number of human activities and the regional limitations of urban green space system planning, the structure of urban green spaces is closer to that of artificial woodlands than natural forests ^[53].

Previous studies have demonstrated a significant positive correlation between biodiversity and ecosystem productivity ^[54]. One study of natural forests concluded that there is a "hump-shaped" relationship between species richness and forest productivity ^[55]. Biodiversity has a positive contribution to green space productivity. This phenomenon is attributed to the fact that green spaces with high biodiversity have higher complementarity in resource use and therefore can produce and store more carbon with limited resources ^[56].

These studies confirm the contribution of biodiversity to green space productivity; however, there still needs to be studies that can prove whether this rule applies to urban green spaces. Another study demonstrated the significant scale-dependence of the relationship between green space biodiversity and productivity ^[57]. This relationship was weaker in the larger-scale sample plots ^[58]. A 2015 study estimated biodiversity at multiple scales and demonstrated that 1000 meters scale are the best measure of biodiversity ^[59]. The tendency of vegetation biodiversity with sample area is consistent with the "species-area" relationship ^[60]. Larger green areas have more space and more species as a buffer against external disturbances, and are less affected by external environmental disturbances, so the prediction results of their biodiversity are more accurate; In contrast, small areas of green space are more susceptible to climate, wildlife and human activities, which makes biodiversity prediction more difficult ^[57]. The synergistic effect between vegetation species is also weakened in small green space areas. Especially in urban environments, ecosystem services are often enhanced by changing the composition of the ecosystem, and this action often leads to a reduction in biodiversity ^[61]. A study in 2018 also demonstrated that species richness varied more in small green areas than in large ones ^[62].

Vegetation structure represents the physical environment that generates, supports, and maintains biodiversity, and vegetation structure is the basis for forest species diversity. Green spaces with complex vegetation structures generally have higher biodiversity ^[63]. Compared to the green space area, the stand structure's complexity is equally essential for maintaining green space biodiversity ^[64]. When forest density and canopy structure complexity increase, biodiversity and carbon stocks also appear to increase ^[65]. At the small scale, biodiversity is primarily influenced by biological processes among vegetation; however, at the large scale, biodiversity is often determined by statistics. The spatial center limit theorem can well explain this phenomenon ^[57]. A study in 2017 summarized the impact of biodiversity on carbon storage and sequestration, concluding that biodiversity, as related by species, traits, and stand structure, explained 64%

of the variation in carbon storage and sequestration ^[56].

1.2.1.2 Research Progress of Remote Sensing Technology and Green space Carbon Sink

With the development of remote sensing technology, landscape architecture has extensively used satellite images as the data base for research. Remote sensing satellite data can provide a wealth of spectral information, texture information, and optical sensor information at a low cost. Remote sensing data have been widely applied to research in related disciplines requiring above-ground biomass mapping. In remote sensing data, vegetation indices, texture features, and leaf area indices can provide technical support for the spatial quantification of above-ground biomass ^[66].

By combining the red and near-infrared bands obtained from the sensor, this study can get optical information that responds to canopy structure, chlorophyll content, plant phenology, and leaf growth conditions. Vegetation indices can reflect the ability of ground vegetation to absorb light and quantify environmental stress; for example, a decrease in NDVI demonstrates a reduction in chlorophyll or vegetation leaves ^[67]. Vegetation growth status can be compared by vegetation indices at different times and spaces. The commonly used vegetation indices are normalized vegetation index^[68] (NDVI)、vertical vegetation index^[69] (PVI) and Tasseled cap green vegetation index^[70] (TC-GVI) . Every type of vegetation index can improve the accuracy of above-ground biomass estimation. However, due to the large amount of information redundancy between different vegetation indices, which leads to a multicollinearity effect between vegetation index indices. Therefore, increasing the number of vegetation indices could not improve the accuracy of the study results ^[71]. At the same time, the vegetation index tends to saturate areas with high vegetation biomass. This phenomenon reduces the accuracy of vegetation indices in predicting biomass ^[72].

Several studies have demonstrated that using spectral information in combination with image texture information can improve the model's accuracy ^[73]. Some studies have also concluded that image texture features correlate more with biomass than spectral information ^[73,74]. Because image texture features can distinguish spatial information, it is possible to identify selected objects in an image by image texture features ^[75]. Therefore, applying texture features ^[75] can effectively improve the accuracy of biomass measurements ^[76]. Compared to spectral features, texture features can better sense changes in forest biomass after disturbance ^[77]. One of the most commonly used image texture feature indices is the grayscale co-occurrence matrix information (GLCM) , the usability has been verified in many studies ^[78]. Franklin determined the ideal structure of age distribution in Canadian coniferous woods by setting the extraction window size of the GLCM homogeneity index to 15m and 25m ^[79]. A study in 2011 significantly improved the performance of the biomass prediction model by applying texture feature parameters to remote sensing images, increasing the R^2 of the model to 0.88 ^[71].

Despite the large number of studies that have demonstrated the usability of image texture features in biomass prediction, there are still some potential problems in practice: The process of extracting texture

features from remote sensing images often generates a large amount of redundant information which is difficult to manage ^[80]. It is undeniable that adding image texture information to the spectral data can optimize biomass and carbon estimation, models.

1.2.1.3 Research Progress on Radar Technology and Greenland Carbon Sink

Previous studies has shown that utilizing a combination of radar data and remote sensing satellite data can increase the accuracy of forest biomass estimating models ^[81–83]. Lidar is an active observation technology. Unlike remote sensing satellite technology, LiDAR can estimate forest height and stand structure information by emitting laser pulses and measuring the signal return time ^[84]. Compared to remote sensing satellite observation techniques that passively capture optical reflection information, it isn't easy to saturate the information obtained from LIDAR measurements ^[85,86]. Laser pulses can penetrate the multi-layered canopy structure of the forest folklore and obtain detailed vertical structure information from the reflected signals. This method solves the saturation problem of high biomass forest carbon stock assessment ^[85]. The carbon storage and sequestration of green space vegetation are determined by the stand structure of the vegetation, including diameter at breast height, height under branches, crown height, crown width, trunk density and branch distribution. Previously, due to technical limitations, height was the only forest structure parameter that could be obtained directly by LiDAR ^[87]. Recent studies have shown that by analyzing the point cloud information obtained from LiDAR scans, it is possible to obtain the forest stand structure, vegetation cover ^[82] and forest stand intensity ^[88]. In addition to the average vegetation information on a regional basis, LiDAR also has the ability to obtain detailed stand structure on an individual vegetation basis ^[89].

Numerous studies have demonstrated the usability of LiDAR for forest biomass estimation ^[90]. By combining remote sensing data with LiDAR point cloud data to increase the accuracy of the results, a study in 2022 showed the potential of radar data in measuring forest carbon density ^[91]. Baccini corrected the anisotropic growth model at the study area scale using LiDAR data and field survey data ^[92]. And further, the forest biomass obtained by radar data extraction was used as an input variable to map the global carbon storage ^[93]. Although studies on biomass and carbon stocks are still primarily based on the use of remote sensing imagery, the field is benefiting from the application of LiDAR technology as time goes on ^[94]. Both remote sensing satellites and airborne LiDAR technology have received high attention in the global carbon monitoring system, mainly used for measuring, estimating and verifying carbon stocks and sequestration, providing technical support for the UN's REDD+ program ^[95].

1.2.2 Methodology for estimating carbon storage in urban green spaces

Urban vegetation is an essential component of terrestrial ecosystems and has a profound impact on the carbon cycle at regional and global scales ^[96]. Research proves that urban vegetation plays a positive role

in reducing the carbon content in the atmosphere^[97]. Urban green spaces promote carbon absorption in the atmosphere in two ways: The direct carbon sequestration is through the absorption of CO₂ by vegetation growth, while indirect carbon sequestration is mainly through reducing energy consumption in urban buildings, reducing the urban heat island effect and guiding green transportation, etc^[98]. At the same time, urban green spaces will release some carbon, such as the natural death of plants, mowing of lawns, etc^[99]. Research on carbon sequestration in urban green spaces has become a popular research topic in landscape architecture because of their location closest to greenhouse gas-producing areas. Although the coverage of urban green space is much smaller than natural vegetation^[100], but many studies have demonstrated the importance of urban green space in the global carbon cycle^[101].

Compared with the natural forest carbon storage model, the carbon storage model for urban green space has two characteristics: First, the spatial distribution of urban green space is highly fragmented^[83]; Secondly, urban green spaces are more affected by human activities, such as irrigation, fertilization, pest control and pruning, etc^[102]. All these features make the calculation of carbon stocks in urban green areas more difficult and inaccurate. It has been suggested that due to the unstable state of ecosystems in cities^[103], the carbon storage in urban green spaces is probably underestimated^[104]. The application of remote sensing images in the field of carbon storage estimation has dramatically contributed to the progress of research on the spatial and temporal distribution of carbon storage in urban green areas. Although remote sensing imaging technology brings new opportunities for calculating carbon stocks in urban green spaces, this technology has some limitations. Spatial heterogeneity causes the resolution of most current satellite images to be insufficient to accurately reflect the spatial distribution of carbon storage in urban green spaces; Massive shadows caused by the three-dimensional structure of urban buildings create a large number of gaps in the urban carbon storage estimation process; Sensors of remote sensing satellites are disturbed by the large amount of human activity in urban areas^[105,106]. On the other hand, the development of multi-source remote sensing technology provides a new opportunity for the estimation of urban green space carbon stocks, such as multispectral, hyperspectral, and LIDAR^[107]. The rapid development of observation instruments such as satellite-borne LiDAR, vehicle-mounted LiDAR, and UAVs have provided a large amount of validation data for estimating urban green space carbon storage and advanced the development and improvement of urban green space carbon storage models.

1.2.2.1 Research progress on carbon storage models

In urban areas, the impact of high-intensity human activities on the carbon stocks of urban green spaces is much higher than the impact on natural ecosystems. Even though many scholars have made a lot of efforts in applying natural forest natural storage models to urban green spaces, however, these methods still cannot completely overcome the influence of human activities on the accuracy of carbon storage estimation. The carbon storage calculation methods commonly used in the existing studies are (1) Field

survey methods, (2) Model estimation methods, and (3) Remote sensing estimation.

The key to measuring the carbon density of urban green space by field survey method is the determination of the optimal sample scale. The most common way to obtain the vegetation carbon storage of the study area ecosystem is by multiplying the carbon density per unit area in the sample square with the area of the whole study area. This method has been used in many studies in China and the United States with positive results ^[108,48]. The field survey method is limited in its implementation by two issues: The first is that this method requires a lot of human and material resources to conduct outdoor surveys; Secondly, the calculation of biomass and carbon storage requires the allometric growth equations of a large number of species. The complex structure of green spaces in cities, the impact of high-intensity human activities and the diverse planting configurations bring many difficulties to the implementation of the field survey method.

Many studies have been conducted to calculate the carbon storage of urban green space by model estimation method. This method was first developed based on data from surface resource surveys conducted in the United States, such as the CTCC (The center for urban forest research tree carbon calculator) and UFORE (Urban Forest Effects Model). In addition, the youngest models are CityGreen, NTBC and i-Tree. Among them, the CityGreen model usually requires a moderate amount of data for analysis, and this model takes more time to analysis, and better suited for regional carbon stock estimation and analysis ^[109]. The i-Tree model has a wide range of applicability, and the minimum scale allows for carbon storage estimation on an individual vegetation basis ^[110]. The NFBC model is also applicable to the carbon storage estimation of single vegetation individuals, but it is only applicable to the carbon storage of specific tree species, The ability to deal with complex community structures is weak ^[111]. Considering the complex three-dimensional structure of urban green space vegetation communities, the i-Tree eco model has a greater advantage in estimating and assessing the carbon storage of urban green spaces ^[112].

The remote sensing estimation method has facilitated scholars' research on the spatial distribution patterns of carbon storage in urban green areas in many ways ^[113,114]. With the decreasing price of high-resolution remote sensing images and the release of public data, the application potential of remote sensing data for urban green space carbon storage estimation is increasing year by year. There are two main forms in the way of application: The first one is to use interpolation in the information extracted from remote sensing images after sampling through sample areas to estimate carbon storage in all areas in the spatial scale; Another way is to establish a carbon storage estimation model based on outdoor survey data and remote sensing information, which can be used to quickly estimate the spatial distribution of surface carbon storage in subsequent studies. Although this method has been applied extensively in related studies, there are still some issues that need to be addressed in future studies, For example, the saturation problem of remote sensing information extraction and the error of estimating model application in different regions need to be solved. On the other hand, obtaining the subsurface carbon storage by remote sensing estimation method is difficult, subsurface carbon storage measurements at small scales are needed as additional

experimental material.

As one of the less studied components of terrestrial ecosystems, urban green space carbon storage has received more and more attention. The development of remote sensing and LiDAR technologies has provided increasingly extensive technical support for studies related to carbon storage in urban green spaces. In the context of achieving carbon neutrality, research on carbon sequestration in urban green spaces still needs more attention.

1.2.2.2 i-Tree eco model

The i-Tree eco model is a software application for cities developed by the USDA Forest Service and is commonly used to quantify and estimate the ecosystem provided by urban green spaces. This model was first published in 2012 and was developed from the Urban Forest Effects model (UFORE) ^[115]. Previous versions were mainly used to simulate the absorption of atmospheric pollution during non-precipitation periods by the sorption of urban green space vegetation.

The application of the i-Tree eco model needs to be based on detailed vegetation information throughout the study area or on data collected in sample plots. The i-Tree eco model takes into account the effect of species type on carbon storage and sequestration, which is one of the reasons why the estimation accuracy of this model is higher than other carbon storage calculation models. The i-Tree eco model can obtain accurate spatial distribution of carbon storage and carbon sequestration in urban green space by vegetation stand information. Compared with the results of carbon storage estimates obtained by remote sensing techniques and field survey methods, the results of the model are less influenced by human activities and subjective choices of researchers. In the calculation process of the model, the information of tree height, diameter at breast height and crown width of vegetation are involved in the calculation, which improves the scientific and rational nature of the simulation results.

The i-Tree eco model has been widely used in landscape architecture, such as developing urban green space master plans, informing environmental regulatory issues, maintaining the balance between different types of ecosystem services, and aiding decision-making on the equity of urban green space ecosystem services.

1.3 Research content and objectives

1.3.1 Main research content

1) Quantifying the Spatial Distribution of Carbon Storage and Sequestration in China Green Expo

In this part, China Green Expo was used as the study area, and a vegetation species census was conducted through outdoor surveys of the study area, and species distribution maps were drawn. Using the

sample method, samples of herbaceous plants were collected in 1 m² units and dried in the laboratory for dry weight measurement. Scanning the China Green Expo using LIDAR backpack to get the point cloud model, and processing in Lidar360 software to get the tree stand structure information and shrub volume information. Based on the information obtained from the field survey and radar point cloud processing results, this study used the i-Tree eco model to calculate the information of tree carbon storage and carbon sequestration. Based on data collection, remote sensing interpretation and shrub volume data, this study gained information on carbon sequestration of herbaceous vegetation, carbon storage and carbon sequestration of shrubs in China Green Expo. Finally, this study can get information on the spatial distribution of species diversity, stand structure, carbon storage and carbon sequestration in China Green Expo.

2) Get the growth factors of 169 tree species and evaluate them in combination with carbon sequestration capacity

This section concerns the growth characteristics and carbon sequestration capacity of 169 species of trees growing in the China Green Expo. There is a wealth of research on plant anisotropic growth equations. However, the use of plant anisotropic growth equations in production practice is limited and urban management are facing with the problem of difficulty in calculating the age of urban forest. Some studies in Europe and the United States have found that tree age can be calculated quickly by plant growth factors, but there is a lack of attention to plant growth factors in China (Tree age = DBH × growth factor) (DBH: Diameter of breast height). Some scholars have already started to focus on the carbon sequestration capacity of different tree species, however, these studies do not integrate their carbon sequestration capacity with their applications in urban environments, thus making it difficult to provide theoretical support for production practices. Therefore, this study combined species information, stand structure information and carbon storage information to extract the growth factors of 169 species of trees. This thesis performed a cluster analysis of the direct factors affecting the carbon storage of species and evaluated the carbon sequestration capacity of arboreal species based on the results of the analysis.

3) Estimating the influencing factors and scale dependence of carbon density based on multiple data analysis methods

This section concerns the relationship between carbon density and drivers of China Green Expo, and the scale dependence of the driving relationship between them. China Green Expo is a comprehensive park for the purpose of greening exhibition, so it is used as the research object to study the carbon density of urban parks in this study.

There are more studies on carbon storage and sequestration in natural green areas, but less studies on urban green spaces. The reason for this phenomenon is due to the small size of urban parks, which makes it difficult to conduct multi-scale studies. The construction of the China Green Expo provides us with this

opportunity. It is essential to study the changes in carbon density in urban park green space under multi-scale observation and analyze the changes of carbon density influencing factors under different scales to explain the carbon sink capacity of urban green space. Therefore, in this study, carbon storage, carbon sequestration, spatial structure information, forest stand structure information, and remote sensing information were extracted separately by the moving pane method at different scales. Then analyze the influence factors and the change of carbon density values at different scales. Finally, the driving relationships between the influencing factors and carbon density at different scales were analyzed by full subset regression, structural equation modeling and HP analysis to find the main influencing factors at multiple scales.

1.3.2 Main research objectives

Through the above-mentioned research content, the following research objectives will be achieved:

1) Clarify the spatial distribution of carbon density, species diversity and stand structure in Zhengzhou-China Green Expo, and verify the applicability of extracting high-precision carbon density from park green areas by LiDAR technology;

2) Identify the carbon sequestration capacity of 169 tree species, and evaluate the carbon sequestration capacity of species in relation to the growth pattern of trees in the region. Providing species selection options for optimal design of urban park green spaces based on carbon enhancement functions;

3) Clarifying the tendency of the carbon density statistics in urban parks to vary with the scale of the sample, and finding the best sample size suitable for urban green space carbon density field survey;

4) Establish multi-scale driving relationships between carbon density and influencing factors, and identify the main drivers of carbon density in different scales. Finally, provides theoretical support for the optimization of urban park green space with the goal of carbon sequestration.

5) Based on the research results, an optimized design was carried out with the goal of enhancing the carbon sink function of China Green Expo.

1.4 Scientific problems to be solved

The key scientific questions to be addressed in this study are as follows:

- 1) What are the differences in the carbon sequestration capacity of different tree species in urban green spaces? How can the results of research on the carbon sequestration capacity of tree species be applied in landscape plant design?
- 2) Is the sampling scale applicable to natural ecosystems also applicable to urban parks? What is the best scale for sampling urban park green space by sample method?
- 3) What are the main drivers of carbon density in urban green spaces? Does the main driver change at different scales?

1.5 Technology Line

The technical lines used in this thesis are as follows:

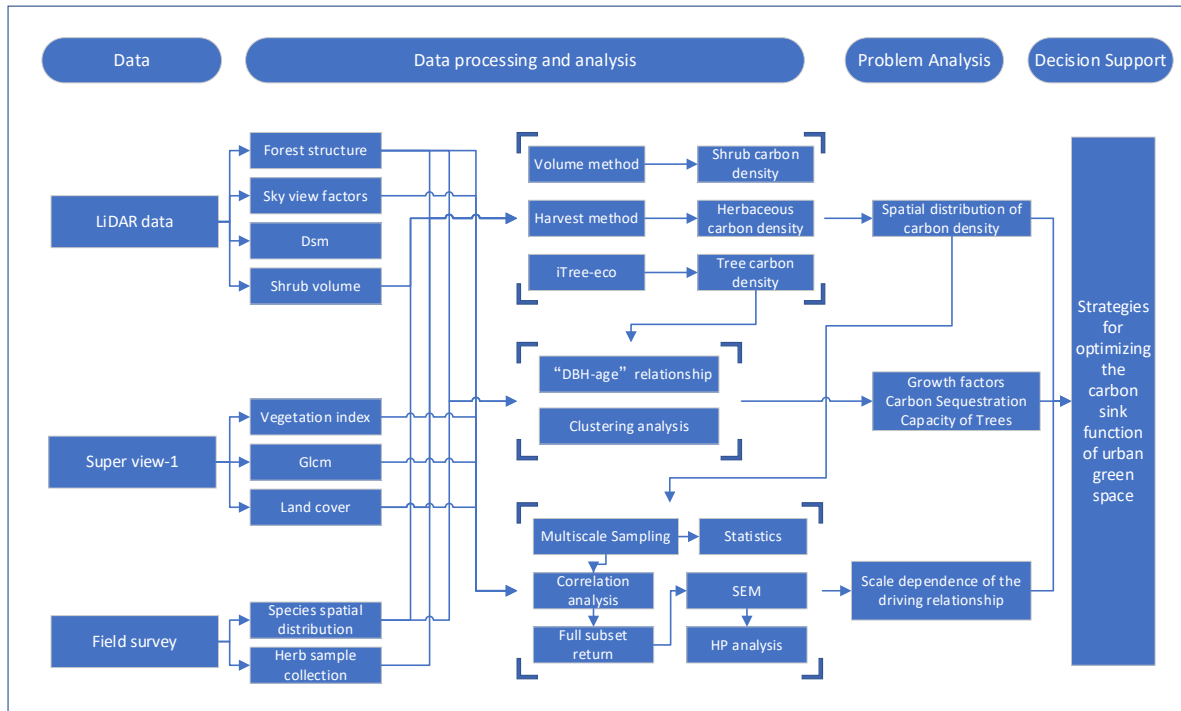


Figure 1-1 Technology Roadmap

2 Research area and methodology

2.1 Nature profile

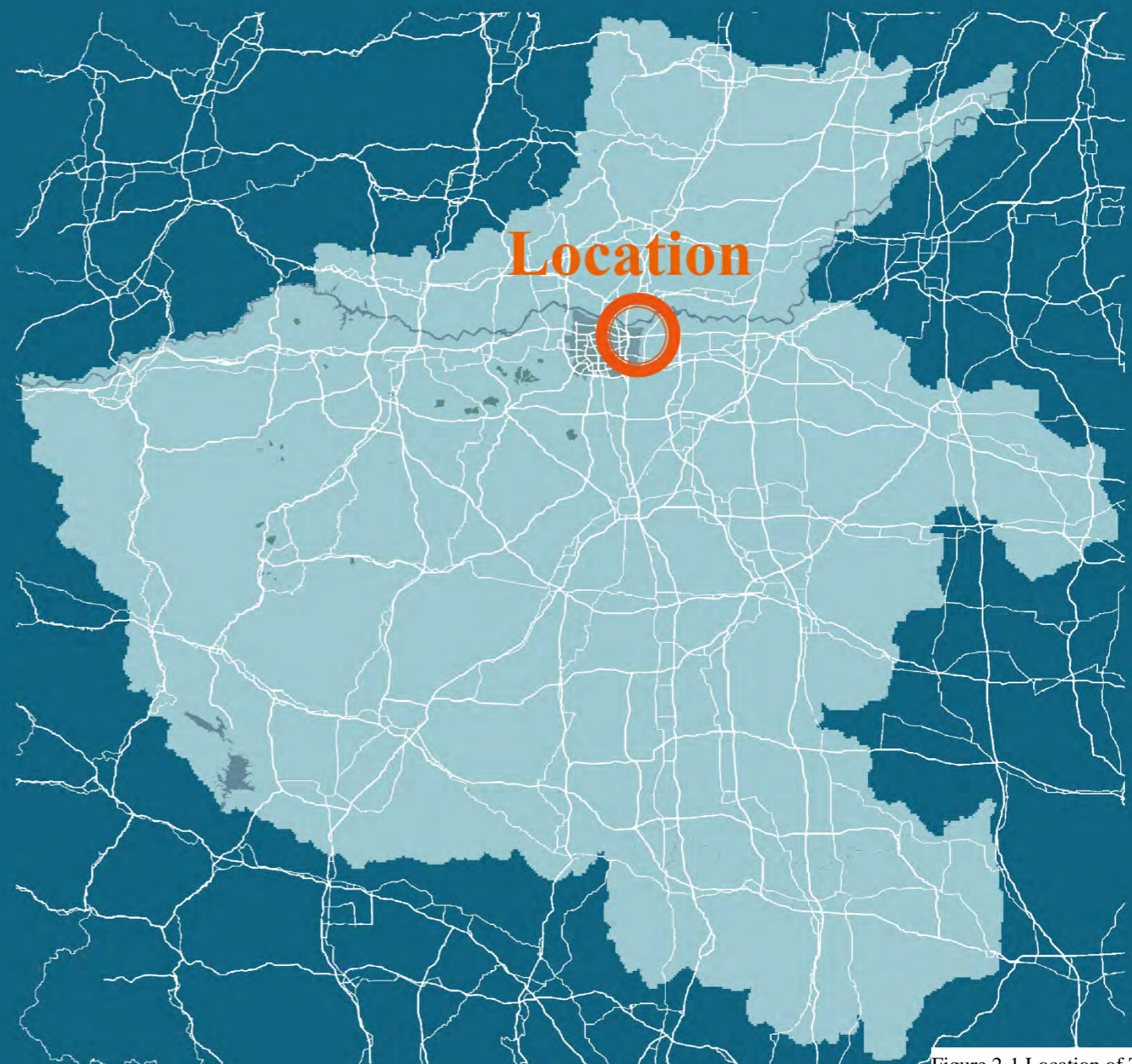
2.1.1 Geographic location

Zhengzhou is the capital of Henan Province, located in the north-central part of Henan Province, in the middle and lower reaches of the Yellow River. Zhengzhou City faces the Yellow River to the north and is connected to Song Shan Mountain to the west. The topographic tendency of Zhengzhou is high in the southwest and low in the northeast, located between the geographical coordinates 112°42'~114°14'E and 34°16'~34°58'N. The total area of the whole region is 7567km². Over the past few decades, the urbanization of Zhengzhou has gradually accelerated, with the population increasing from 8.62 million in 2010 to 12.6 million in 2020. Zhengzhou City was awarded the title of "National Ecological Garden City" in 2020, with a greening area of 13m² per person and a greening coverage of 40.83% in the built-up area of the city.

China Green Expo is located in Zhengzhou City, Henan Province, at the center of the geographical coordinate system of 113°E and 34°N. The park has a total area of 196ha and an average annual growing season of 307 days. The construction of China Green Expo began in August 2009 and was completed in September 2010 after a total construction time of one year and two months. The China Green Expo was built to showcase the characteristics and achievements of urban greening construction in various regions of China and to popularize the knowledge of greening throughout the country. The China Green Expo consists of 91 theme parks, of which different theme parks have different forest composition, tree age and landscape garden style.



Location of Henan Province in China



The project is located in Zhengzhou City, Henan Province, in a suburban location with convenient transportation.

About 56 minutes drive from Zhengzhou city center

About 1 hour drive from Kaifeng city center

Figure 2-1 Location of Zhengzhou City



China Green Expo is located in the eastern part of Zhengzhou City, adjacent to the "Zhengzhou-Kaifeng Expressway" in the north, surrounded by water on three sides.

Amusement Park

Zhengzhou-Kaifeng Road

Research area

G107 Road

Culture Road

Figure 2-2 Location of China Green Expo

2.1.3 Topography

Zhengzhou is located at the interface of the second and third terrain steps in China. The north-eastern part is lower, located in the alluvial plain of the Yellow River; The southwest is higher, with the middle and eastern sections of the Song Shan Mountain as the main composition (Figure 2-3, a). The mountainous area of Zhengzhou City is 2375.4km², accounting for 31.6% of the total area of the city; The area of hills is 2256.2km², accounting for 30% of the total area of the municipality; The plains cover a total area of 2,879.7km², accounting for 38.4% of the total area of the city. This research area is located in the eastern plain at elevations between 75-100 m.

The terrain of China Green Expo is relatively flat, with an average elevation of 97m; high in the northwest and low in the southeast, while the maximum height difference is less than 1m (Figure 2-3, b). The uneven distribution of some small hills has little impact on the overall environment. The soils in the area were basically sandy tidal soils and light loamy tidal soils with low organic matter content, averaging less than 8.0 g/kg. The soil pH is between 7.3-7.8, which is suitable for vegetation growth.

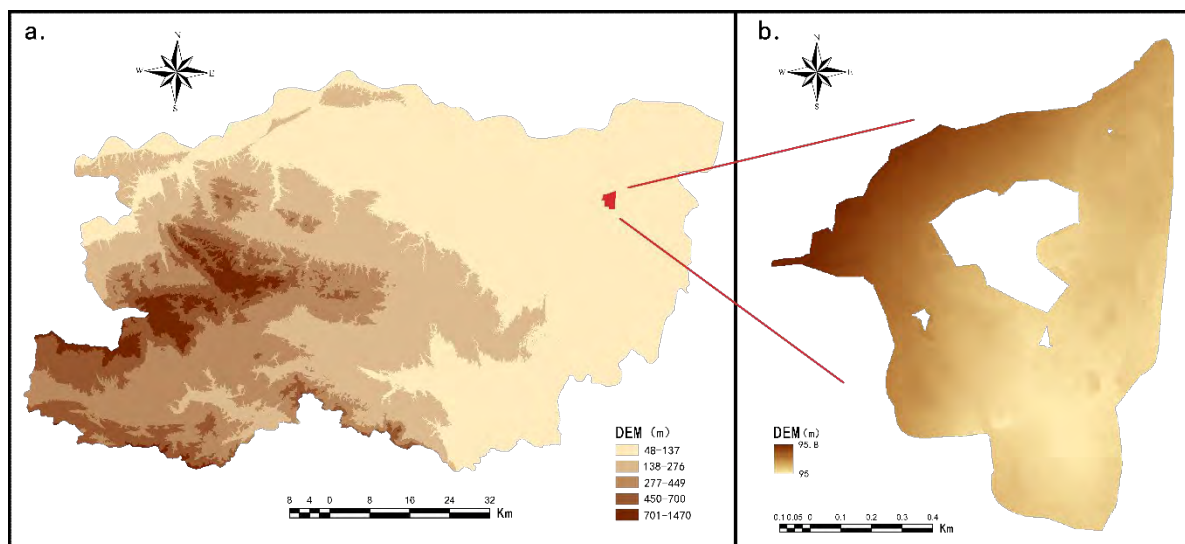


Figure 2-3 Digital elevation model ^[116] (DEM); a. DEM of Zhengzhou city; b. DEM of China Green Expo

2.1.4 Hydrologic conditions

Zhengzhou has a dense network of rivers in its territory, spanning two major basins: the Yellow River and the Huaihe River. The location of China Green Expo belongs to the Huaihe River Basin. The Huaihe River Basin covers a total area of 5,499.5 square kilometers within the Zhengzhou city boundary, accounting for 73% of the city's area. The main tributaries of the Huaihe River Basin within the area of Zhengzhou City are the Yinghe River, the Jialu River and the Yunliang River. In 2020, the total water resources of Zhengzhou was 859.12 million cubic meters, of which the total surface water resources was 527.36 million cubic meters.

China Green Expo is close to the Jalu River in the southwest and the Yellow River Diversion Canal in the east. The average groundwater level is 4~6m, and the groundwater resources are relatively abundant, but there is a risk of internal flooding during the abundant water period. Following extreme precipitation events, the flooding will last for a longer period of time.

2.1.5 Vegetation profile

Zhengzhou city is rich in plant resources. It belongs to the warm temperate deciduous broad-leaved forest vegetation type in the flora division and is located at the junction of two vegetation zones. The area has excellent soil conditions, hydrological conditions and suitable temperatures for the formation of a rich plant landscape ^[117].

The China Green Expo is located on the north-south climate zone of China, with abundant plant resources available. According to the 《Zhengzhou City-China Green Expo Plant List》 published during the construction period of the China Green Expo, there were 146 families, 344 genera, 1,088 species and their varieties of plants when the Zhengzhou City-China Green Expo was completed. The total number of tree species is 442 and the total number of shrub species is 323. Among them, the provincial protected plants included in the list of key protected plants in Henan Province are *Pinus bungeana*, *Juniperus squamata*, *Ostrya japonica*, *Polygonum honanense*, *Malus honanensis*, *Aesculus hippocastanum*, *Acer oblongum*, *Aesculus chinensis*, *Paliurus hemsleyanus*, *Opisthopappus taihangensis*, *Dendrobium nobile*, Holly etc.^[118]. The plants listed as national key plants include the *Cycas*, *Ginkgo biloba*, *Podocarpus*, *Metasequoia glyptostroboides*, *Calocedrus macrolepis*, *Thuja sutchuenensis*, *Taxus wallichiana*, *Pinus parviflora*, *Pseudotsuga sinensis*, *Liriodendron chinense* etc.^[119].

2.2 Landscape Function

2.2.1 The original design concept

With "ecology, innovation, and harmony" as the core concepts of the park's planning, the Green Expo Park is designed to be an ecological park that incorporates innovative green technologies and natural recreational activities. The park aims to serve as a showcase and experience center for green environments, technologies, and cultural activities, fully reflecting the theme of the Green Expo (Figure 2-4). Moreover, it is intended to become an integral part of Zhengzhou's future ecological green space system, and a distinctive attraction for public leisure and recreational activities in the city's green core.

By organizing 15 themed projects that showcase the theme of "Green Integration into Life" and embody the park's planning concepts of "ecological conservation, technological innovation, and harmonious living," the Green Expo provides visitors with a comprehensive understanding of the close relationship between greenery and human life (Figure 2-5).

By constructing a natural overall layout, with a dense and diverse functional and spatial arrangement, a rich landscape and plant system, the Green Expo creates an eco-friendly green park. At the same time, the park employs green buildings, sets up high-profile landmarks and designs landscape facilities that reflect the characteristics of Central Plains culture as artificial landscapes and environmental features. Through these efforts, the park constructs a distinctive public leisure and recreational space that embodies the harmony between humans and nature, reflects the characteristics of Central Plains culture, and has unique features.

2.2.2 Site transportation and functional analysis

The main entrance is located on the north and east sides of the park, which includes entrance squares and public service facilities (Figure 2-4). The northern entrance square covers an area of 5.3 hectares and is located on the north side of the park. Large parking lots are planned on both sides of the square to meet the parking requirements of large buses and private cars. The parking lots adopt an ecological parking design with trees and shade. The east entrance square covers an area of 1.2 hectares and has a semi-circular design, including entrance management facilities. A large parking lot is planned on the south side of the square to meet the parking requirements of large buses and private cars. The parking lot adopts an ecological parking design with trees and shade.

The road system is divided into three levels (Figure 2-6). The first level is the vehicular roadway: the red line width of the roads on both sides of the north square is 21 meters, with a roadway of 12 meters and sidewalks of 4.5 meters on each side. The inner and outer double rings within the park are the main vehicular and landscape roads, with a roadway width of 6 meters. The road on the southern hillside is defined as a secondary vehicular road with a width of 6 meters. The second level is the pedestrian walking routes: The planned design relies on the central pedestrian theme axis and the walking loop around the central lake, as well as the main branching layout of pedestrian tour routes, with a width of 3 meters for pedestrian traffic. The third level is the waterfront pedestrian roadway: forming a circular pedestrian network around the central lake to create a unique road system within the area. The width of the wooden boardwalk is controlled within 1.5 meters.



Figure 2-4 Current Planning and Design

Aerial photography



Facilities for children



Animals



Transportation



Flowers



Theme Garden



Figure 2-5 Functions of the park

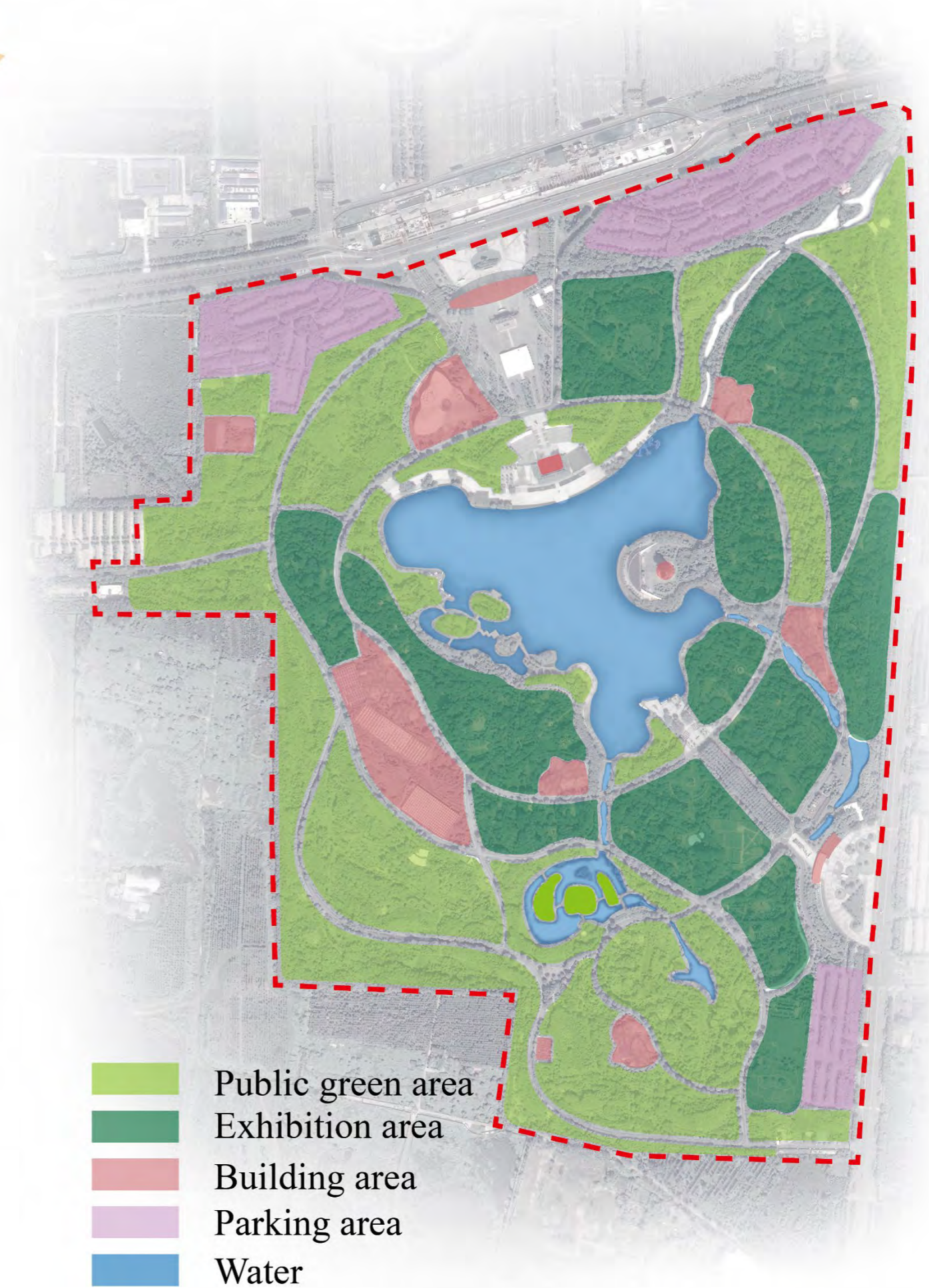
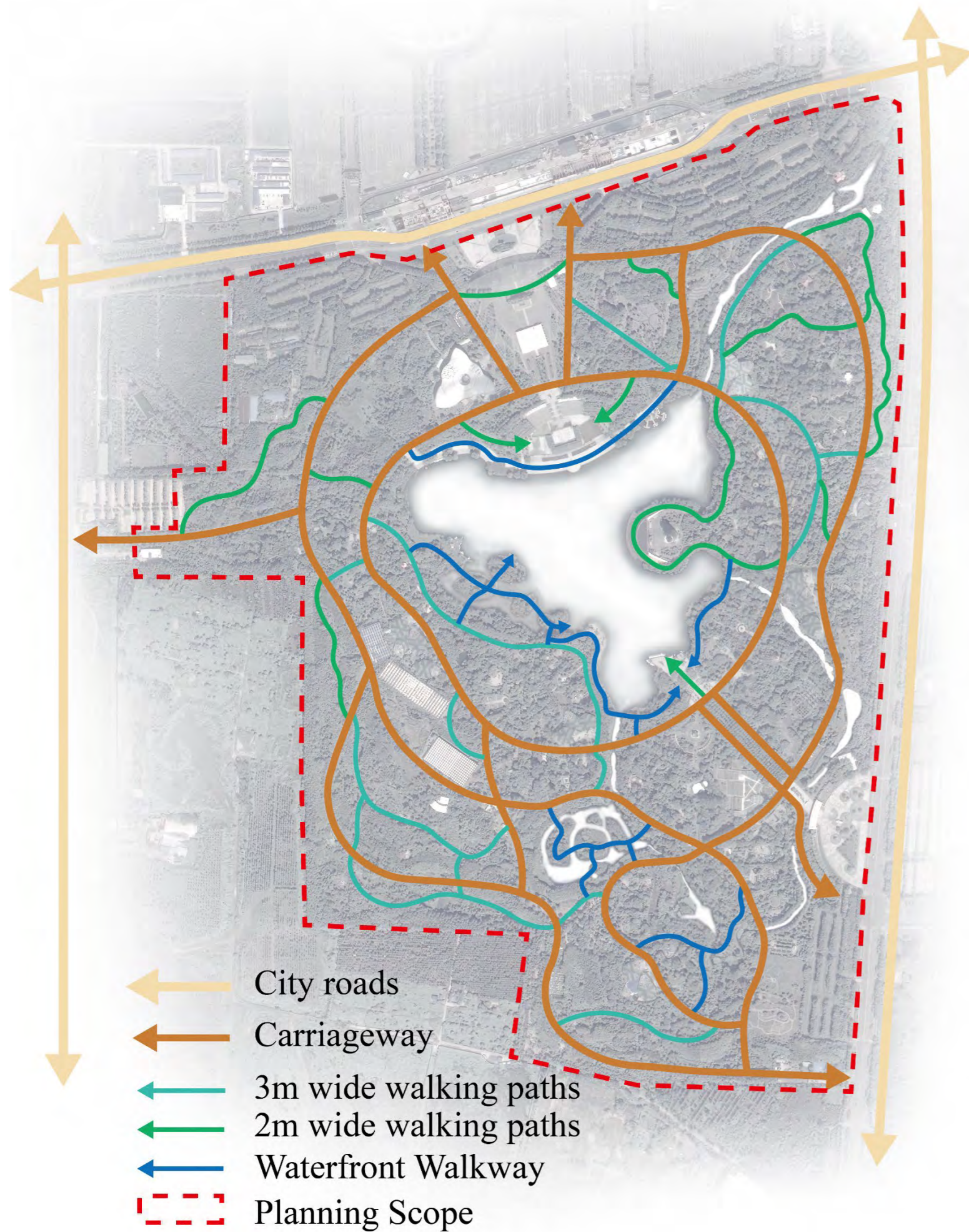


Figure 2-6 Road system analysis and land use analysis

2.3 Materials and Methods

2.3.1 Field survey

2.3.1.1 Tree species survey

This thesis conducted a survey of tree species information in China Green Expo during July and August 2021, and the survey information included species and spatial distribution information for each tree.

2.3.1.2 Herbal plant sampling

The samples of herbaceous vegetation in China Green Expo were collected during July and August 2021 using the harvesting method. The carbon storage of herbaceous plants under sunny conditions is about 70 times higher than that in areas with higher forest depression ^[120,121]. This thesis set up 10 sample squares of 1×1m in the understory area and the area with good light conditions, then harvested and collected the herbaceous vegetation in the sample squares. The locations of the samples were evenly distributed in China Green Expo. The collected herbaceous plants were brought back to the laboratory for drying and weighing to get the total biomass, then the biomass was multiplied by the "biomass-carbon stock" conversion factor of 0.5 to get the carbon storage ^[122]. Finally, this study obtained the carbon storage density of herbs under the forest and sunny environment of China Green Expo, the formula is:

$$C_H = \left[\frac{1}{10} \times (W_1 + W_2 + \dots + W_{10}) \right] \times 0.5 \div 1 \quad \text{Equation 1}$$

In the formula, C_H is the herbaceous above-ground carbon storage density in kg/m². W_1, W_2, \dots, W_{10} are the herbaceous biomass in samples, and 0.5 is the "biomass-carbon storage" conversion factor.

In the published studies so far, the carbon sequestration capacity of herbaceous plants is mostly observed by respirometry. However, this technique is highly influenced by environmental conditions and requires a large amount of work, which makes it difficult to perform at larger study scales. In natural environments, herbaceous plants often leave a large amount of falling leaves by natural withering. In contrast, in artificial environments, herbaceous plant biomass fallout is often caused by manual pruning. Therefore, this study calculated the annual carbon sequestration of herbaceous plants by the biomass obtained from the lawn pruning. A study on the biomass of grassland vegetation in China proved that the below-ground biomass of grassland vegetation is 6.15 times higher than the above-ground biomass ^[123]. The frequency of lawn pruning in the management system of the China Green Expo is about 10 times a year. The biomass removed per pruning is about one-third of the above-ground biomass of the herbaceous plants. Therefore, this study can calculate the annual carbon sequestration density of herbaceous plants based on the carbon storage density of herbaceous vegetation by the following equation:

$$C_S = C_H \div 7.15 \times \frac{1}{3} \times 10 \quad \text{Equation 2}$$

In the equation, C_S is the annual carbon sequestration density of herbaceous plants in $\text{kg}/\text{m}^2 \cdot \text{yr}^{-1}$. C_H is the aboveground carbon storage density of herbaceous plants.

Table 2-1 Carbon storage density and carbon sequestration density of herbaceous vegetation

	Carbon storage density (kg/m^2)	Carbon sequestration density ($\text{kg}/\text{m}^2 \cdot \text{yr}$)
Sunny area	0.28	0.1
Underwood area	0.043	0.018

In the subsequent research process, the spatial distribution of grassland vegetation was obtained by combining remote sensing images. Finally, this study obtained the carbon storage density and carbon sequestration density of herbaceous vegetation in China Green Expo and the spatial distribution.

2.3.2 Radar data

A complete radar point cloud model was obtained during July-August 2021 using the Li-Backpack radar for a full park-wide scan of the China Green Expo. Li-Backpack radar is a LiDAR scanning system developed by Beijing Digital Green Earth for acquiring high precision 3D point cloud data in 3D space.

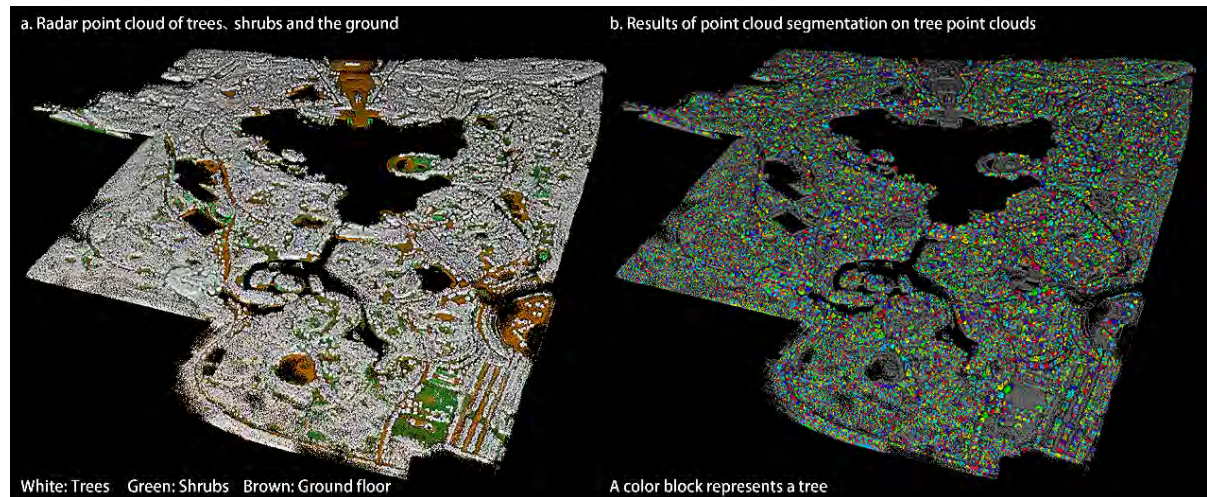


Figure 2-7 LiDAR point cloud data; a. Radar information classification; b. Single wood segmentation

2.3.2.1 Radar point cloud pre-processing

LiDAR360 software was used to perform operations such as pre-processing and post-analysis of the data. LiDAR360 software is a professional processing platform for point cloud data issued by Beijing Digital Green Earth Company, which supports the processing of multi-source radar point cloud data. LIDAR point cloud data pre-processing includes denoising, cropping fragmentation, resampling and ground point filtering.

- 1) Denoising. The denoising process is applied to eliminate invalid radar point clouds created by environmental influences.
- 2) Cropping fragmentation. Crop fragmentation is the removal the invalid point cloud from the file by visual recognition.

- 3) Resampling. This resampling step reduces the point cloud density and facilitates the operation of the processing program.
- 4) Ground point filtering. Filter out the point clouds belonging to the ground.

To eliminate the effect of the study area topography on the LiDAR point cloud data, a global digital elevation model dataset with a resolution of 30m was used for correction. The 30m resolution digital elevation model (DEM) dataset was issued by Hawaker et al. in 2022 ^[116]. This DEM dataset has the highest accuracy than any other existing study, and it reduces the elevation error in the forest area from 5.15m to 2.88m.

With the visual interpretation method, the LiDAR point cloud data were classified into trees, shrubs, ground points and building points.

2.3.2.2 i-Tree eco model

The tree point cloud data were processed in LiDAR360 software for single tree segmentation to obtain tree location information, tree height, DBH, crown width, crown area and crown volume information. This thesis used ArcGIS pro software combined with the distribution information of tree species obtained from field surveys to obtain complete information of tree stand structure.

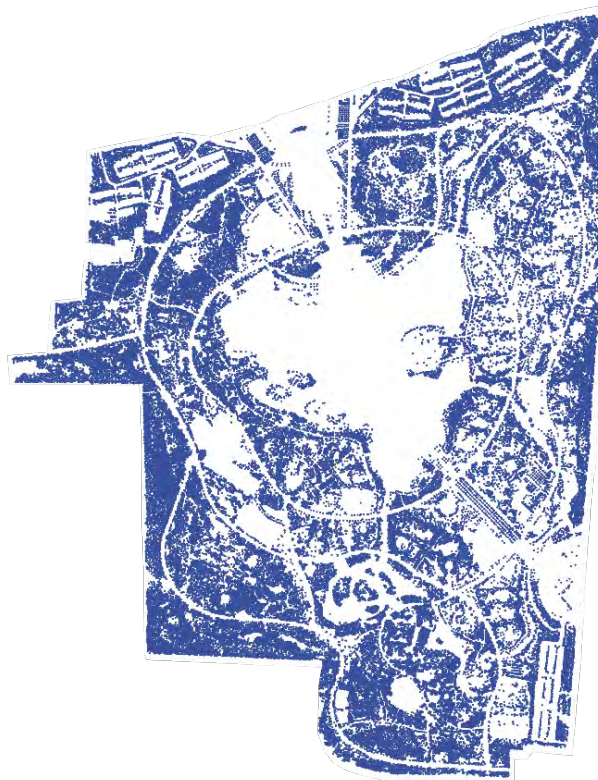


Figure 2-8 Single wood segmentation results

The accuracy of carbon storage calculated based on the anisotropic growth equation is much higher than that estimated based on remote sensing images or radar information ^[124,125], thus this study calculate tree carbon storage and carbon sequestration in the i-Tree eco model. The i-Tree software was released by

the U.S. Forest Service as a software suite primarily for forestry analysis and benefit assessment of urban areas. The i-Tree eco model can provide information on forest stand structure, pollution removal, energy impact, rainfall interception, carbon storage and sequestration in urban areas. The anisotropic growth equations for tree carbon storage and carbon sequestration used in the i-Tree-eco model are as follows:

$$C_t = aD^b \quad \text{Equation 3}$$

In the equation, C_t represents the carbon storage and sequestration of the tree, a and b are two constants, and D is the DBH of the tree.

2.3.2.3 SVF and shrub carbon density

Based on LiDAR point cloud data, the digital surface elevation model (DSM) and shrub vegetation elevation data were extracted in LiDAR360 software. The resolution of both DSM and shrub elevation information is 0.1m. Import the DSM data into the saga-GIS software and processing to get the Sky View Factors (SVF) information [126]. SVF information can be used to represent the spatial scale of the visible sky.

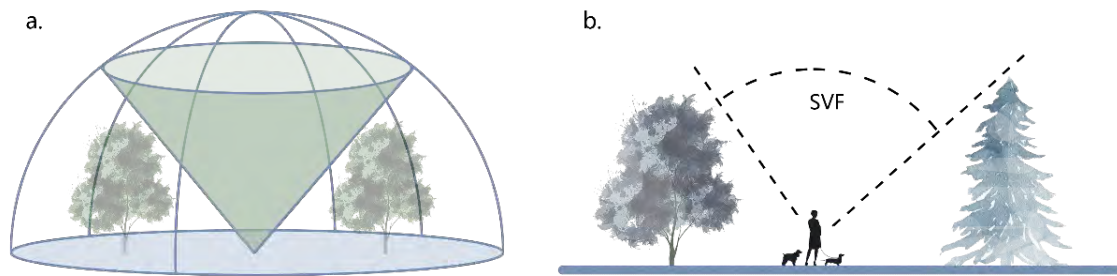


Figure 2-9 SVF diagram; a. SVF in 3D space; b. SVF in the visitor's perspective

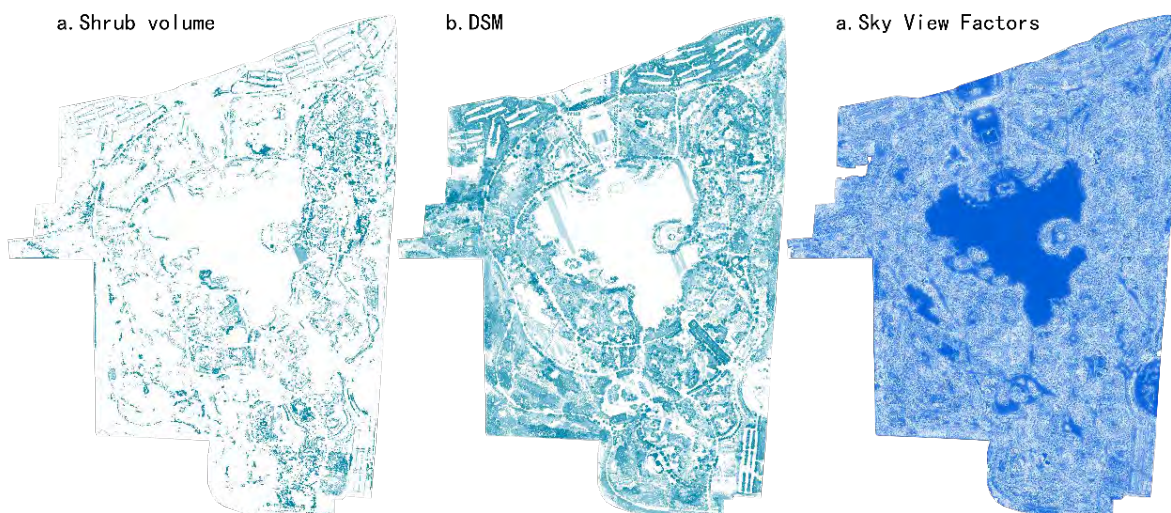


Figure 2-10 Radar extracted information; a. Shrub volume; b. DSM; c. Sky View Factors

In this study, the spatial distribution of shrub volume was obtained by multiplying the shrub elevation information by a resolution dimension of 0.1m. The average carbon storage and carbon sequestration to

volume ratios of shrubs in Zhengzhou were 22 kg/m³ and 2.7 kg/m³·yr. Multiplying the shrub volume data of China Green Expo with shrub carbon density, this study obtained shrub carbon storage and carbon sequestration.

Table 2-2 Carbon density of shrubs in urban parks green spaces in Zhengzhou

	Carbon storage density (kg/m ³)	Carbon sequestration density (kg/m ³ ·yr)
Shrub	22	2.7

The carbon storage and sequestration of shrub vegetation are calculated as follows :

$$C_s = V \cdot E \quad \text{Equation 4}$$

In the equation, C_s is the carbon storage and sequestration of shrub vegetation, V is the volume of shrubs, and E is the carbon storage density and carbon sequestration density of Zhengzhou City obtained from outdoor survey, E in kg/m³ and kg/m³·yr, respectively.

2.3.3 Remote sensing image data

The remote sensing image data used in this study were taken by the Superview-1 commercial remote sensing satellite. The Superview-1 remote sensing satellite was launched on December 28, 2016, the satellite captured images with a panchromatic resolution of 0.5m and a multispectral sensor resolution of 2m; The satellite's sensor has five bands: panchromatic, blue, green, red and near-infrared. The satellite is the first commercial satellite with high agility and multi-mode imaging capability in China.

The images used for the study were acquired on September 8, 2021, on a day when the weather in the study area was good, free of cloud cover and clear of impact. Studies for other cities at the same latitude show that the above-ground net primary productivity of vegetation is greatest between June and September of each year ^[127]. Therefore, this study chose images with cloud-free dates in September.



Figure 2-11 Superview-1 Satellite Remote Sensing Images

Table 2-3 Remote sensing image used in this study

Superview-1	Date	Path & Row
1	2021.09.08	1012200950020001_01
2	2021.09.08	1012200950020001_02

Table 2-4 SuperView-1 satellite band parameter information

Sensors	Band	Band Name	wavelength/nm	Resolution/m
Panchromatic	Band1	Pan	450-890	0.5
	Band2	Red	760-622	2
multispectral	Band3	Green	520-590	2
	Band4	Blue	450-520	2
	Band5	NIR	770-890	2

2.3.3.1 Image pre-processing

To improve image quality and enhance the accuracy of information representation of images, it is necessary to conduct pre-processing operations. The preprocessing operations performed in this study were carried out in the ENVI software. Since ENVI software is still not adapted to the format of SuperView-1 images, this study installed the China Satellites Support plugin in the Envi App Store to process SuperView-1 satellite images (<https://envi.geoscene.cn/appstore/>). The pre-processing steps in this study mainly include atmospheric radiation correction, geometric correction and image cropping.

- 1) Atmospheric radiation correction. Atmospheric radiation correction is to eliminate the electromagnetic radiation in the process of propagation by the atmospheric gas molecules, water vapor, aerosols and other atmospheric components of the absorption and scattering of radiation value changes.
- 2) Geometric correction. The geometric correction is to correct the image distortion caused by various factors such as stability of satellite orbit and imaging attitude, instantaneous field-of-view position and size of the detector, uneven terrain, scan deviation, atmospheric refraction level, and Earth rotation.
- 3) Image cropping. The image is cropped according to the vector boundary of the study area to obtain the image within the study area.

2.3.3.2 Vegetation Index Extraction

Vegetation index is an index information that can reflect vegetation characteristics obtained by calculating different spectral bands of remote sensing satellite detection data. Vegetation index showed significant correlation with biomass. A large number of vegetation index types, such as ratio vegetation index (RVI), difference vegetation index (DVI), and normalized vegetation index (NDVI) have emerged in the current related studies. In previous studies, NDVI is the most frequently used vegetation index because

NDVI has a better correlation with urban vegetation biomass. Meanwhile, some studies have also obtained better results by applying RVI. Therefore, this study extracted NDVI and RVI based on SNAP software.

The equation for NDVI is as follows:

$$NDVI = \frac{(IR_{factor} * near_{IR} - red_{factor} * red)}{(IR_{factor} * near_{IR} + red_{factor} * red)} \quad \text{Equation 5}$$

The equation for RVI is as follows:

$$RVI = \frac{(IR_{factor} * near_{IR} - red_{factor} * red)}{(red_{factor} * red)} \quad \text{Equation 6}$$

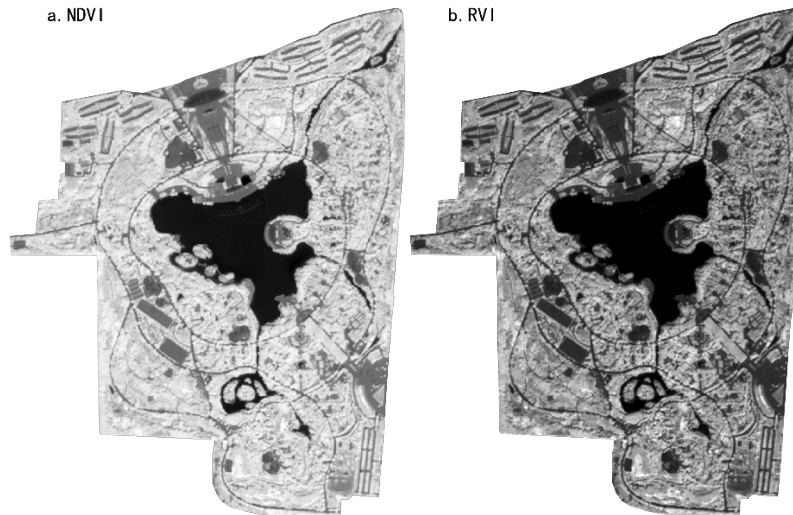


Figure 2-12 Vegetation index; a. NDVI; b. RVI

2.3.3.3 Texture feature extraction

Image texture features can reflect spatial variations in the image, which embody the properties of slow changes or periodic changes in space. In existing studies the image texture features are often extracted by the Gray Level Co-generation Matrix (GLCM) method proposed by Haralick et al. in 1973 [75]. The impact texture features extracted in GLCM include three groups of contrast, orderliness and statistical values; these metrics have been well validated in studies about biomass prediction [128,73]. In this study I applied three metrics from the statistical group: GLCM-mean, GLCM-variance and GLCM-correlation. In this study, I carried out principal component analysis on remote sensing images in Orfeo Toolboxes software to extract the bands that cover the widest range of information. Based on the band information obtained from the principal component analysis, this study calculated the image texture features in the SNAP software. To avoid generating too much redundant data during the GLCM calculation, this study choose 32 degrees of gray volume for the calculation [129].

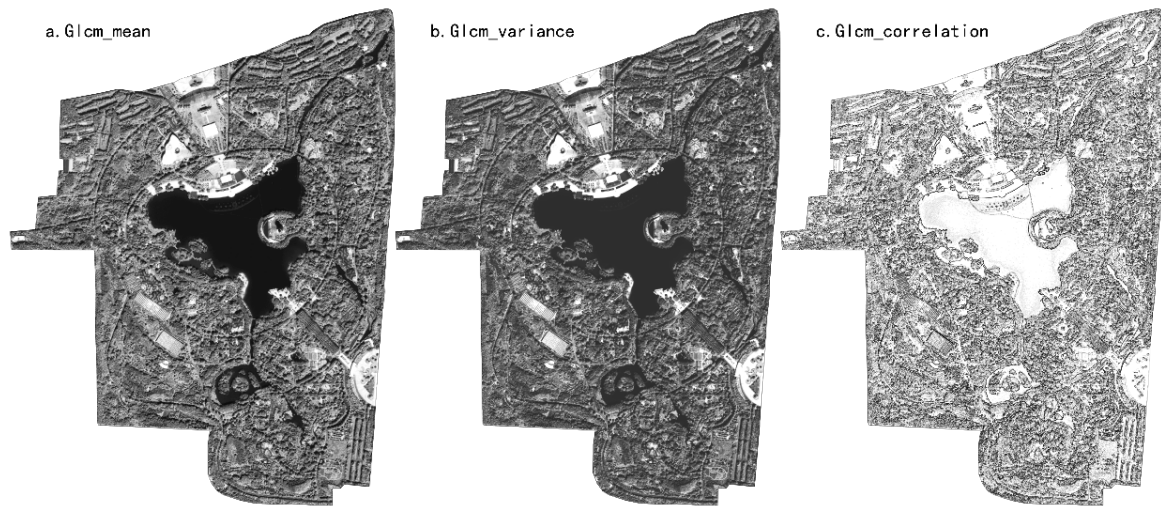


Figure 2-13 Texture features of remote sensing images; a. Glcm_mean; b. Glcm_variance; c. Glcm_correlation

2.3.3.4 Supervised classification and accuracy verification

This thesis followed the method proposed by Myint in 2011 ^[130,131], I fused band information, vegetation indices, texture features and DSM information of remote sensing images to obtain an image map with high heterogeneity. Based on the obtained image maps, this study conducted supervised land use classification by maximum likelihood method in ENVI software and obtained the land use classification results with high accuracy ^[132]. Land use was divided into four categories: High vegetation, Low vegetation, Impervious surfaces, and Water bodies. High vegetation includes trees and tall shrubs; Low vegetation includes herbs and low shrubs; Impervious surfaces include traffic roads and building surfaces; And water bodies include rivers and lakes in the park.

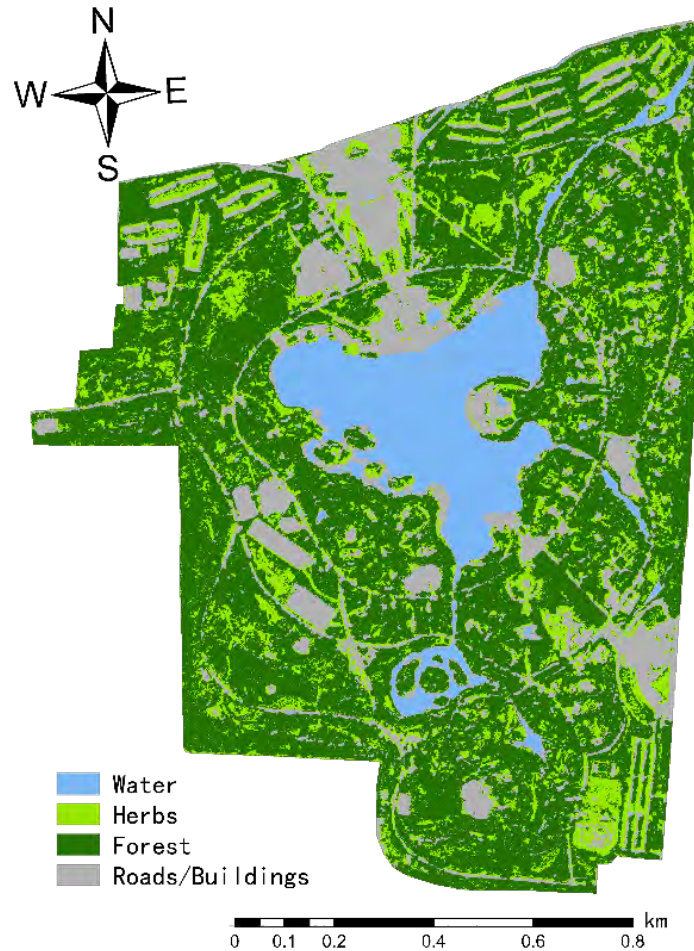


Figure 2-14 The land use information of China Green Expo

The results of the precision validation show that the classification results can satisfy the requirements for the assessment of land use change ^[133]. Combining land use information and herbaceous vegetation carbon density, this study obtained the spatial distribution of herbaceous vegetation carbon storage and carbon sequestration density in the study area.

2.3.4 Biodiversity Information

For this study, the species diversity indices used were the Shannon-Wiener diversity index^[134], the Simpson diversity index^[135] and the Menhinick diversity index^[136]. The Shannon-Wiener diversity index can represent the number of species and the uniformity of individual distribution among species; The higher value of Simpson's diversity index indicates the greater heterogeneity of species distribution; Menhinick's diversity index represents the number of species per unit area in a community. These three species diversity indices are insensitive to changes in sample size and their usability has been validated in many studies ^[136].

The Shannon-Wiener diversity index is calculated by the following formula:

$$H = - \sum_{i=1}^S (P_i \ln P_i) \quad \text{Equation 7}$$

In the equation, S represents the number of species; P_i is the proportion of species in the community.

The Simpson Diversity Index is calculated by the following equation:

$$D = 1 - \sum_{i=1}^S \frac{N_i(N_i-1)}{N(N-1)} \quad \text{Equation 8}$$

In the equation, N_i values the number of the "i" species and N represents the total number of individuals of all species.

The Menhinick Diversity Index is calculated using the following equation:

$$D_{Mn} = \frac{S}{\sqrt{N}} \quad \text{Equation 9}$$

In the equation, S is the number of species and N represents the total number of individuals of all species in the sample.

2.3.5 Data analysis

2.4.5.1 Spatial distribution of site vegetation status and carbon density

This thesis obtained detailed information on forest stand structure based on outdoor survey data and LiDAR point cloud data. Then the site vegetation information was analyzed by Excel and Origin software.

This thesis processed the outdoor survey data, LiDAR point cloud information and remote sensing image information to obtain the carbon storage and sequestration density of trees, shrubs and herbaceous vegetation; Then obtain the spatial distribution of carbon density in China Green Expo by raster calculator in ArcGIS pro software.

2.3.5.2 Growth factors and carbon sequestration capacity of tree species

This thesis was based on the results of tree stand structure and carbon density calculations, and data analysis was completed using SPSS and R language software, and pictures were drawn using Origin.

In the first part of this study, the "DBH-carbon" anisotropy of tree species was first fitted in SPSS. Compared to the anisotropic growth equations obtained from previous studies, the results this study obtained are more applicable to our study area. Next, this study wrote code in R based on the "if" function. The "DBH-age" relationships for each tree species were obtained by entering the anisotropic growth equations for each species obtained in this study. In order to improve the usability of the "DBH-age" relationship, each species was clustered in R based on the distribution of DBH and age of tree species. Cluster analysis by K-means clustering using the "cluster" package in R language^[137]. The clustering results were used to round the "DBH-age" relationship of each species to obtain the growth factors.

In the second part, R language, Excel and Origin software were used for processing and analysis. Clustering of tree species by growth factors, age of rapid growth period and growth rate using K-means method^[137]. Based on the clustering results, This thesis discussed the carbon sequestration capacity, growth

characteristics and landscaping methods of each tree species in landscape architecture.

2.3.5.3 Multiscale analysis of carbon density and influencing factors

ArcGIS pro, Envi, Snap, SPSS, R language and Origin software were used to accomplish the data analysis in this study.

In the first part of the study, this study used the sliding window method in ArcGIS pro for multi-scale sample extraction of carbon storage density, carbon sequestration density and influencing factors. Using circular samples with scales of 10m, 20m, 30m, 40m, 50m, 100m, 200m, 300m, 400m, 500m, 600m, 700m, 800m, 900m and 1000m respectively. In order to avoid duplicate sampling of the same scale for the same area, different numbers of sample squares were set up at different scales in this study. 10,000 samples were taken from 10m to 50m in diameter, respectively; 1000 samples were taken from 100m to 500m in diameter; 100 samples were taken for each of the 500m to 1000m diameter sample squares. Each sample can represent a plant community, so this study performed the scale variation of carbon density and influencing factors as well as multi-scale driving analysis by this method. The location of each sample is randomly generated in ArcGIS pro and evenly distributed in the study area (Figure 2-15). Compared to natural green spaces, urban park green spaces are filled with a large number of water bodies and impervious surfaces, and these areas seriously affect the use of sample methods in urban park green spaces. In order to eliminate the effect of water bodies and impermeable surfaces on the carbon density statistics, the carbon density obtained from this study only considered the areas covered by vegetation.

In the second section this study use multiple statistical methods to analyze and determine the multi-scale driving relationships between carbon storage, carbon sequestration and influencing poppies^[138]. Firstly, this study conducted a correlation analysis using SPSS software to check whether the influencing factors were significantly correlated with carbon storage and carbon sequestration at the level of 0.05. Entering too many influences in a study often results in data redundancy. To eliminate this effect, this study used the R-leaps software package to perform a full subset regression analysis of the influencing factors and carbon density; the aim was to obtain the optimal regression model between the influencing factors and carbon density^[139,140]. The optimal regression models obtained from full subset regression often have the same R^2 for multiple models, which affects the selection of the best model. Thus this study used the Bayesian Index (BIC) to determine the optimal regression model based on the results of R^2 and BIC^[141]. However, this result hardly allows us to understand the covariance component that affects the individual influences. Therefore, this study proceeded to develop structural equation modeling (SEM) and hierarchical partitioning (HP).

Structural equation modeling is a way to analyze the relationship between variables based on the covariance of the variables^[142]; Hierarchical analysis is a multiple regression analysis method that identifies the strongest causal links among multiple co-linear relationships. Therefore, our study used SEM

to analyze the driving effects of stand structure, remote sensing information and spatial information on carbon density, as well as the covariance between the various influencing factors. This operation is based on the Lavaan package in R language ^[143]. Compared with the traditional regression analysis, this study can obtain multiple covariance relationships among the influencing factors ^[144]. Meanwhile, the full subset regression results are analyzed hierarchically based on the Hier package in R language ^[145,146]. Thus, this study can determine the independent effects of each influencing factor in the optimal subset.

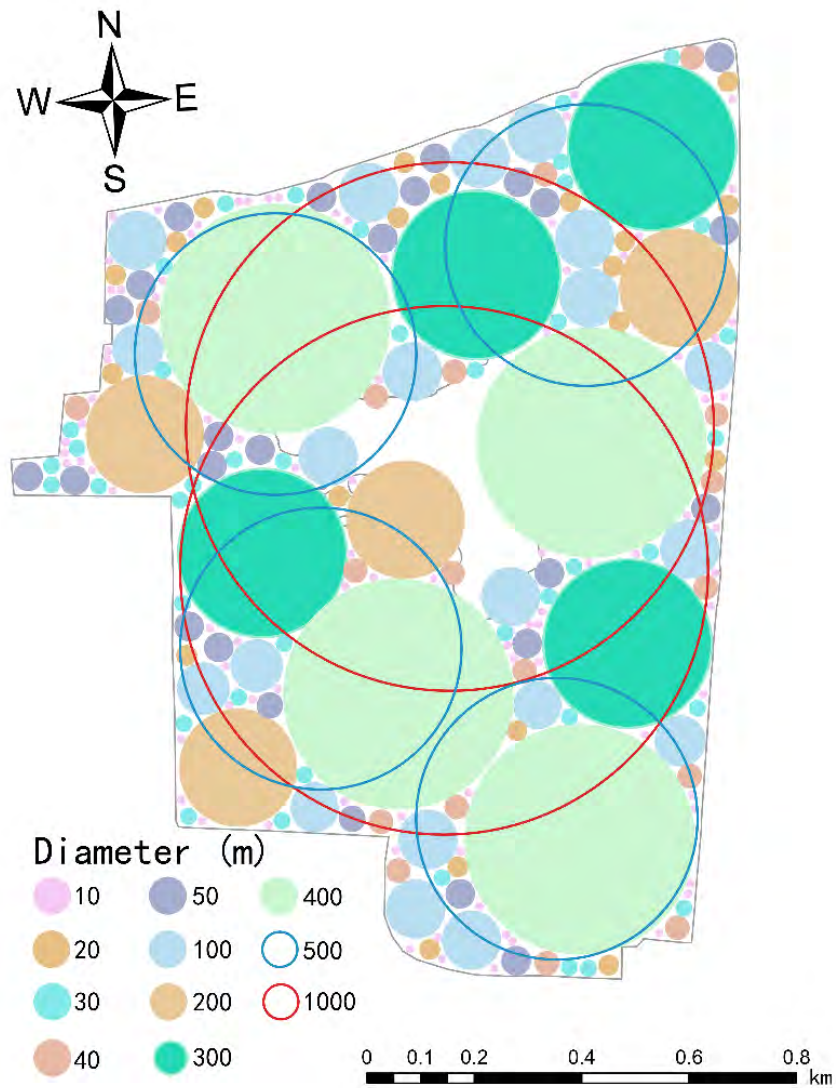


Figure 2-15 Multiple scale sampling method diagram

3 Vegetation Status and Carbon Density Distribution in China Green Expo

3.1 Status of vegetation in China Green Expo

This thesis counted the landscape trees in the China Green Expo. There are 53 species of flowering trees, 26 species of fruiting trees, 29 species of colorful trees, and 5 species of dry trees in the study area (Table 10-1). There are 169 species of trees in the China Green Expo, with a total of 108,241 trees. The largest number of tree species are *Platanus acerifolia* (Aiton) Willdenow, *Ligustrum lucidum* Ait, *Cedrus deodara* (Roxb.), *Salix babylonica*, *Ginkgo biloba*, *Prunus cerasifera* 'Atropurpurea' and *Koelreuteria paniculata*, etc. The total number of these tree species accounts for 48.5% of the total number of trees in the China Green Expo. The average DBH of the trees in the study area was 32.3 cm. The DBH of tree species in the study area was mainly distributed in the range of 10-50 cm, and trees in this DBH range accounted for 72% of the total number of trees. Meanwhile, carbon sequestration by trees in the 10-50 cm DBH range accounted for 59% of the total carbon sequestration by trees in the study area. Trees with a diameter at breast height greater than 50 cm have a small proportion in the park, but their carbon storage accounts for 62.7% of the total carbon storage of trees in the study area. The carbon storage of trees in the range of 70-80cm in DBH accounted for 19.5% of the total carbon storage of the whole park. The total carbon storage and sequestration of trees, shrubs and herbaceous plants was 48.58 Gg and 3.26Gg·yr⁻¹. Among them, trees provide a large amount of carbon storage and sequestration, The carbon storage of trees, shrubs and herbs were 43.17 Gg, 5.31 Gg and 0.1 Gg, respectively; The annual carbon sequestration provided by trees, shrubs and herbaceous plants are 2.57 Gg·yr⁻¹, 0.64 Gg·yr⁻¹ and 0.05 Gg·yr⁻¹. The carbon storage and sequestration of trees far exceeds that of shrubs and herbs. However, it is not difficult to find that the annual carbon sequestration of shrubs and herbs is higher than their carbon storage. Carbon density of deciduous and evergreen plants is very similar. However, the higher number of evergreen trees means that evergreen trees have less carbon density than deciduous plants. There are 40 species of evergreen trees and 129 species of deciduous trees in the China Green Expo. The total number of evergreen trees was 36,780 and the total number of deciduous trees was 71,460. The ratio of evergreen to deciduous trees in China Green Expo is 3:7, which is a reasonable configuration.

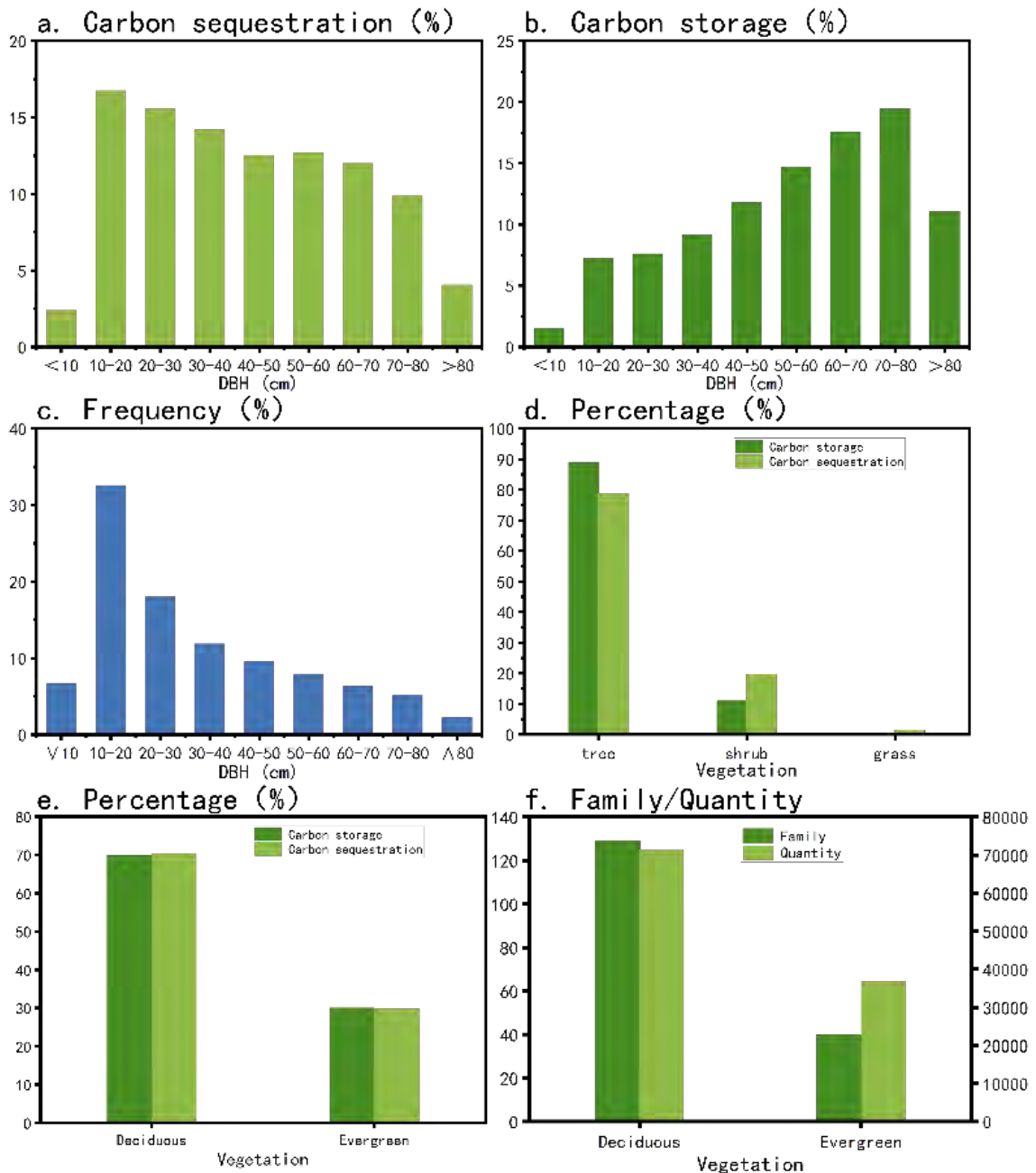


Figure 3-1 Statistical of tree information; a. Carbon sequestration information of trees in different diameter range at breast height; b. Carbon storage information of trees with different DBH; c. Number of trees with different DBH; d. Proportion of carbon storage and sequestration by trees, shrubs and herbaceous preparations; e. Carbon storage and sequestration of deciduous and evergreen trees; f. Number of deciduous and evergreen trees

There are a total of 54 families and 97 genera of trees in the study area. Among them, the carbon storage of single family of trees accounts for more than 5% of the total carbon storage of the whole garden are *Rosaceae*, *Salicaceae*, *Oleaceae*, *Pinaceae*, *Platanaceae* and *Sapindaceae*. The single family of trees sequestering over 5% of the total carbon sequestered in the whole garden are *Salicaceae*, *Oleaceae*, *Platanaceae*, *Pinaceae*, *Rosaceae* and *Sapindaceae*. The families with the highest number of trees are

Oleaceae, Rosaceae, Pinaceae, Platanaceae, Salicaceae, Sapindaceae, Ginkgoaceae and Aceraceae.

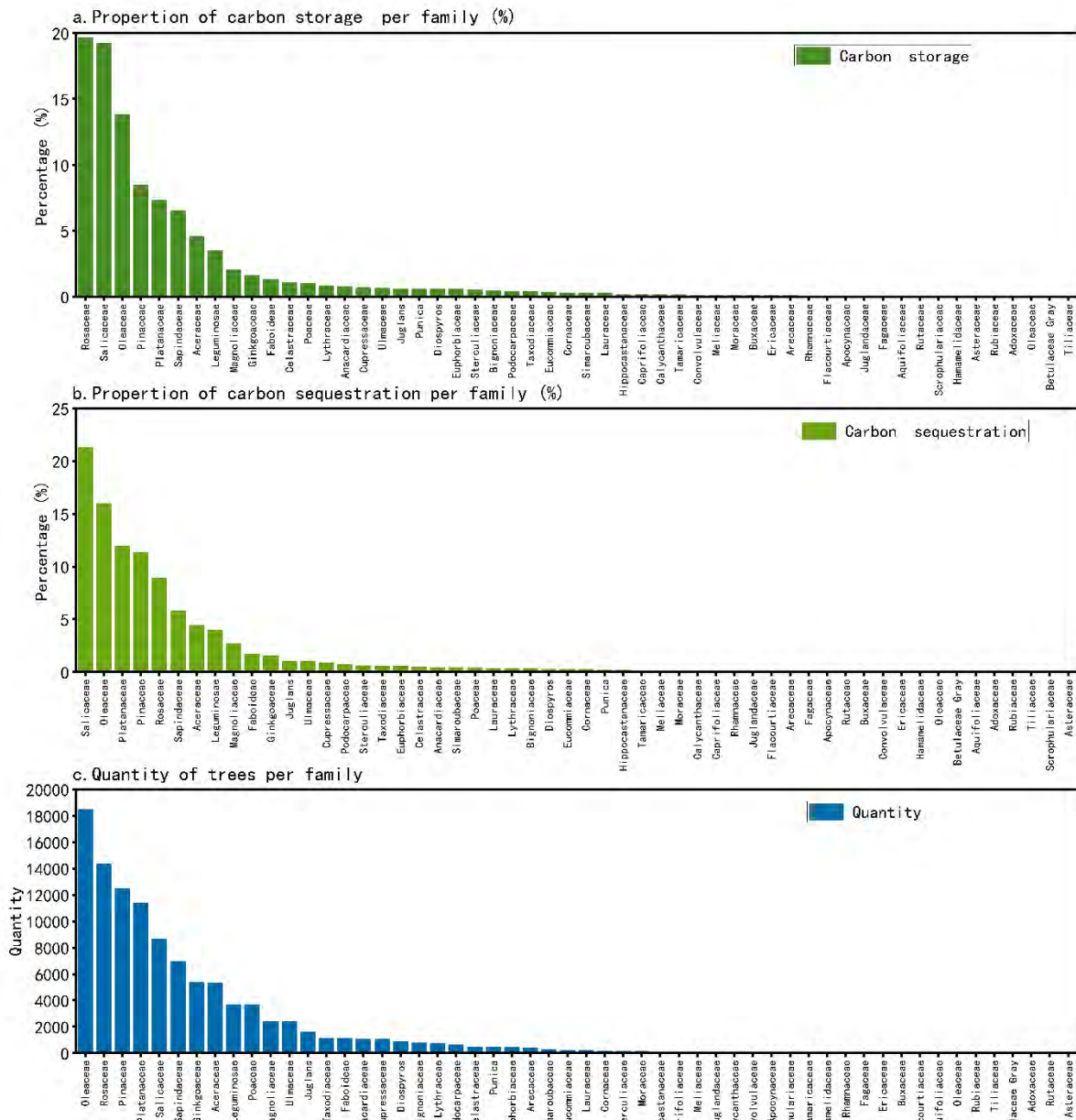


Figure 3-2 Statistics of trees in various families; a. Carbon Storage statistics of trees in each family; b. Carbon Sequestration Statistics of Trees by Family; c. Statistics on the number of trees in each family

The total carbon storage and sequestration of *Salix* are much higher than those of other genera, accounting for about 20% of the total carbon storage and sequestration of the whole garden. The amount of carbon sequestered by the genera *Platanus* and *Cedrus* exceeded 10% of the total amount of carbon sequestered by China Green Expo. The carbon storage and sequestration of the remaining genera of trees are less than 10% of the total amount of China Green Expo.

Platanus acerifolia (Aiton) Willdenow and *Ligustrum lucidum* were the most abundant, with 11,050 and 11,024 trees, respectively. The total number of trees exceeds 4,000, including *Salix babylonica*(5413), *Ginkgo biloba* L(5350), *Prunus cerasifera* 'Atropurpurea'(5286), *Koelreuteria paniculate*(5171) and

Fraxinus chinensis(4618). Tree species with numbers over 1000 include *Photinia serratifolia*, *Celtis sinensis*, *Osmanthus sp*, *Pterocarya stenoptera*, *Bambusoideae*, *Salix matsudana*, *Eriobotrya japonica*, *hyllostachys sulphurea*, *Pinus bungeana*, *Acer buergerianum*, *Yulania denudate*, *Koelreuteria bipinnata*, *Sophora japonica*, *Prunus serrulate* and *Robinia pseudoacacia*. The number of trees of all other species was less than 1000.

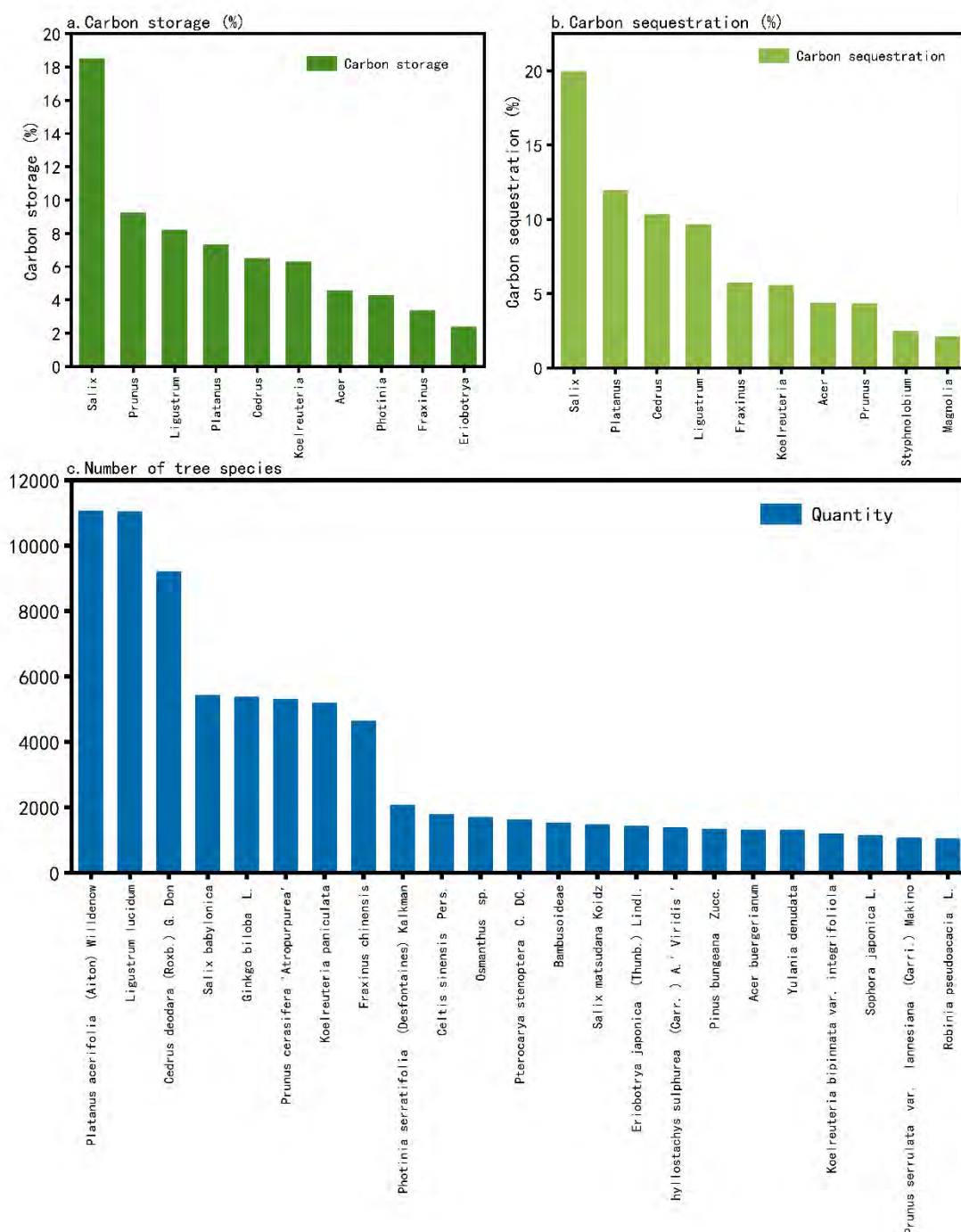


Figure 3-3 Genus and species tree information statistics; a. Carbon storage statistics of tree genera; b. Carbon sequestration statistics for tree genera; c. Number of tree species statistics

3.2 Spatial distribution of vegetation carbon density in China Green Expo

The density of carbon storage and sequestration of trees, shrubs and herbs in China Green Expo showed a heterogeneous spatial distribution. The maximum density of tree carbon storage is 1186kg/m^2 , the maximum density of carbon sequestration is $60\text{kg/m}^2\cdot\text{yr}$. In the eastern area where the landscape effect is well created, the tree carbon density is low and shows a high degree of fragmentation. The maximum shrub carbon storage density is 420kg/m^2 , the maximum shrub carbon sequestration density is $50\text{kg/m}^2\cdot\text{yr}$. The carbon density of shrubs is higher in the east side area where the landscaping is more effective. The carbon density distribution of herbs was significantly influenced by trees and shrubs, showing higher values only in a few areas (0.28kg/m^2 and $0.1\text{kg/m}^2\cdot\text{yr}$).

The spatial distribution of carbon storage and carbon sequestration density in China Green Expo is shown in the Figure 3-4. The maximum values of total carbon storage density and total carbon sequestration density in the China Green Expo were 1175kg/m^2 and $62\text{kg/m}^2\cdot\text{yr}$.

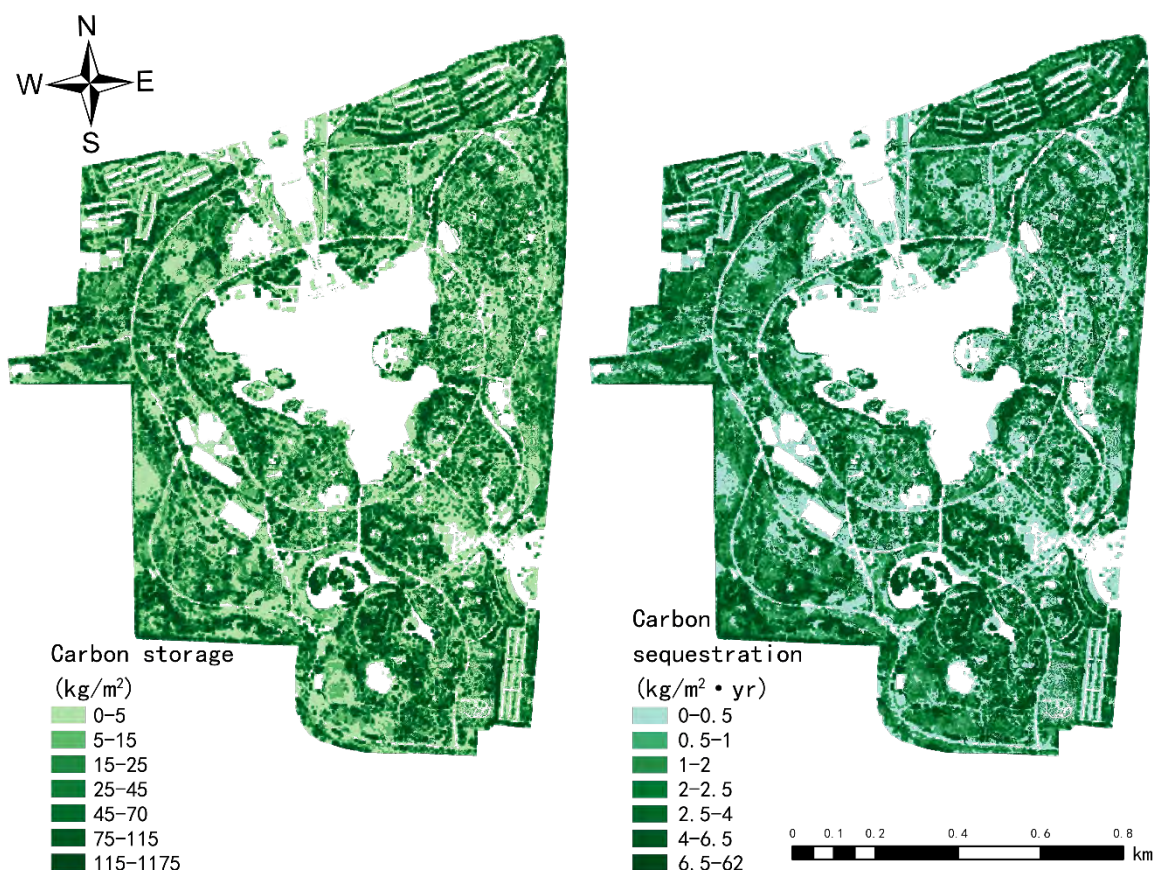


Figure 3-4 Spatial distribution of carbon storage density and carbon sequestration density

4 Growth factors and carbon sequestration capacity of tree species

4.1 Growth factor analysis of 169 tree species

In this study, based on LiDAR data and outdoor survey results, the "DBH-carbon" relationship was fitted on the basis of carbon storage and carbon sequestration. The relationship of "DBH - carbon" for each tree species is consistent with the relationship in the Figure 4-1-a. During the early stages of DBH growth, a large increase in carbon sequestration occurred; Once the DBH increases to a certain value, the amount of carbon sequestration decreases with increasing DBH; When the carbon sequestration decreased to a very small level, it stopped decreasing and showed a small increase with the continued increase in DBH. The R^2 of the fitted relationship of "DBH-carbon sequestration" for all species is shown in Figure 4-1-b. The fit results are normally distributed centered at 0.85, so the fit is positive. The slope of the linear relationship "DBH- carbon sequestration" was normally distributed with a center of 2.1 for all species during the rapid growth period. The mean DBH of each tree species was normally distributed with a center of 0.33m. The first inflection point of the "DBH- carbon sequestration" fitted relationship is shown in the Figure 4-1-e. This thesis input the fit results for each species into R language and obtained the "DBH-age" relationship by compiling the code based on the "if" language.

Finally, this study obtained growth factors for 169 tree species (Table 10-2). The tree species with growth factors greater than 1 include *Trachycarpus fortunei* (1.32), *Catalpa bungei* (1.3), *Ilex chinensis* (1.18) and *Euonymus alatus* (1). Species with larger growth factors have a slower rate of growth of DBH. The tree species with growth factors less than 0.3 include *Paulownia fortunei* (0.12), *Tilia tuan* (0.14), *Fraxinus chinensis* (0.17), *Chaenomeles cathayensis* (0.18), *Bischofia javanica* (0.18), *Ulmus parvifolia* (0.19), *Ulmus pumila* (0.21), *Firmiana simplex* (0.21), *Sambucus australasica* (0.22), and *Acer spp* (0.23). Species with smaller growth factors have a faster growth rate of DBH. Among them, 57% of all tree species had growth factors between 0.4 and 0.6. The values of growth factors of 169 tree species conformed to a normal distribution.

4.2 Carbon sequestration capacity of 169 tree species and application in landscape garden planning

Considering the "DBH of inflection", "DBH-carbon sequestration" relationship and growth factors, This thesis used the "k-means" package in R language to cluster 169 tree species. Before running the k-means clustering analysis, the data used for the clustering analysis were first normalized in SPSS software. And This thesis checked the optimal number of clusters in R language by "nbclust" function and "clusGap" function respectively. The results of the test showed that the optimal number of clusters was 9. The results of the cluster analysis are shown in the Figure 4-1. The clustering results are positive, and the separation between different clusters is abundantly clear. This thesis finally combined the results of cluster analysis and the application of tree species in landscape gardening.

The application of landscape plants in landscape gardening is influenced by many factors. In my study,

I evaluated the clustering of individual tree species in relation to their carbon sequestration capacity, growth characteristics of tree species and landscape plant applications. With the increase of DBH, when the carbon sequestration stops increasing, it means that the growth of this tree will slow down. In this study, I use the "DBH of inflection" to represent the size of the tree species. This thesis used growth factors to represent the growth rate of tree species (yr/cm). Also, I use the coefficient of linear relationship "DBH-carbon sequestration" to represent the carbon sequestration capacity of tree species. With the increase in DBH, some species showed a significant increase in carbon sequestration. Thus, such tree species have a higher carbon sequestration capacity. Combining the above three indicators, I evaluated the suitability of nine species clusters for landscape application.

The tree species in Cluster 4, Cluster 5 and Cluster 6 have larger DBH and are often planted as large trees in landscape planting, requiring larger living space; Can provide space for birds to live and provide good shade. However, the growth rate and carbon sequestration capacity of these trees vary greatly, so they need to be planted in combination with design requirements. Cluster 5, Cluster 6 and Cluster 9 had smaller growth factors and faster growth rates of DBH; These species can form a good plant landscape in a short time in landscape garden applications. Cluster 1, Cluster 2 and Cluster 8 have a higher rate of increase in carbon sequestration thus have a higher capacity of carbon sequestration.

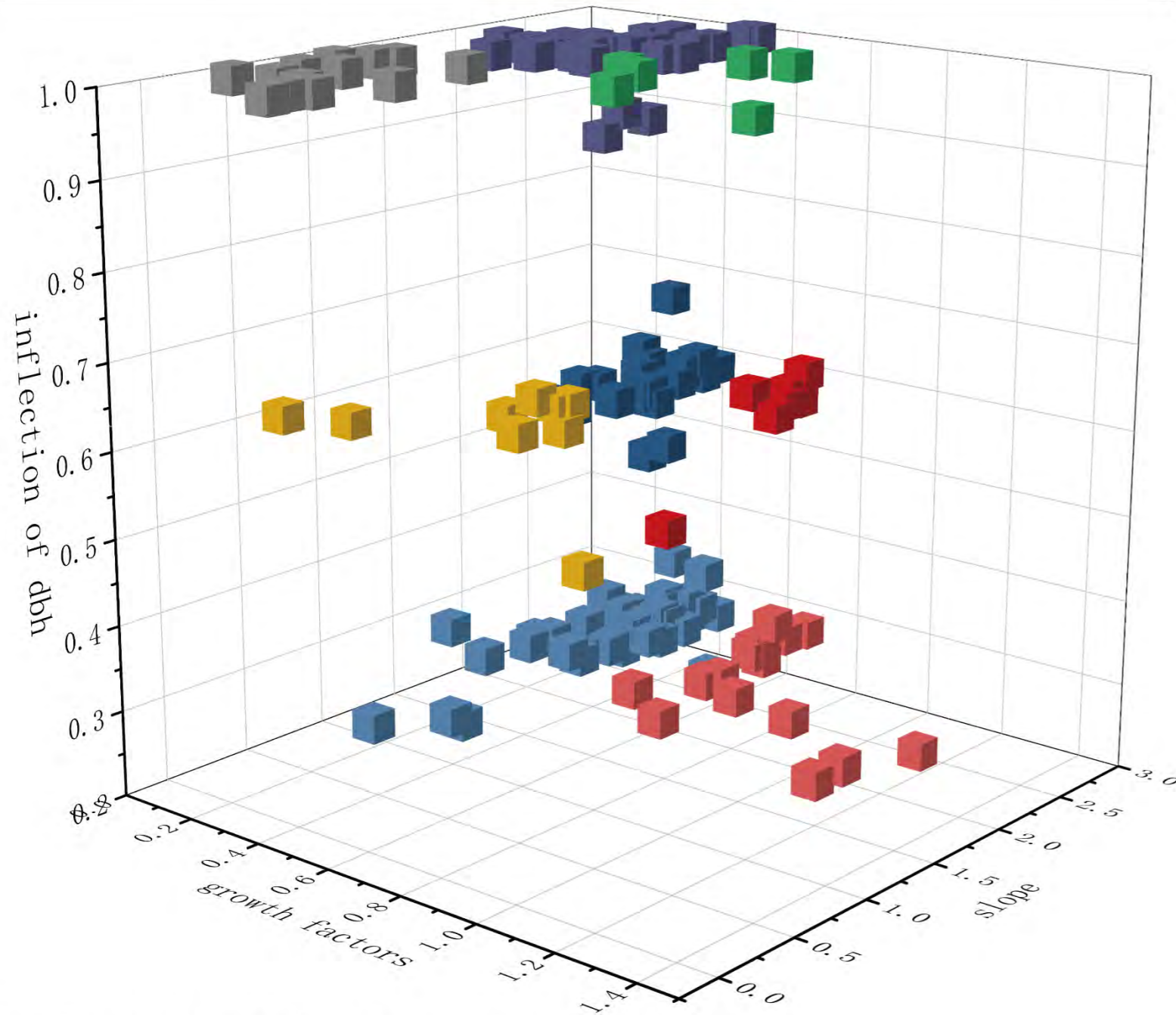
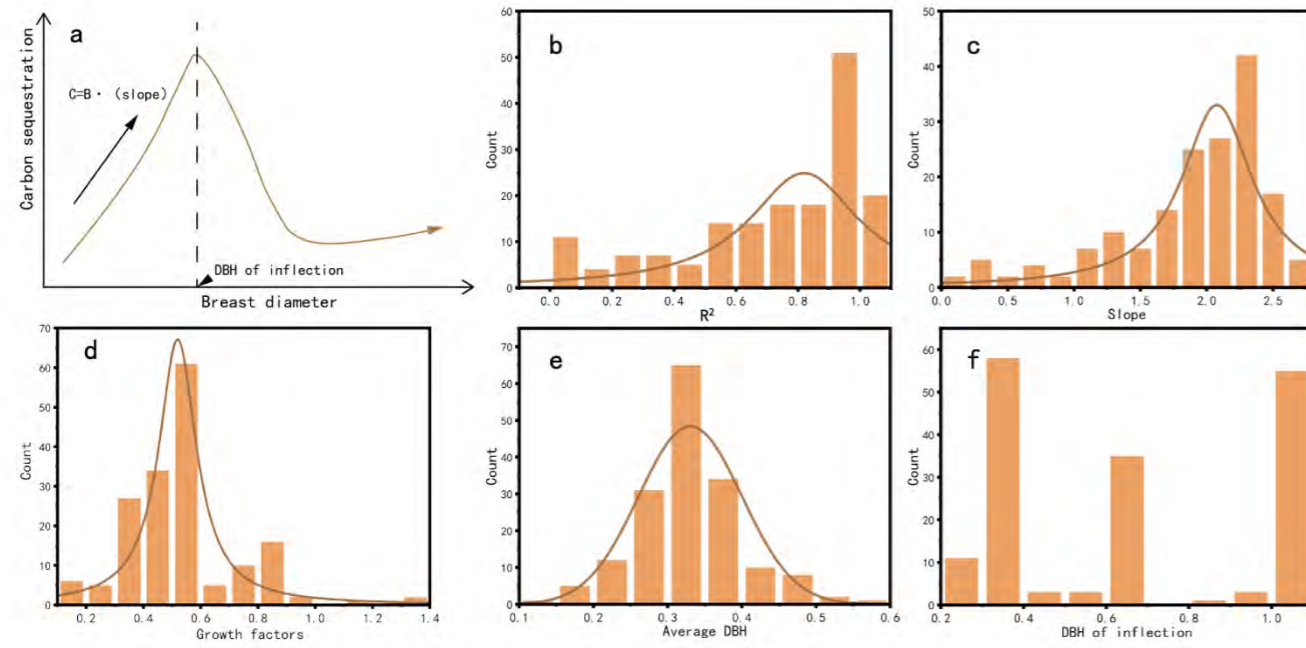


Figure 4-1 Results of cluster analysis of carbon sequestration capacity of 169 tree species

1

- (1) The trunk diameter is of medium size.
- (2) The increase in trunk diameter is slow.
- (3) With an increase in trunk diameter, carbon sequestration increases significantly.

2

- (1) The trunk diameter is of medium size.
- (2) The growth rate of trunk diameter is moderate.
- (3) With an increase in trunk diameter, carbon sequestration increases significantly.

3

- (1) The trunk diameter is of medium size.
- (2) The growth rate of trunk diameter is moderate.
- (3) With an increase in trunk diameter, carbon sequestration increases slightly.

4

- (1) The trunk diameter is on the larger side.
- (2) The growth rate of trunk diameter is relatively fast.
- (3) With an increase in trunk diameter, carbon sequestration increases slightly.

5

- (1) The trunk diameter is on the smaller side.
- (2) The growth rate of trunk diameter is moderate.
- (3) With an increase in trunk diameter, carbon sequestration increases significantly.

6

- (1) The trunk diameter is on the larger side.
- (2) The growth rate of trunk diameter is slow.
- (3) With an increase in trunk diameter, carbon sequestration increases moderately.

7

- (1) The trunk diameter is on the larger side.
- (2) The growth rate of trunk diameter is relatively fast.
- (3) With an increase in trunk diameter, carbon sequestration increases moderately.

8

- (1) The trunk diameter is on the smaller side.
- (2) The growth rate of trunk diameter is slow.
- (3) With an increase in trunk diameter, carbon sequestration increases moderately.

9

- (1) The trunk diameter is on the smaller side.
- (2) The growth rate of trunk diameter is relatively fast.
- (3) With an increase in trunk diameter, carbon sequestration increases slightly.

5 Multiple scale driving force analysis of carbon density

In this study, I analyzed the carbon density and influencing factors under multiple scales separately. Clarified the variability of carbon density and influencing factors caused by the difference of sample scales. Finally, I obtained the driving relationships between the influencing factors and carbon density at different scales, as well as the multiple covariance relationships between the influencing factors.

5.1 Multiscale variation of carbon density and influencing factors

The carbon density of green space, trees, shrubs and herbaceous plants all showed a non-linear decreasing trend with increasing sample scale. The statistical values of carbon storage density and carbon sequestration density showed unstable variations in smaller-scale samples. The standard errors of the statistical values also showed a tendency to decrease with increasing sample size. The statistical value of tree carbon density showed the first lowest value in the sample with a diameter of 600 m; As the sample scale continues to increase, a minimum value occurs when the sample diameter grows to 1000m. The statistical value of shrub carbon density showed a minimum value when the sample diameter increased to 100m. The minimum value of herbaceous carbon density statistics occurred when the sample diameter increased to 300m. The tendency of green space carbon density with sample scale is similar to that of tree carbon density, the first minimum value occurs for trees when the sample diameter grows to 600m; With the continuing increase of the sample scale, the minimum value occurs at the sample diameter of 1000m. The tendency of carbon storage density and carbon sequestration density with sample scale was the same.

When the diameter of the sample is 1000m, the average value of green space carbon storage density is 40.63kg/m^2 and the density of green space carbon sequestration is $2.65\text{kg/m}^2\cdot\text{yr}$.

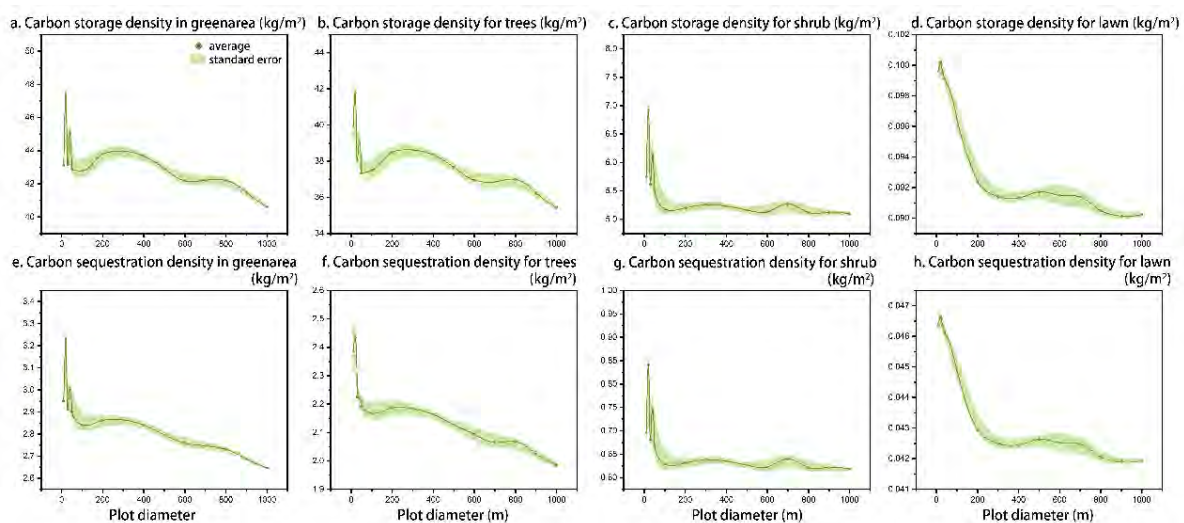


Figure 5-1 Tendency of carbon density statistical values with sample scale; a,e. Green space; b,f Trees; c,g. Shrubs; d,h. Herbaceous vegetation

With the increase of sample scale, the segmentation function can well explain the standard deviation changing tendency of CD. The standard deviation of CD of green space, trees, shrubs and lawns showed

different tendencies on the two sides of the 100m diameter sample square. When the sample diameter was larger than 100m, the effect of increasing the sample scale on the standard deviation of CD decreased. When the sample diameter reached 1000m, the standard deviation of CD was almost zero. The trend of the standard deviation of CSD with sample scale is the same as that of CD.

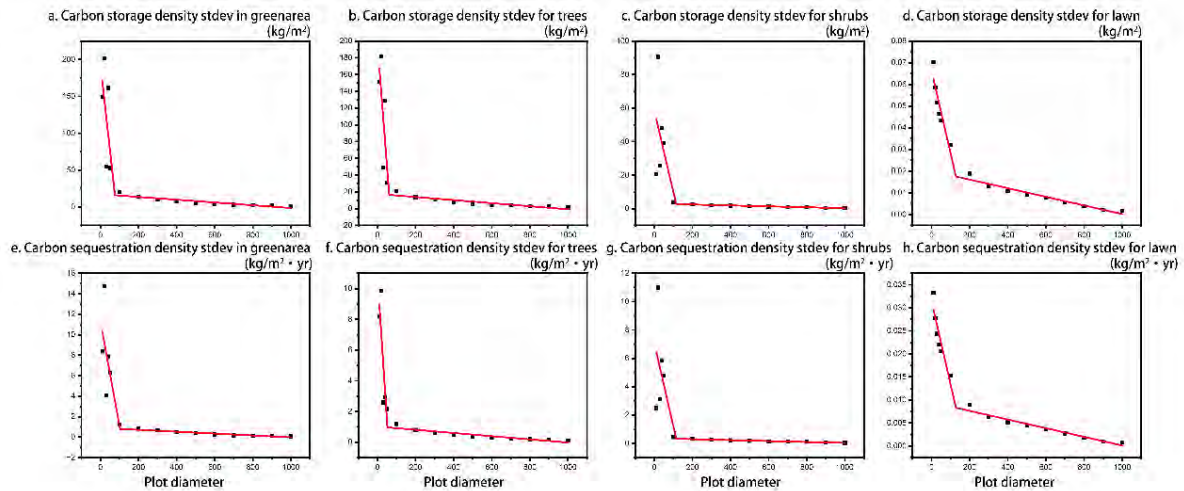


Figure 5-2 Tendency of the carbon density standard deviation with sample scale in urban park green space; a,e. Green space; b,f. Trees; c,g. Shrubs; d,h. Herbaceous vegetation

Except for the tree/green ratio, the mean values of all spatial factors and remote information showed opposite trends on both sides of the 700m diameter sample square. A similar tendency was observed for Sum cut off area per square meter, Sum DBH per square meter and Tree per ha among the forest structure indicators. The change tendency of the tree/green ratio was similar to that of Shannon wiener diversity and Simpson. The mean value was almost zero at the most minor sample scale, which increased and slowed down with the increasing sample scale. However, the mean values of Mean tree height, Mean crown diameter, Mean crown area and Mean crown volume showed opposite changing tendency with increasing sample scale.

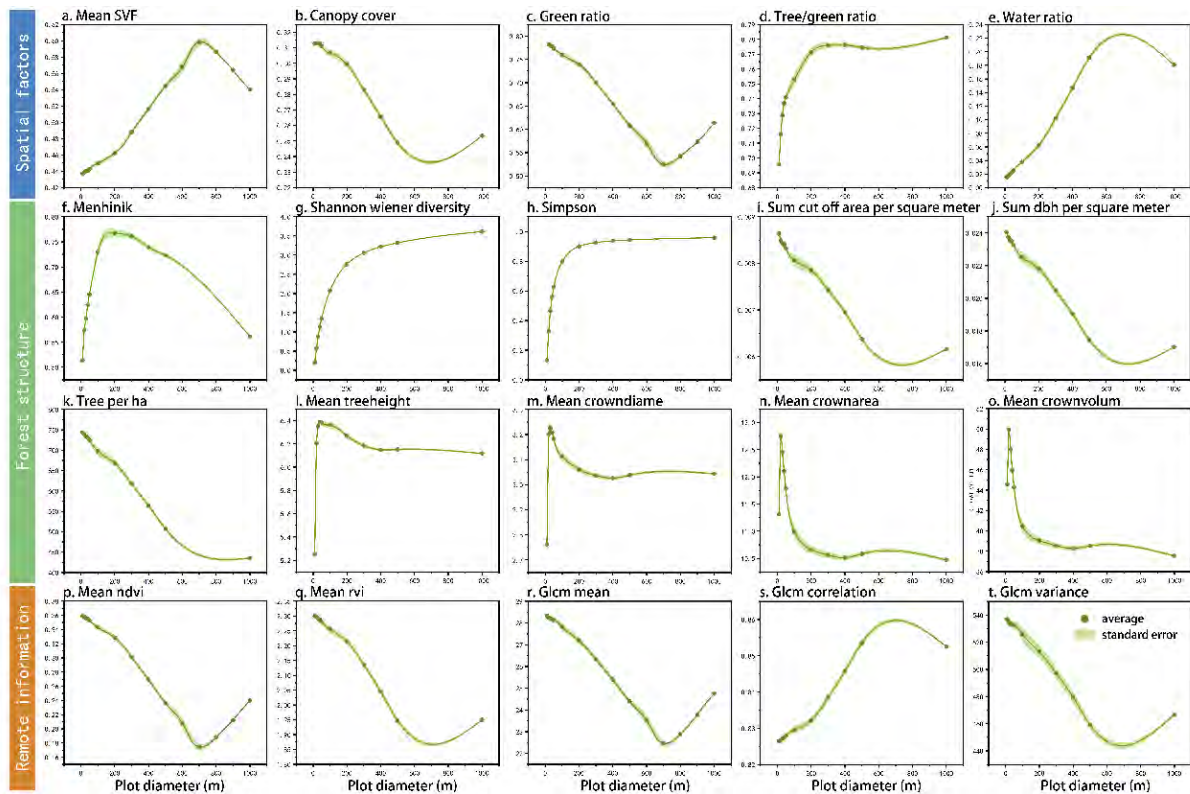


Figure 5-3 Tendency of influencing factors with sample scale

5.2 Correlation analysis of carbon density and influencing factors

The carbon density of urban park green space is closely related to spatial factors, remote sensing information and stand structure information, and the significance of its correlation varies with the scale of the sample. Overall, the degree of correlation between carbon density and influencing factors has a tendency to gradually increase with increasing sample scale.

For the spatial factors (mean vegetation canopy cover, green space percentage, SVF), their correlation with carbon storage density was unstable in the smaller scale samples. In smaller-scale samples, places with lower green space rates and smaller SVF have higher green space carbon storage density. In a sample with a diameter of 1000m, the carbon storage density was higher in the areas with larger vegetation canopy cover, green area ratio and SVF. The “Trees/green ratio” and the water ratio were positively correlated with carbon storage density in all sample scales. Areas with a higher proportion of green space covered by trees and areas with larger water bodies have higher carbon storage density.

For remote sensing information (RVI, NDVI, Glcm_mean, Glcm_correlation, Glcm_variance), the vegetation index showed an unstable correlation relationship with carbon storage density. Both RVI and NDVI showed negative correlations with carbon storage density in smaller scales and positive correlations in larger sample scales. In the small-scale sample, carbon storage was higher in areas with lower vegetation index; In the larger scale sample, carbon storage was higher in areas with larger vegetation index. Meanwhile, the correlation between NDVI and carbon storage density was higher than that of RVI in smaller sample scale; Although NDVI and RVI show missing correlations with carbon storage density at

some scales, This thesis could also find that the correlation between RVI and carbon storage density was higher than NDVI after the sample scale increased to 400m. The texture features have always shown a negative correlation with carbon storage density, and the degree of correlation between texture features and carbon storage density is greater than that of vegetation index.

For the stand structure information, "sum of DBH" and "sum of truncated area" showed a stable and positive relationship with carbon storage density. In samples with diameters less than 1000m, areas with higher tree density have higher carbon storage density; In the sample of 1000m diameter, the area with less tree density has higher carbon storage density. Mean crown diameter, mean crown area, mean crown volume and mean tree height were significantly and negatively correlated with carbon storage density in all scales; In areas with a higher average stand structure index, the carbon storage density is relatively low. Simpson diversity index, Shannon wiener diversity index and Menhinik diversity index showed a significant negative correlation with carbon storage density; Areas with high biodiversity have relatively low carbon storage density.

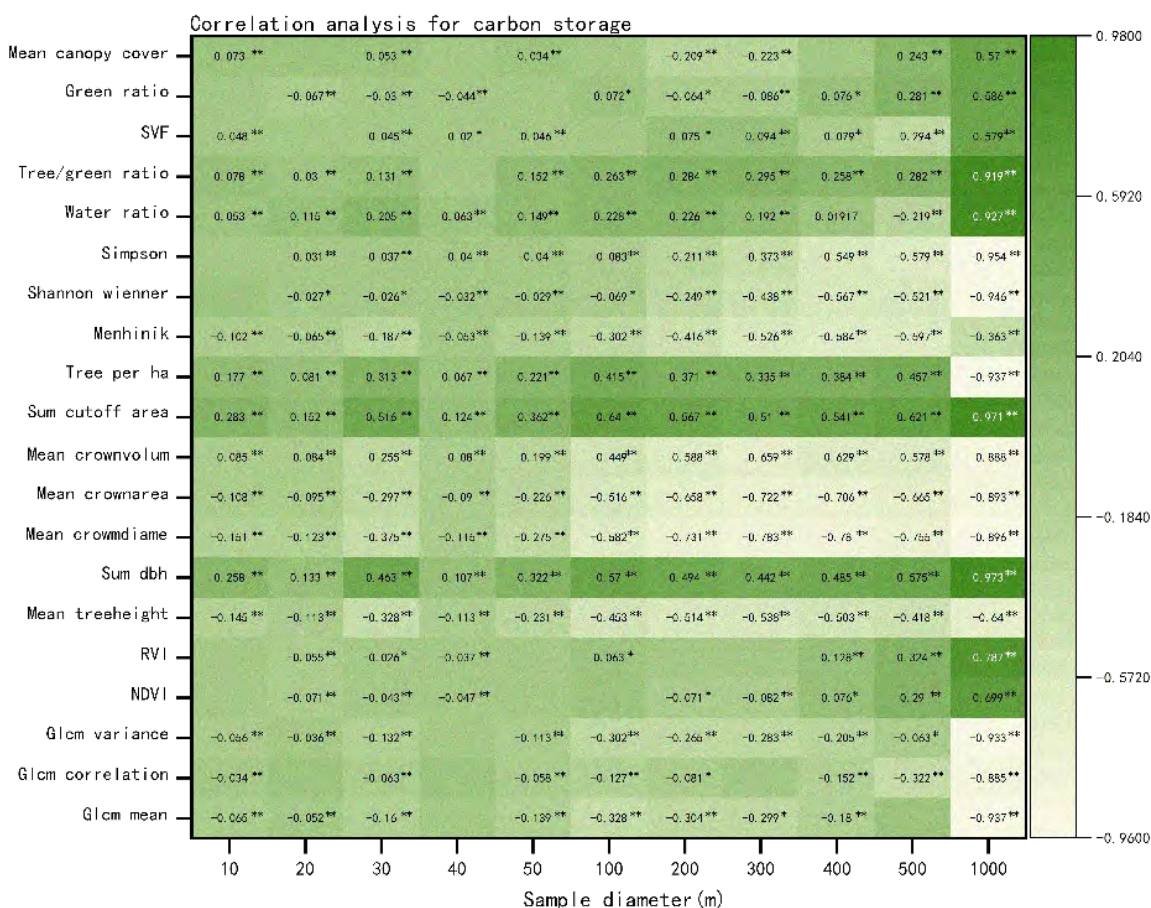


Figure 5-4 Correlation analysis of influencing factors and carbon storage density

The correlation between the density of carbon sequestration and the influencing factors is similar to that of carbon storage density. The correlation between the carbon sequestration density and the influencing factors increased with the increase of sample scale. Spatial factors and remote sensing information were insignificantly correlated with carbon sequestration density in smaller scales. Simpson's diversity index and

Shannon Wiener diversity index were not significantly correlated with carbon sequestration density in 10m diameter sample.

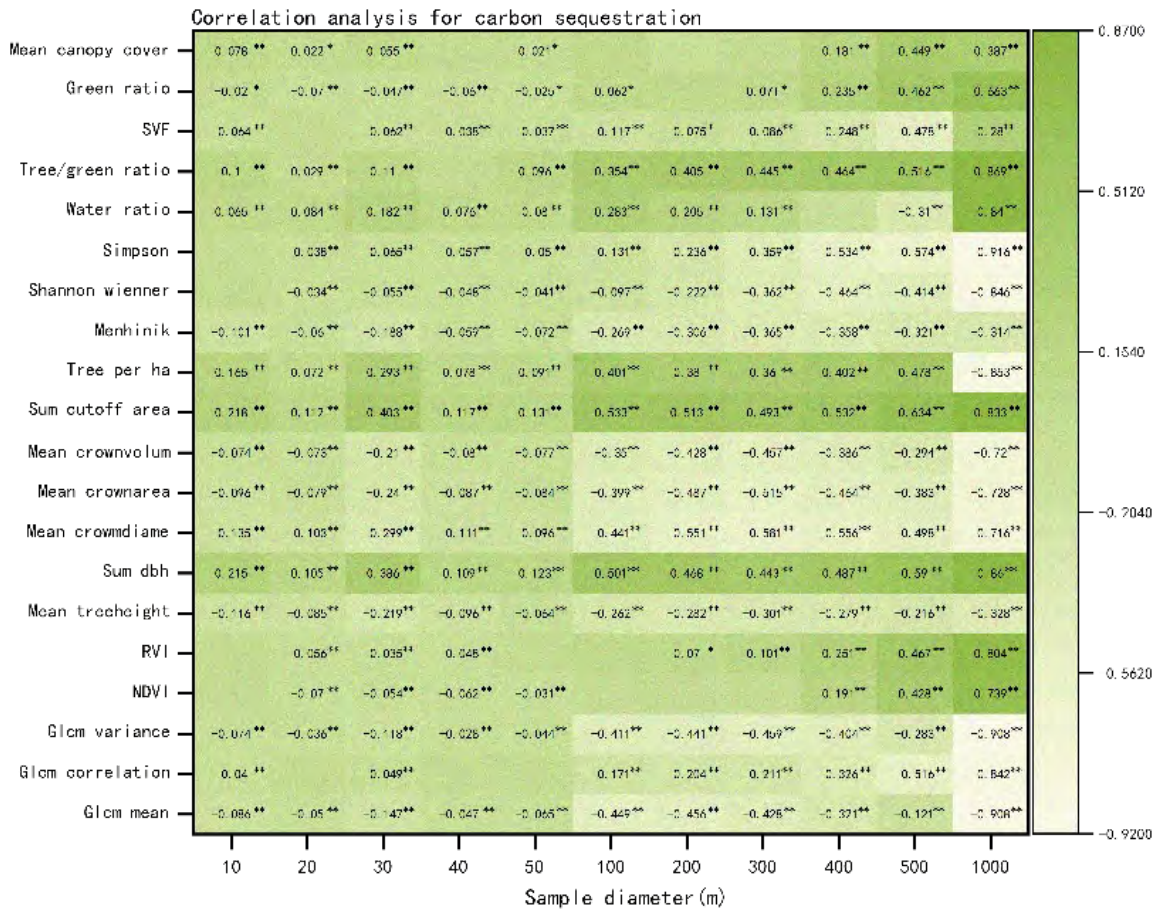


Figure 5-5 Correlation analysis of influencing factors and carbon sequestration density

The explanatory degree of each influence factor on carbon density increased with the increase of sample scale, but the explanatory degree of each influence factor was different. The interpretation of carbon storage density by remote sensing information in small-scale samples was low, only 0.005 in a sample scale of 10m in diameter. The explanation of carbon storage density by spatial factors is higher than that by remote sensing information, but both are smaller in small-scale samples; Only when the sample diameter increased to 100 m, the spatial factor (0.131) and remote sensing information (0.123) explained more than 0.1 for the carbon storage density. Compared with the spatial factors and remote sensing information, the forest stand structure information can explain the carbon storage density better. The interpretation of carbon stock density by spatial factors and remote sensing information was close to 0.9 when the sample diameter increased to 1000m, while the interpretation of carbon storage density by stand structure information was close to 0.99.

The degree of interpretation of remote sensing information, spatial factors and stand structure information on the density of carbon sequestration was similar to that of carbon storage density.

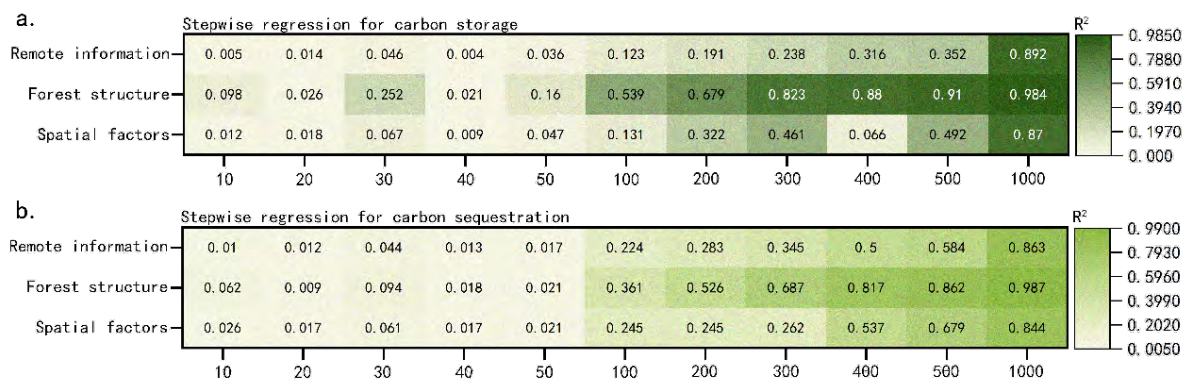


Figure 5-6 Stepwise regression analysis; a. Stepwise regression analysis of carbon storage density; b. Stepwise regression analysis of carbon sequestration density

5.3 Analysis of the multi-driver relationship between carbon density and influencing factors

According to the results obtained from the Figure 5-2, it can be found that the carbon density standard deviation has stabilized when the sample diameter increases to 100m. Therefore, I choose the statistics with sample diameter of 100m and 1000m respectively for full subset regression analysis. With the results of the full subset regression analysis, I combine R2, BIC index and the number of elements in the subset to determine the optimal subset.

Spatial factors, stand structure information and remote sensing information showed large differences in the explanation of carbon density in different size sample scales. Therefore, I further used structural equation modeling and hierarchical analysis to find out the driving effects of the three types of influences on carbon density and the autocorrelation effects among the three types of influences.

The influencing factors this study selected explained more than 99% of the variation in CD and CSD in a sample of 1000m diameter (Figure 5-7). At the same time, there was a high covariance between forest structure, remote information and spatial factors, which implies that the SEM model has information redundancy at a sample diameter of 1000 m. The water ratio was the most explanatory influence factor for the spatial factors. The best driver of CD in forest structure was Simpson; however, the best driver of CSD was Sum DBH. In remote information, the influence of the texture feature index on CD and CSD was much greater than that of the vegetation index. Meanwhile, the driving power of RVI on CD was higher than that of NDVI.

In contrast, the explanation of CD and CSD by influencing factors in a 100 m diameter sample was only 64% and 54%, respectively. Meanwhile, the covariance between forest structure, remote information and spatial factors was small or even absent. The most influential spatial factor on CD was Tree/green ratio. The forest structure's most significant drivers of CD and CSD were Sun cutoff area and Sum DBH, respectively. Stepwise regression results for all scales show that: the effects of various influences on CD and CSD become more significant as the sample scale increases (Figure 5-7).

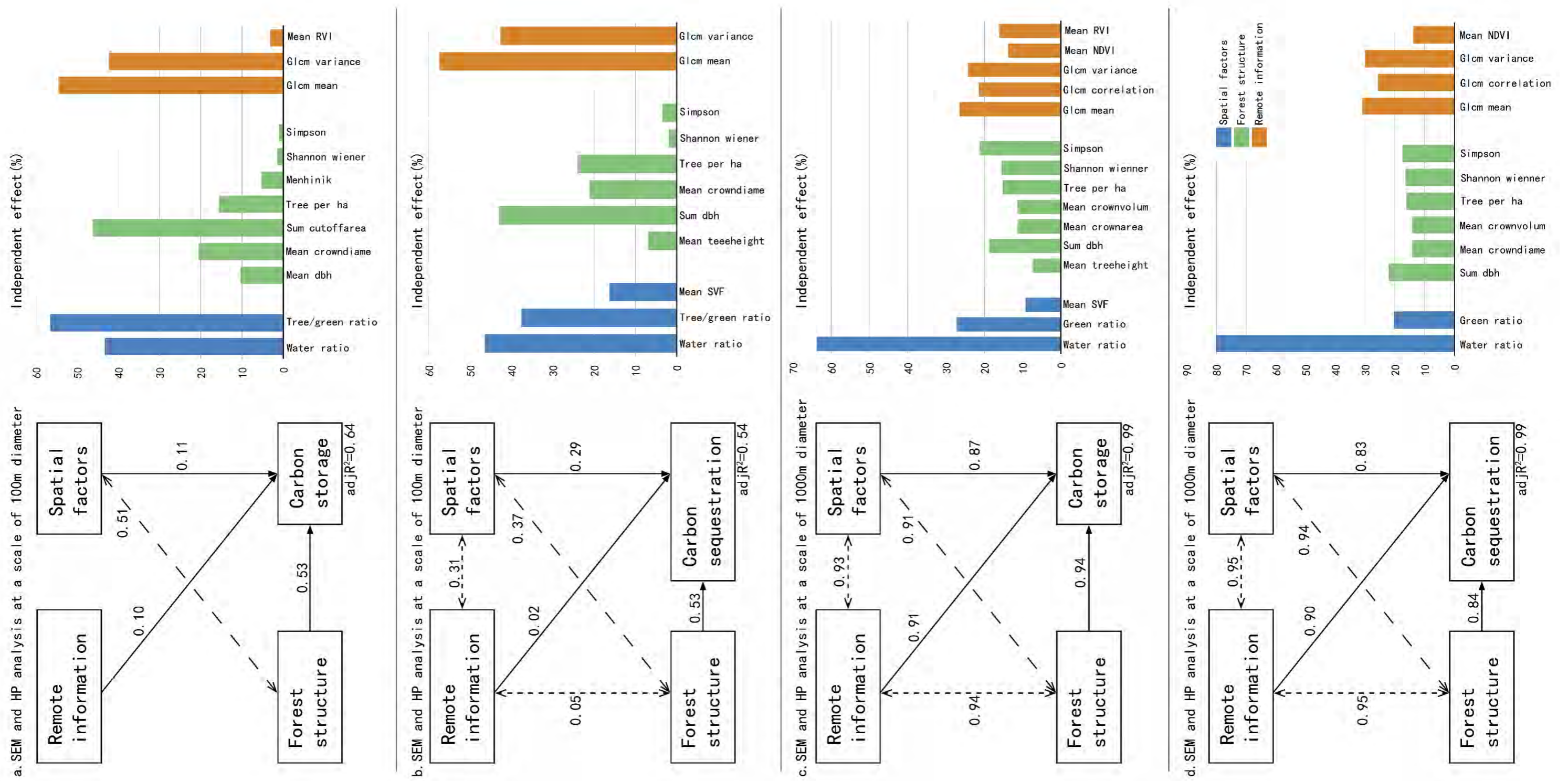


Figure 5-7 SEM model and HP analysis; a. carbon storage density-100m; b. carbon sequestration density-100m; c. carbon storage density-1000m; d. carbon sequestration density-1000m

6 Discussion

6.1 Comparison with related researches

The carbon storage density of China Green Expo is 30.72 kg/m², which is much higher than the carbon density of urban vegetation (1.9-3.5 kg/m²) estimated in previous studies for Zhengzhou city [147,148]. It is possible that this phenomenon can be attributed to the expanding urban area of Zhengzhou, which has led to the gradual dominance of impervious surfaces over green spaces, resulting in a decrease in the carbon storage of parks [149]. Meanwhile, a study on the distribution of carbon density in China shows that the average forest carbon density in China is 3.6 to 3.89kg/m², and the carbon density of China Green Expo obtained in this study is significantly higher than this value [150]. This phenomenon may be caused by the difference between natural and planted forests. The vegetation in the China Green Expo is better cared for than in planted forests. The vegetation in the China Green Expo is better cared for than in planted forests [53]. The carbon density of green spaces is disturbed by multiple factors such as structural complexity, biodiversity, human disturbance, environmental conditions, and vegetation types [82,65,57,56]. Previous studies have demonstrated a positive correlation between forest structural complexity and biodiversity [151,63], where areas with complex structures tend to maintain higher biodiversity [152]. Although the results of our study showed that the effect of biodiversity on the carbon density of urban park green spaces was small. However, the results of previous studies show that higher biodiversity promotes resource complementation in the community and therefore has higher biomass; A study quantified the effects of forest structure and biodiversity on carbon storage and sequestration, which could reach 64% of the explanatory degree [152]. There are two possible reasons for the difference between our findings and previous studies: First, the forest age and species richness are significantly correlated, and the effects of both on carbon density may appear to be confounded. Thus the effect of species richness on carbon density may be caused by the age of the forest, and the effect of both on ecosystem services occurs interactively [153,154]. Another reason may be caused by the difference between natural and planted forests. There are often complex interspecific relationships between species in natural forests, such as parasitic, epiphytic, symbiotic, and physiological relationships; While, since only mechanical relationships between vegetation and landscape effects are considered in urban green space planning, the influence of species diversity on carbon density in urban green spaces is smaller. The effect of climatic variables on ecosystem function is close to that of forest structure, as temperature and precipitation can influence the primary productivity of vegetation [155,156]. The China Green Expo has a complex three-dimensional vegetation structure, as well as good conservation management. In contrast, natural forests are influenced by the environment and thus have much lower carbon density than the China Green Expo. Although the growth of understory vegetation is restricted in planted forests compared to natural forests [157,158], the impact on shrubs is covered by the fact that the carbon storage of trees is much higher than that of shrubs in well-managed parks (Figure 3-1).

Compared with the results of our research, the carbon density in Beijing is 6.7kg/m^2 [149], significantly higher than the carbon storage density of Zhengzhou. This variation may be attributed to the different geographical locations. The northern region of China accounts for 12.5% of the country's forest biomass, while the eastern region accounts for 10.8% [150]. It is also attributed to some carbon enhancement policies adopted by Beijing, such as the “Million Acres Trees Campaign” and the “Country Parks Circle Projects” [159]. However, the CD of Zhengzhou is much higher than that of Xi'an (2kg/m^2) at the same latitude [148]. The difference in composition of dominant tree species may be one of the reasons [160]. Urban tree species are divided into keystone species, backbone species and general species. The keystone species are fewer in species but larger in number, forming the character of the city and playing a unifying role in the landscape and color; While the general tree species have more species, less number, colorful and play a role of change in the landscape. Acacias, poplars, sycamores, and pines are the main tree species in Xi'an [161], While the dominant tree species in China Green Expo are *Platanus acerifolia*(10.2%), *Ligustrum lucidum*(10.2%), *Cedrus deodara*(8.5%), *Salix babylonica*(5%) etc (Figure 3-3). Another reason for the low carbon storage density of urban green spaces in Xi'an may be caused by the low carbon emissions: Xi'an's carbon emissions are about half of Zhengzhou's carbon emissions in 2022 [162]. Low carbon emissions may lead to less vegetation carbon sequestration [162]. Compared to the results of studies in other countries, the CD in Florida, USA is 10.7kg/m^2 and 14.2kg/m^2 in Michigan [163,164]. It is about one-third and half of the CD of the China Green Expo but significantly higher than the CD of Zhengzhou. This indicates that there is great potential to improve the carbon sink capacity of parks in Zhengzhou (Table 6-1). China Green Expo provides an excellent case for vegetation carbon sink research. Therefore, in order to promote carbon sinks and achieve carbon neutrality goals as soon as possible, a detailed analysis of the drivers of urban greenarea carbon density is essential.

Table 6-1 Carbon Storage Density Information Statistics in different regions

Regions	Carbon storage density kg/m^2	Data source
China Expo Park	30.72	This thesis
Zhengzhou, China	1.9-3.5	[147,148]
Peking, China	6.7	[149]
Xian, China	2	[148]
China	3.6-3.89	[150]
Florida, USA	10.7	[163]
Michigan, USA	14.2	[164]

Compared to homogeneous natural forests, parks tend to have an uneven distribution of carbon density. his study uses i-Tree eco software to calculate carbon storages by anisotropic growth equations, which helps to illustrate the spatial variation of CD. Numerous studies have extracted carbon density by remote sensing images and LiDAR techniques. Because of the saturation of wavelength information in remotely sensed images at high biomass and the significant effect of the sensor resolution size on the estimation results [165,166], and thus, it is difficult to obtain high-precision park CD information from remote sensing images

[167,72]. Also, the information extracted directly from LiDAR data does not reflect well the information of biomass and carbon storage in the site. An analysis in Wisconsin, USA, found that biomass extracted directly from LiDAR data had an error of up to 35 % [168]. But, LiDAR-derived metrics such as canopy height, diameter at breast height, and canopy cover are widely used in many studies [84,82]. In comparison to field surveys, LiDAR has a huge advantage in measuring vegetation structure information. Compared with previous studies, the CD and CSD calculation method used in this study is more accurate with an innovative approach. Estes et al. found little overlap in the ecological literature between studies analyzing field survey information and those analyzing remote sensing image data [169]. However, linking field survey data and remotely sensed data is particularly important for translating ecological processes to regional and global scales [170]. Thus, this thesis highlighted the scale differences in CD, CSD and various data. Our findings demonstrate the importance of scale in ecological processes that affect CD and CSD.

6.2 Growth factors and tree planning application

There are four methods commonly used to calculate the age of trees: The first method is to extract the trunk tissue from the trunk at breast height section and measure the age of the tree according to the annual rings, this method is harmful to the trees; The second is the CT scan method, this method has some damage to the tree and the equipment is very expensive; The third is the C₁₄ determination method, which also requires taking the tissue of the tree's diameter at breast height section and has an error of more than 20 years; The last one is the "growth factor" which is less used nowadays, this method estimates the tree age from the measured diameter at breast height information. Currently, there are few studies on tree growth factors in China; while in other countries, only a few tree species have been studied. There are two reasons for the low number of studies in this area: Firstly, the growth of trees is affected by the environment and there will be large inter-individual differences, so the age of trees calculated from the growth factors will have some errors; Secondly, in different regions and in different climatic contexts, each species has specific growth factors and the obtained research results are difficult to be applied in other regions. In this study, this study extracted a large amount of tree information from the study site and obtained accurate tree growth factors based on the site conditions. The formula for calculating tree age from DBH and growth factor is as follows:

$$Y = D \times G \quad \text{Equation 10}$$

Where Y is the age of the target tree in yr, D is the diameter at breast height of the tree in cm, and G is the growth factor of the tree obtained in this study in yr/cm.

The results of our study showed some differences compared to those obtained in other countries and regions, and the differences in the study results are shown in Table 6-2. This thesis consider that there are two reasons for the difference: The first is the difference in climatic background, which leads to different growth rates of the same species in different regions; Secondly, the results of this study were calculated

based on the growth rate of tree species during the rapid growth period (Figure 4-1), while the results obtained from other related studies were based on the entire life cycle of tree growth. The growth rate of tree vegetation decreases rapidly at the end of the rapid growth period of trees, and there are two explanations for this phenomenon: First, the reduced growth rate at the end of the rapid growth period may be caused by vegetation cell senescence; The second theory suggests that this phenomenon is caused by the respiratory burden and hydraulic limitation of vegetation ^[171]. China's urbanization only reached 35% in 2000, and will reach 73% in 2050. Therefore, most of the trees in urban green spaces were planted within the last 20 years and did not have enough time to go through the full tree growth cycle. As shown in the Table 6-2, the age of most tree species obtained in this study for rapid growth cessation was over 25 years. Therefore, compared with the growth factors calculated based on the whole tree growth cycle, the growth factors obtained in this study based on the growth conditions of tree species during the rapid growth period are more suitable for application in urban green spaces.

Table 6-2 The "growth factor" in different regions

Growth factors	Thesis results (yr/cm)	Other regions (yr/inches)	Rapid growth period (yr)	Source
<i>Gleditsia sinensis</i>	0.52	3	16	[172]
<i>Acer palmatum</i>	0.81	4.5	25	[173]
<i>Cornus officinalis</i>	0.51	7	16	[174]
<i>Cercis canadensis</i>	0.57	7	35	[174]
<i>Fraxinus chinensis</i>	0.42	6	38	[175]
<i>Betula platyphylla</i>	0.44	5	44	[176]
<i>Juglans regia</i>	0.44	4.5	44	[177]
<i>Populus tomentosa</i>	0.45	2	45	[176]
<i>Ficus religiosa</i>	0.3	3	30	[176]

The concept of landscape gardening is not only limited to a park or a scenic spot, many countries have been focusing on the planning of plant landscapes since the spatial planning of the country. Considering the preservation of natural vegetation, a large number of green areas have been purposefully planned and planted. Because of China's "carbon neutrality" goal, urban green space carbon sequestration strategies have received more and more attention. Combined with the results of our study (Figure 6-1), this study can refer to the trees in Table 10-3-Cluster 2 and Cluster 5 when selecting the urban keystone tree species. The tree species in both clusters are characterized by larger DBH, rapid growth and higher carbon sequestration capacity, such as *Sophora japonica*, *Firmiana platanifolia*, *Pterocarya stenoptera*, *Liriodendron chinense*, *Populus canadensis*, *Cedrus deodara*, *Triadica sebifera* etc. For the selection of general urban tree species, if planners want to enhance the carbon sequestration capacity of green areas, they can refer to the tree species in Table 10-3-Cluster 1 and Cluster 8, such as *Euonymus maackii*, *Koeleruteria paniculate*, *Celtis julianae*, *Lonicera japonica*, *Diospyros kaki*, *Prunus subg*, *Pseudocycdonia sinensis* etc.; If planners want to enhance the landscape effect of the green space, they can refer to the tree species characteristics in Table 10-1 for species selection.

The garden paths in urban parks occupy a considerable proportion of the green space. Thus, the plant configuration on both sides of the garden road will directly affect the landscape of the urban park green space. Therefore, this study can select the tree species that become landscape faster on both sides of the garden path, referring to Table 10-3- Cluster 5, Cluster 6, Cluster 9 (Figure 6-1). For example, *Koelreuteria bipinnata*, *Styphnolobium japonicum*, *Pterocarya stenoptera*, *Platanus acerifolia*, *Firmiana simplex*, *Ulmus pumila* etc. Both sides of the main road often use regular arrangement; it is better to dominate by flowering trees to enrich the color of the garden. Species selection can be accomplished by referring to the Table 10-1 of flowering plants, Such as *Ilex chinensis*, *Lonicera japonica*, *Gardenia jasminoides*, *Amygdalus triloba*, *Albizia julibrissin*, *Amygdalus persica*, *Chimonanthus praecox*. Secondary roads are the main roads within each region of the park, generally with a width of 2-3m. The tertiary path is for visitors to stroll through a peaceful rest area, generally 1-1.5m wide. The planting along secondary and tertiary roads is relatively more flexible and diverse. For example, shade and flowers can be provided by planting trees on one side of the road. If planners want to enhance the carbon sequestration capacity of vegetation, they can refer to Table 10-3- Tree species in Cluster 1 and Cluster 8; The characteristics are moderate volume of trees, moderate rate of landscape formation, and strong carbon sequestration capacity; Such as *Sophora japonica*, *Euonymus bungeanus*, *Pinus tabuliformis*, *Prunus cerasifera*, *Syringa oblata* etc.

There are three forms of water bodies in landscape gardens: lakes, pools, and rivers. In larger gardens water bodies often exist in the form of lakes, which are often surrounded by group planting to form large-scale plant landscapes. Planners can select tree species with higher carbon sequestration capacity, larger DBH and faster growth rate, refer to Table 10-3-Cluster 1, Cluster 2 and Cluster 8 (Figure 6-1); Such as *Salix matsudana*, *Salix babylonica*, *Cinnamomum camphora*, *Photinia serratifolia*, *Pinus tabuliformis*, *Prunus serrulate* etc. In smaller gardens, the form of the water body usually dominated by pools. Plant arrangements often highlight individual gestures or use plants to divide the water space and create layers, while also creating a lively and tranquil landscape. Tree species with high carbon sequestration capacity and small volume can be selected to enhance the carbon sequestration capacity; Refer to the Table 10-3-Cluster 1, Cluster 2, Cluster 7 and Cluster 8, Such as *Celtis julianae*, *Acer pictum*, *Ligustrum lucidum*, *Liquidambar formosana*, *Acer palmatum*, *Prunus subg*, *Prunus cerasifera* etc. The river form is rarely used in parks. In the design of the river landscape, tall trees are often planted on both banks. Gardens in European countries also often use regular canals with tall trees planted on both banks. Therefore, in the river landscape, planners can choose large trees which can form a landscape quickly; Refer to the Table 10-3-Cluster 5 and Cluster 6, Such as *Sophora japonica*, *Firmiana platanifolia*, *Platanus acerifolia*, *Acer negundo*, *Populus canadensis*, *Aesculus chinensis*, *Metasequoia glyptostroboides* etc.



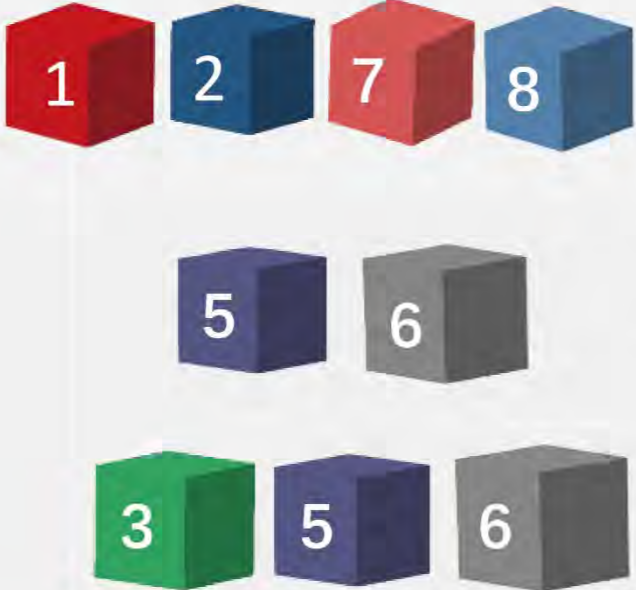
Urban landscape	Recommended tree species	Reasons for recommendation
<p>Foundational tree species</p> <p>common tree species</p>		<p>The tree species in both of these clusters are characterized by larger trunk diameters, faster growth rates, and stronger carbon sequestration abilities.</p> <p>The tree species in both of these clusters are small trees with high landscape value and strong carbon sequestration abilities</p>
Park Road	Recommended tree species	Reasons for recommendation
<p>Main road</p> <p>Second road and path</p>		<p>The quality of the plant configuration on both sides of the main road will directly affect the landscape of urban parks and green spaces. Therefore, fast-growing and strong carbon-sequestering tree species with ornamental value should be selected on both sides of the park road.</p> <p>The planting design along secondary roads and paths can be more flexible and diverse, and require tree species with moderate size, moderate ornamental value, and strong carbon sequestration capacity.</p>
Water landscape	Recommended tree species	Reasons for recommendation
<p>Pond</p> <p>River</p> <p>Lake</p>		<p>The surrounding area of a lake often forms a large area of planted vegetation, and it is recommended to select tree species with strong carbon sequestration ability, larger trunk diameter, and faster growth rate through mass planting to form a large plant landscape.</p> <p>The arrangement of plants near a pond often emphasizes their individual characteristics or is used to divide the water surface space through the distribution of plants, thereby enhancing the hierarchical sense of the landscape. It is recommended to select tree species with strong carbon fixation abilities but small size.</p> <p>The banks of rivers are often planted with tall trees, so it is recommended to choose large trees that have fast-growing and strong carbon sequestration capabilities to enhance the landscape.</p>

Figure 6-1 Planting design recommendations

6.3 Scale dependence of carbon density and influencing factors

The results obtained in this study showed that both the mean and standard deviation of carbon density decreased with increasing sample size (Figure 5-1). Garrigues suggested that the leaf area index was also affected by the sample scale, but the standard deviation of the leaf area index increased with the increasing sample scale ^[166]. A study on natural forests also obtained the opposite conclusion to ours ^[62], confirming significant differences between natural and planted forests ^[53]. Our results showed that the standard deviation of the vegetation indices decreased with increasing sample scale (Figure 5-3). Brown quantified this effect, demonstrating that resolution size explained 20% of the variance in NDVI ^[165]. An alternative study concluded that compared to high-resolution sensors, low-resolution sensors better predicted spatial variation in richness patterns and environmental features ^[178]. Our study quantifies in great detail how the statistical values of remote information vary with scale (Figure 5-3) and further explains the reasons for the differences in statistical values caused by sensor resolution.

Our results show that there is a positive correlation between Shannon wiener diversity index and sample area (Figure 5-3), which is consistent with the Species-area relationship ^[179,60]. As the sample scale increasing, the Shannon wiener diversity index was close to the maximum in 1000m diameter sample scale (Figure 5-3). However, another research showed that the species richness in natural forests saturates before the sample size reaches 1 ha ^[57]. Therefore, this study conclude that the park has a similar biodiversity pattern to natural forests, but their biodiversity saturation scales differ significantly.

A study of natural forests concluded that 44-85 samples are required for each forest type to characterize the mean CD ^[180]. Another study on urban green space also showed that uneven sampling would lead to the underestimation of biomass statistics ^[83]. In this thesis, this study avoided errors from uneven sampling by making a large number of sample squares (100/1000/10000 samples). Robert suggested in 1989 that it was difficult to determine the driving patterns of ecosystems at a single scale ^[181], and this opinion has been verified in many studies ^[182,183,59]. Our results also validate this view (Figure 5-7). Considering that field survey data generally use a sample area of less than 0.3ha ^[184,185], our results demonstrate that in parks, vegetation CD is best measured at the sample scale of 100 m diameter; remote sensing and spatial information is best measured at the sample scale of 100 m or 1000 m diameter; biodiversity information is best measured at the sample scale of 1000 m diameter. This result is not identical to the 250 m and 1000 m grain size proposed by Thuiller ^[59]. There are two possible reasons for this discrepancy: firstly, the circular samples used in this study are similar to the natural community morphology compared to the square samples used by Thuiller; secondly, the differences between natural and planted forests could also lead to different results.

Our results demonstrate that similar CD is obtained in parks based on different sample scales (Figure 5-1). The same conclusion was obtained in a study facing natural forests, where the same average net primary productivity was calculated from samples with scales of 1000m², 1km², and 12500km²,

respectively ^[186]. However, this thesis found that the driving capacity of each influencing factor on CD is not the same at different scales (Figure 5-7), which further suggests that CD is getting the same value for different reasons. A detailed discussion of this phenomenon will be presented in the next section.

6.4 Driving relationship of carbon density

In the sample square with a diameter of 100m, the explanation degree of influence factors on CD (0.64) is higher than that of CSD (0.53), similar conclusions were obtained in Sande's study ^[56]. As the sample diameter increased to 1000m (Figure 5-7), the explanation of carbon density by influence factors increased to 0.99, while the difference in the explanation of carbon storage and carbon sequestration was masked. Previous studies have demonstrated that carbon storage is strongly affected by the average traits of the plant community, while carbon sequestration is strongly affected by the taxonomic diversity of the plant community ^[184,187,56]. Our experimental results validated this opinion, with the biodiversity index explaining more CSD than CD, while the forest structure index is doing the opposite (Figure 5-7) .

Paquette et al. verified the relationship between biodiversity and biology at scales ranging from 0.04 to 0.07ha, respectively ^[51,188,189]. This thesis analyzed parks at larger scales and concluded that the relationship between biodiversity and CD is weaker at small scales, while greater at larger scales (Figure 5-7). Similar conclusion was also reached in a forest-facing study ^[56]. Possible reasons for this phenomenon are that large plant communities have more species and space as buffers, and lower turnover rates with neighboring communities; while small plant communities are vulnerable to environmental influences, thus the drivers of biodiversity are masked ^[190-192]. The correlations between biodiversity and CD were all unidirectional (Figure 5-4, Figure 5-5). This phenomenon implies that in urban park green spaces, the density of carbon storage and carbon sequestration in green spaces tends to decrease with the increase of vegetation species diversity (Figure 6-2). In natural forests, areas with high species diversity tend to have higher carbon storage density and carbon sequestration density; And the carbon density will rise by about 6.4% for each additional species ^[193]. Therefore, the urban parks' "biodiversity-carbon density" relationship differs from that of natural forests. Compared to the "ecological complementarity theory"^[194] and "Species selection effect"^[195] in natural ecosystems, the artificial environment has a greater impact on plant communities. However, the relationship between forest structure and CD was not only unidirectional. The number of trees and canopy cover was negatively correlated with carbon density in the 1000m diameter sample and positively correlated in all other scales of the sample (Figure 5-4, Figure 5-5) . Possible reasons for the positive and negative correlations between forest structure and CD are: on the one hand, large amounts of vegetation increase productivity, leading to higher CD and CSD; on the other hand, the dense vegetation in competition for resources and space leads to less sunlight, water, and nutrients required for individual growth ^[196]. Mean crown diameter, mean crown area, mean planted crown volume, mean tree height, and mean indicators of stand structure information showed significant negative correlations with

carbon storage density and carbon sequestration density (Figure 5-4, Figure 5-5). This phenomenon might be caused by the fact that a single tree's rate of mass increase is negatively correlated to the tree size ^[197].

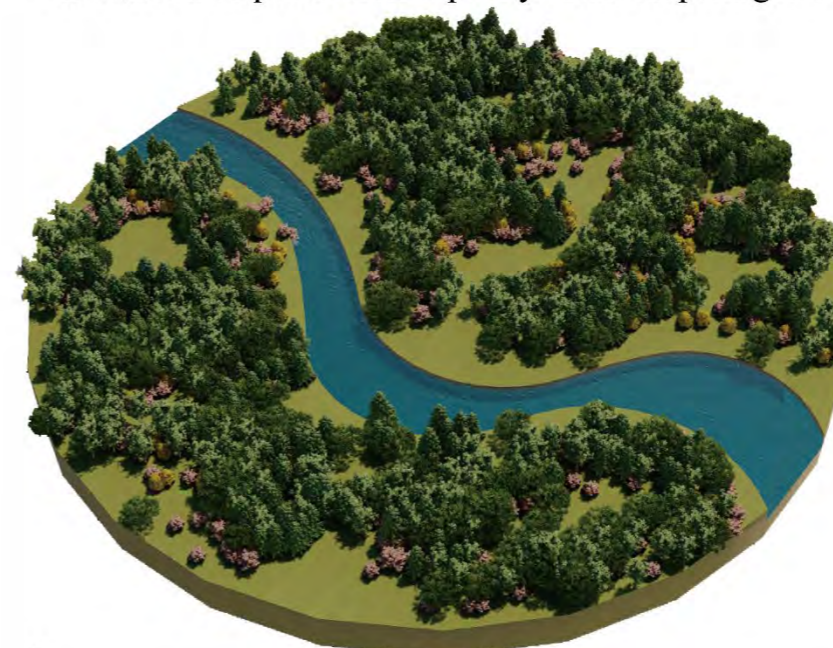
At the 1000m sample scale, the water ratio explains 80% of the covariance between spatial information and CD and 63% of the covariance between spatial information and CSD (Figure 5-7). Therefore, increasing the proportion of water bodies is a viable method to increase the carbon density of urban park green spaces (Figure 6-2). The correlations of both water ratio and CD were positive, and there are two potential reasons for this phenomenon: Primarily, hydrophilic plants are artificially planted nearby the waterbody to avoid the stressful effects of water on the vegetation ^[198]; secondly, the vegetation carbon storage in the study area is limited by water, increasing carbon storage requires more irrigation ^[199]. This thesis uses the Sky View Factor in representing the 3D index of green space, as this index is a good representation of the human senses. The SVF index can only explain less than 10% of the covariance of spatial information and CD, which means that there is little effect of increasing CD through landscape design methods. Also, this means that CD in parks is also associated with edge effects of vegetation structure, which have been observed in natural forest ecosystems ^[200]. Therefore, increasing the edge complexity of vegetation communities is a potential approach to enhance the carbon density in urban park green spaces (Figure 6-2). The results of the study demonstrate that texture information explains more CD than vegetation index at any scale, and the interpretation of texture information is greater in small-scale samples than in large-scale samples. The NDVI explains more about the CD than the RVI, the same as Yao's findings ^[161]. However, the RVI explained more CSD than NDVI. Thus, using RVI in the calculation of CSD will give better results.

a. The standard urban park green space used as a comparative reference.



1000 m

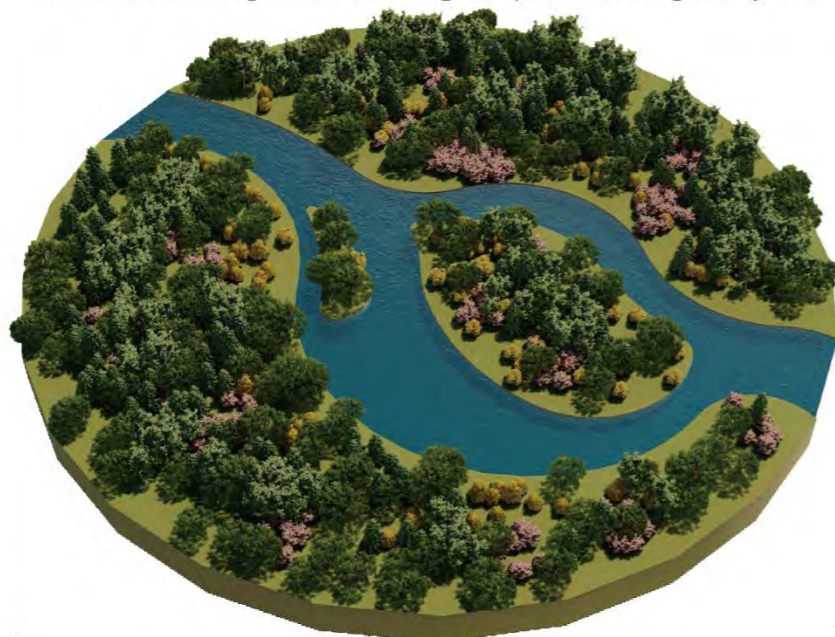
b. Enhancing the complexity of vegetation communities at the edges can increase the carbon sequestration capacity of urban park green spaces.



1000 m

Reason:
Urban green spaces and natural green spaces exhibit similar "edge effects".

c. Increasing the area of water bodies and coverage of tree canopies can enhance the carbon sequestration capacity of urban park green spaces.



1000 m

Reason:
The microclimatic conditions near water bodies are more favorable for vegetation growth and there is ample water supply.

d. Urban park green spaces with low tree species diversity have a higher carbon sequestration capacity.



1000 m

Reason:
In urban park green spaces, higher tree biodiversity can lead to reduced spatial utilization efficiency.

Figure 6-2 Optimization strategies for carbon sequestration capacity of vegetation communities in urban parks: a. Vegetation communities in typical urban park green spaces; b. Vegetation communities in urban park green spaces with increased carbon sequestration capacity based on the "edge effect"; c. Vegetation communities in urban park green spaces with increased carbon sequestration capacity through the expansion of water bodies; d. Vegetation communities in urban park green spaces with increased carbon sequestration capacity by reducing the species richness of trees.

7 Conclusion and outlook

7.1 Main research conclusion

7.1.1 Carbon storage density and carbon sequestration density in China Green Expo

1) There are 108,241 trees in China Green Expo, belonging to 54 families and 97 genera respectively. The keystone species include *Platanus acerifolia*, *Ligustrum lucidum*, *Cedrus deodara*, *Salix babylonica*, *Ginkgo biloba*, *Prunus cerasifera*, *Koelreuteria paniculate* etc; The dominant families with high carbon sequestration capacity are *Rosaceae*, *Salicaceae*, *Pinaceae*, *Platanaceae*, *Sapindaceae* etc; The dominant genera for carbon sequestration capacity are *Salix*, *Platanus*, and *Cedrus*. The majority of trees (72%) were distributed within the 10-50 cm DBH.

2) There are 40 species of evergreen trees and 129 species of deciduous trees in the China Green Expo, with a total of 36,780 evergreen trees and 71,460 deciduous trees. The ratio of evergreen trees to deciduous trees is 3:7. The carbon sequestration capacity of deciduous trees is greater than that of evergreen trees. There are 53 species of flowering trees, 29 species of foliage trees, 26 species of fruit trees and 5 species of trunk observation trees in the China Green Expo.

3) The total amount of carbon storage in China Green Expo is 48.58 Gg, and the total amount of carbon sequestration is 3.26 Gg·yr⁻¹. The carbon storage of trees, shrubs and herbaceous vegetation are 43.17 Gg, 5.31 Gg and 0.1 Gg, respectively; The amount of carbon sequestered by trees, shrubs and herbaceous vegetation are 2.57 Gg·yr⁻¹, 0.64 Gg·yr⁻¹ and 0.05 Gg·yr⁻¹.

4) The average green space carbon storage density and carbon sequestration density of China Green Expo are 40.63 kg/m² and 2.65 kg/m²·yr⁻¹. While the carbon storage density and carbon sequestration density including water bodies and impermeable surfaces are only 30.74 kg/m² and 2.06 kg/m²·yr⁻¹.

5) Under similar climatic background conditions, the carbon density of urban park green space in Zhengzhou is much higher than that of other regions. Even so, there is still great potential for optimizing the carbon density of parkland in Zhengzhou. The carbon sink capacity of urban green spaces can be rapidly increased by publishing policies and optimizing the structure of tree species.

7.1.2 Growth factors and carbon sequestration capacity of tree species in China Green Expo

1) This thesis obtained the growth factors of 169 tree species in China Green Expo species during the rapid growth period. The fit results are excellent ($R^2 \approx 0.8$); This result can be well implied in urban park green spaces under similar climatic background conditions.

2) Species with growth factors greater than 1 include *Trachycarpus fortune*, *Catalpa bungee*, *Ilex chinensis* and *Euonymus alatus*, such tree species have a slow growth rate in DBH; Species with growth factors less than 0.3 include *Paulownia fortune*, *Tilia tuan*, *Fraxinus chinensis*, *Chaenomeles cathayensis*,

Bischofia javanica, *Ulmus parvifolia*, *Ulmus pumila*, *Firmiana simplex*, *Sambucus australasica* and *Acer spp*, such tree species have a faster growth rate in DBH. The growth factors of 57% tree species were distributed between 0.4 and 0.6, which matched the normal distribution.

3) This thesis conducted a cluster analysis for the carbon sequestration capacity of 169 tree species. The results of this study can provide theoretical support for tree species selection in urban planning.

4) This thesis proposes some options of tree species selection based on carbon enhancement function in combination with landscape scenarios.

7.1.3 Multiple scale driving relationship of carbon density in urban park green space

1) Both the carbon density and tree carbon density of urban park green space were obtained at the minimum value in the sample scale of 1000m in diameter; The minimum shrub carbon density was obtained in a sample scale of 100m in diameter; The minimum value of herbaceous carbon density was obtained in a sample scale of 300m in diameter.

2) The standard deviation of carbon density obtained by the sample method gradually stabilizes after the sample diameter exceeds 100m. Considering the large amount of work required for outdoor surveys, the optimal sample diameter for investigating carbon density in urban green parks is 100m; The traditional sample survey scale of forest ecosystems has a large error when applied to urban green spaces.

3) The vegetation community in urban park green space has edge effect; The carbon density was higher in areas with lower SVF indices, also higher in vegetation communities with more complex boundaries.

4) Areas with a higher proportion of green space covered by trees and areas with a higher proportion of water bodies have a higher carbon density. The driving force of water body occupancy on carbon density was significantly greater than other spatial factors at a sample scale of 1000 m in diameter.

5) Remote sensing image texture information has higher driving capacity on carbon density than vegetation index, and this phenomenon is more significant in smaller scale samples. NDVI has a higher driving effect on carbon storage density than RVI, while RVI has a higher driving effect on carbon sequestration density than NDVI. In studies which estimate the density of carbon sequestration in urban parks, the accuracy of the results can be improved by applying RVI.

6) At the scale of 1000m diameter sample, areas with high tree density have higher carbon density; In samples with diameters less than 1000 m, areas with low tree density had higher carbon density. Because of the lower growth rates of larger biomass tree individuals of the same species, carbon density tended to be lower in areas with higher average stand structure index.

7) The diversity of tree species in urban parks shows a similar "species-area" relationship with natural forest. In large scale samples, the effect of species diversity on carbon density in urban park green spaces is particularly significant. The areas with higher species diversity tend to have lower carbon density.

7.2 Research Innovations

1) This thesis uses multi-source data to spatially quantify the carbon density of China Green Expo, which provides a new scheme for estimating the carbon density of urban park green space;

2) Exploring a new method for estimating the age of trees applicable to urban park green space; Combining the carbon sequestration capacity of tree species with landscape garden planning applications to provide a theoretical basis for urban park green space optimization;

3) Exploring the driving ability of carbon density in urban park green space based on multi-scale analysis method; Providing theoretical support for optimal design of landscape architecture;

4) Discovering the difference in the "species diversity-carbon density" driving relationship between urban park green spaces and natural green spaces; Further analysis of possible reasons.

7.3 Shortcomings and Outlook

1) Because of the limitations of urban green space planning, the area of urban park green space tends to be small. For example, the average area of urban parkland in Beijing is only 49.28ha ^[201], Thus the analysis of the scale effect of carbon density in urban park green spaces is severely limited. This thesis is based on the China Green Expo with a total area of 196ha, and the maximum diameter of the sample square used can only reach 1000m. In the following studies, it can be explored the carbon density variation on the larger scale.

2) This thesis focuses on the optimization analysis of carbon sequestration capacity of urban park greenery, with less consideration for landscape effects and other related ecosystem services. In future research, carbon sequestration capacity should be more closely integrated with other types of ecosystem services.

8 Optimization design of China Green Expo

The conclusion drawn from this thesis has significant practical value in the field of landscape architecture planning and design. In this section, targeted optimization design proposals will be put forward based on the current site conditions.

As the purpose of constructing the China Green Expo Park is to exhibit the achievements of urban greening in various regions, most of the areas are used to build theme parks, which are not suitable for renovation and design. Therefore, the optimization design in this study was chosen to be carried out in the public green space areas of the China Green Expo. The optimization design plan was completed based on the guidance of Figure 6-2 and Figure 6-1. Thus, guided by Figure 6-2 and Figure 6-1, this study conducted optimization design on two public green space areas in the China Green Expo Park, as shown in Figure 8-1 and Figure 8-2.

The main function of the road system in urban parks is to connect various areas within the park and serve as a complementary part of the city's road system. The China Green Expo Park has a well-developed and clearly graded road system, with a complete traffic route (Figure 2-6). Through field research and consultation of construction documents in the China Green Expo Park, this study found that there are five types of roads in the park, including two types of carriage way and three types of pedestrian walkways. Because this study proposed targeted tree planting optimization design schemes for each of the five road types, as shown in Figure 8-3, Figure 8-4, Figure 8-, Figure 8- and Figure 8-.

Water features play a very important role in urban parks, providing not only good views and a comfortable living environment for users, but also creating microclimatic conditions suitable for vegetation growth. In the discussion section, we conducted a detailed and profound discussion on the role of water bodies in park green spaces. Water feature design often varies depending on the site conditions. Overall, they can be divided into three types: lakes, rivers, and ponds. In this study, we conducted an in-depth discussion on tree planting for the three water feature types in the discussion section. Moreover, we found that there are a rich variety of water features in the China Green Expo Park. Therefore, we propose a variety of optimized design schemes for different water feature types, combining the site conditions of the China Green Expo Park (Figure 2-6) and the theoretical basis derived from previous discussions (Figure 6-1) (Figure 8-, Figure 8-, and Figure 8-1).

Figure 8-1 China Green Expo Optimized Design Plan 1



Current plan



Optimization



Styphnolobium japonicum



Firmiana simplex



Pterocarya stenoptera



Liriodendron chinense



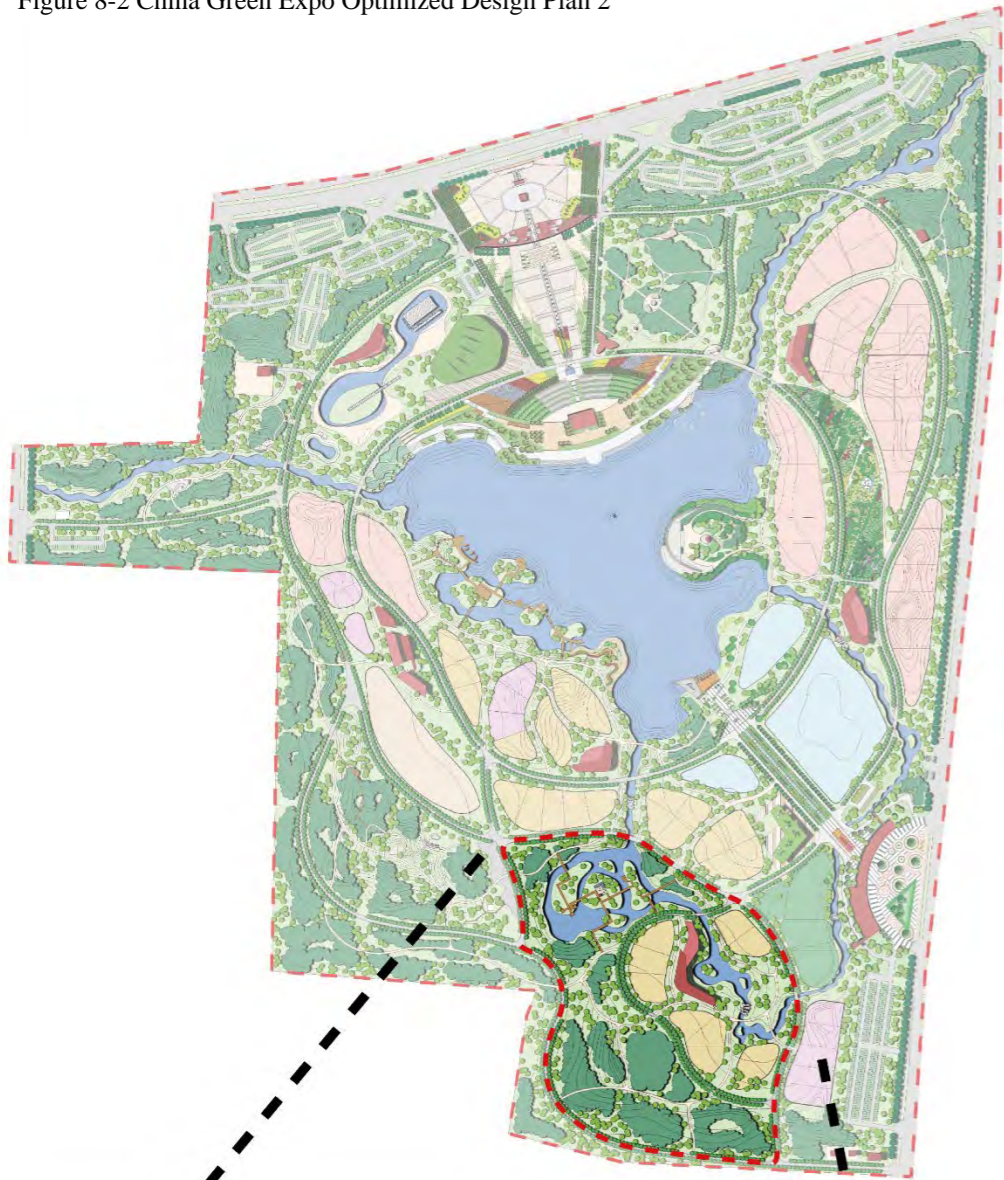
Cedrus deodara



Triadica sebifera

In the new design scheme, the coverage area of arboreal vegetation has been increased, and arboreal vegetation from **2** and **5** has been utilized to achieve the carbon sequestration goal.

Figure 8-2 China Green Expo Optimized Design Plan 2



Current plan



Metasequoia glyptostroboides



Aesculus chinensis



Acer negundo



Optimization

In the optimized design scheme, the area of the water body was increased, the vegetation community with more complex edge structures was designed, and the carbon sequestration goal was achieved by utilizing the arbor vegetation in



Liquidambar Formosana Hance

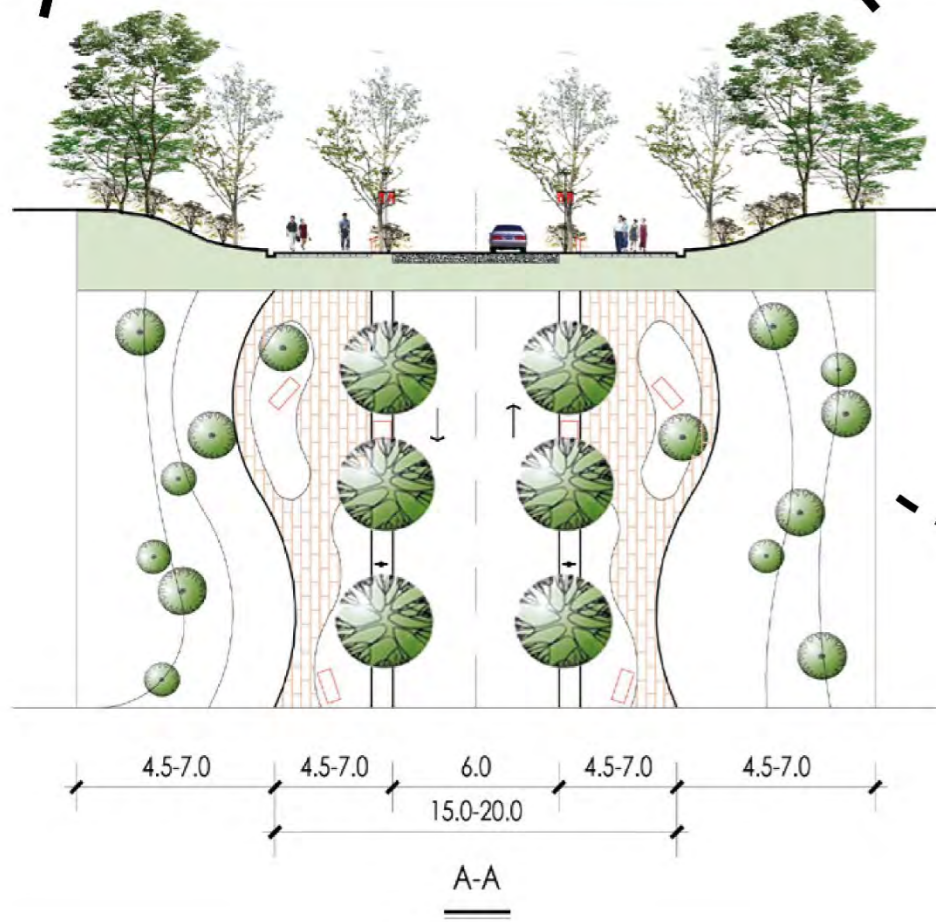
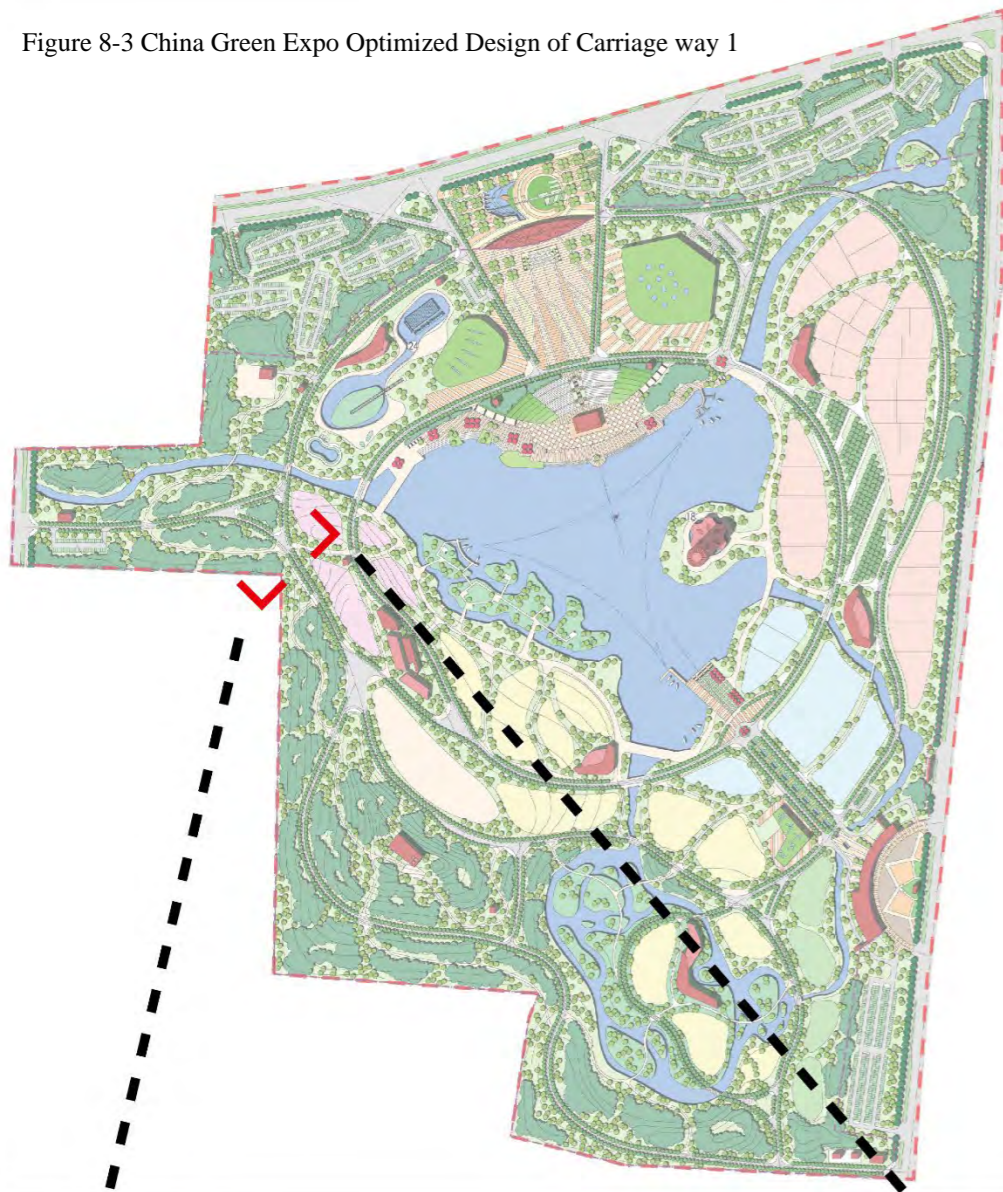


Prunus persica



Prunus cerasifera

Figure 8-3 China Green Expo Optimized Design of Carriage way 1



Due to the presence of main roads throughout various areas within the park, the arrangement of plants on either side will directly affect the landscape of the park's green spaces. Therefore, we have opted for deciduous tree species with shorter maturation periods, selecting suitable species from



Ulmus spp



Robinia pseudoacacia



Firmiana simplex



5 m 6 m 5 m

Figure 8-4 China Green Expo Optimized Design of Carriage way 2



While using fast-growing deciduous tree species on either side of the main roads, flowering trees can also be used to enrich the colors of the park's landscape. Therefore, flowering tree species from 5, 6 and 9 can be selected.



Albizia julibrissin



Prunus persica



Firmiana simplex

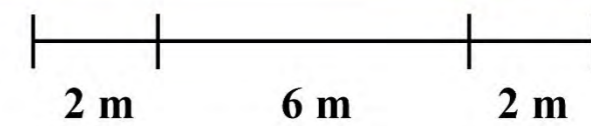
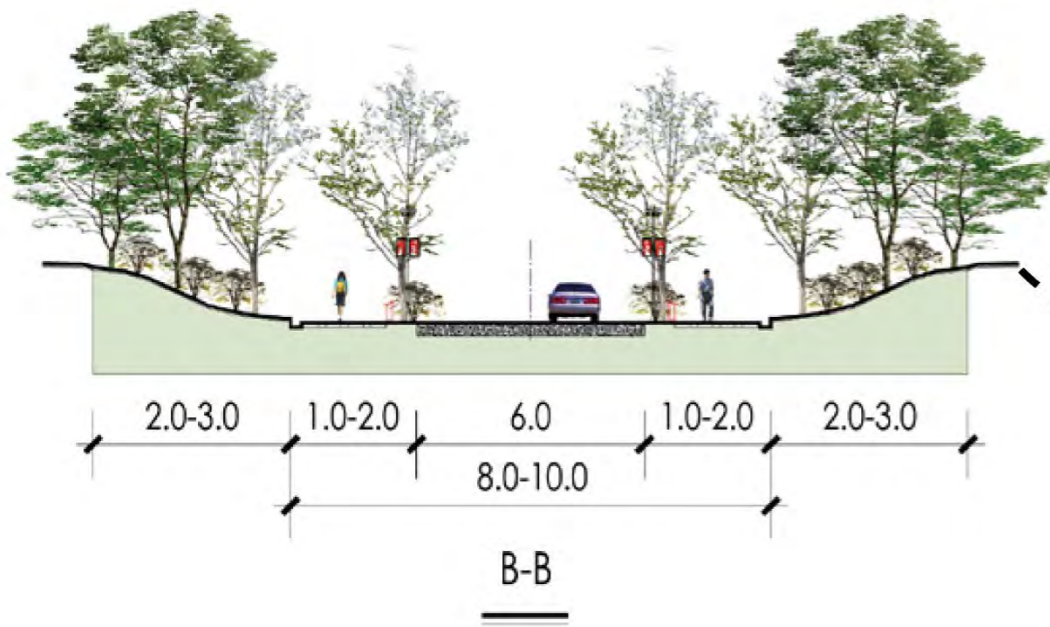
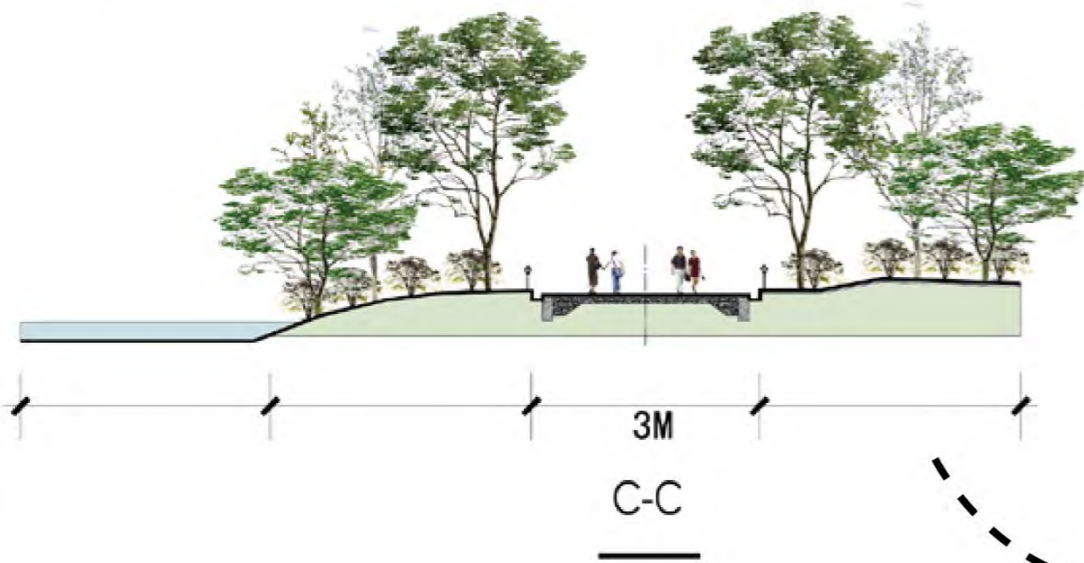
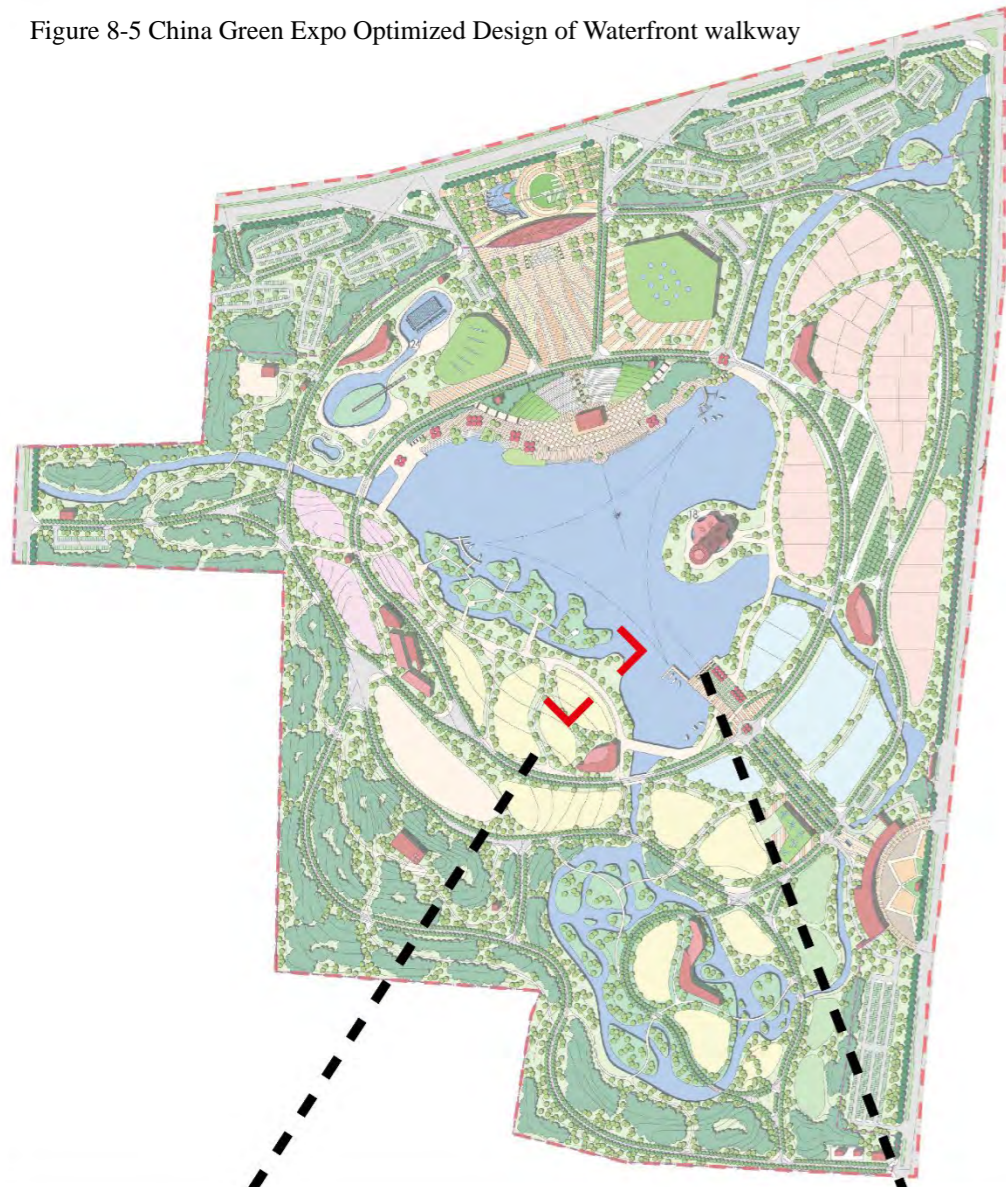


Figure 8-5 China Green Expo Optimized Design of Waterfront walkway



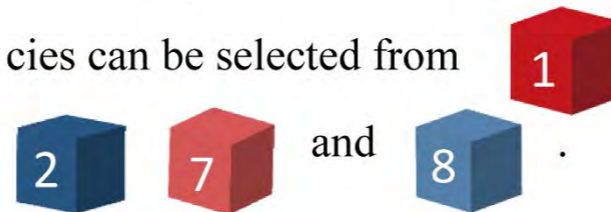
Tamarix chinensis



Prunus serrulata

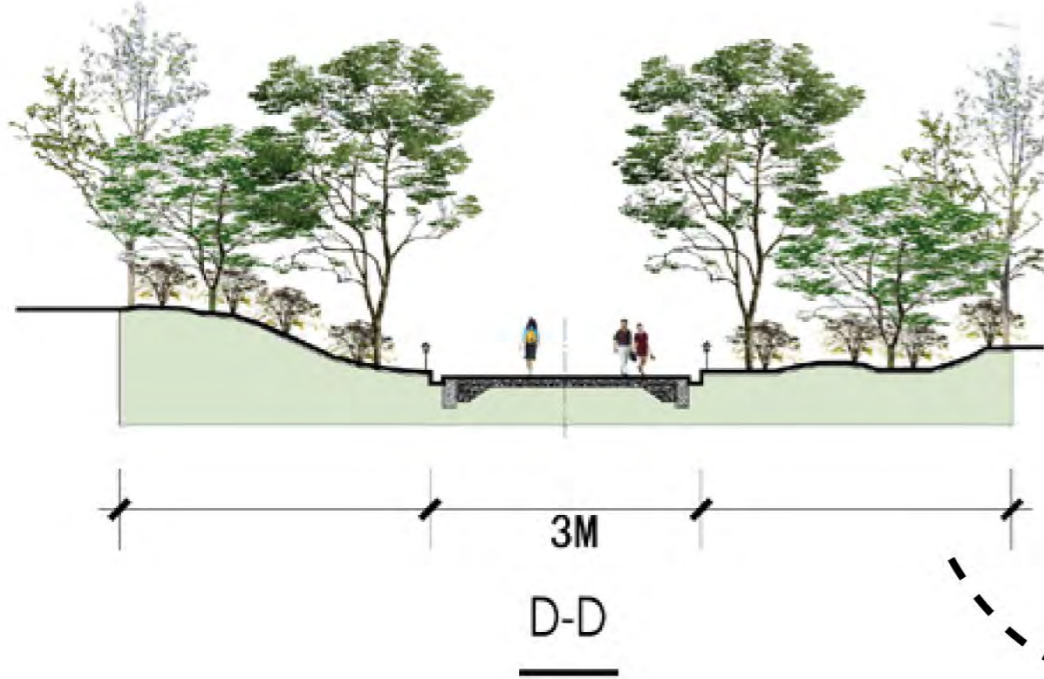
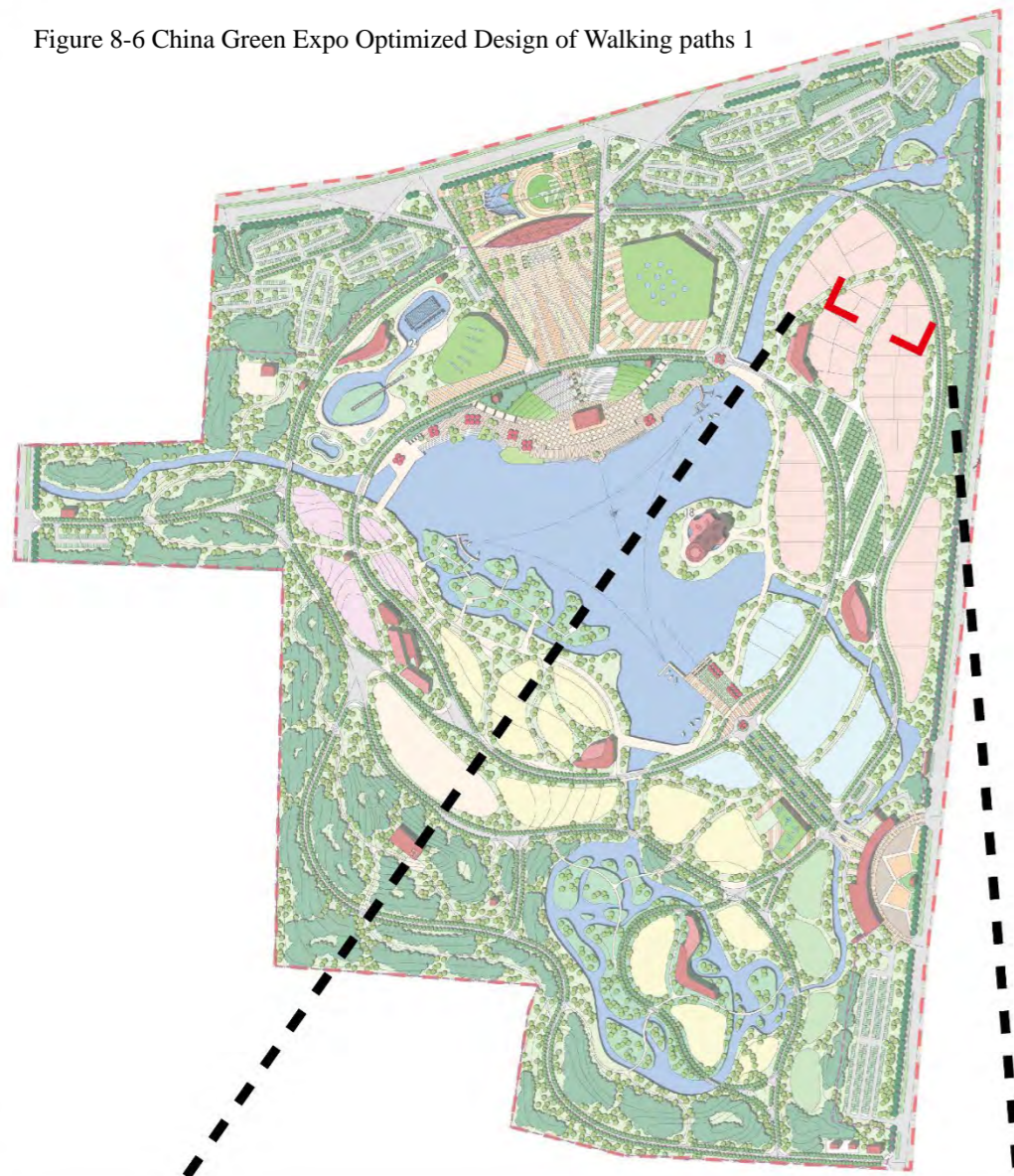


The waterfront trail on both sides has both water views and secondary road properties, therefore we can choose tree species with moderate size, moderate maturation rate, and strong carbon sequestration ability. Tree species can be selected from



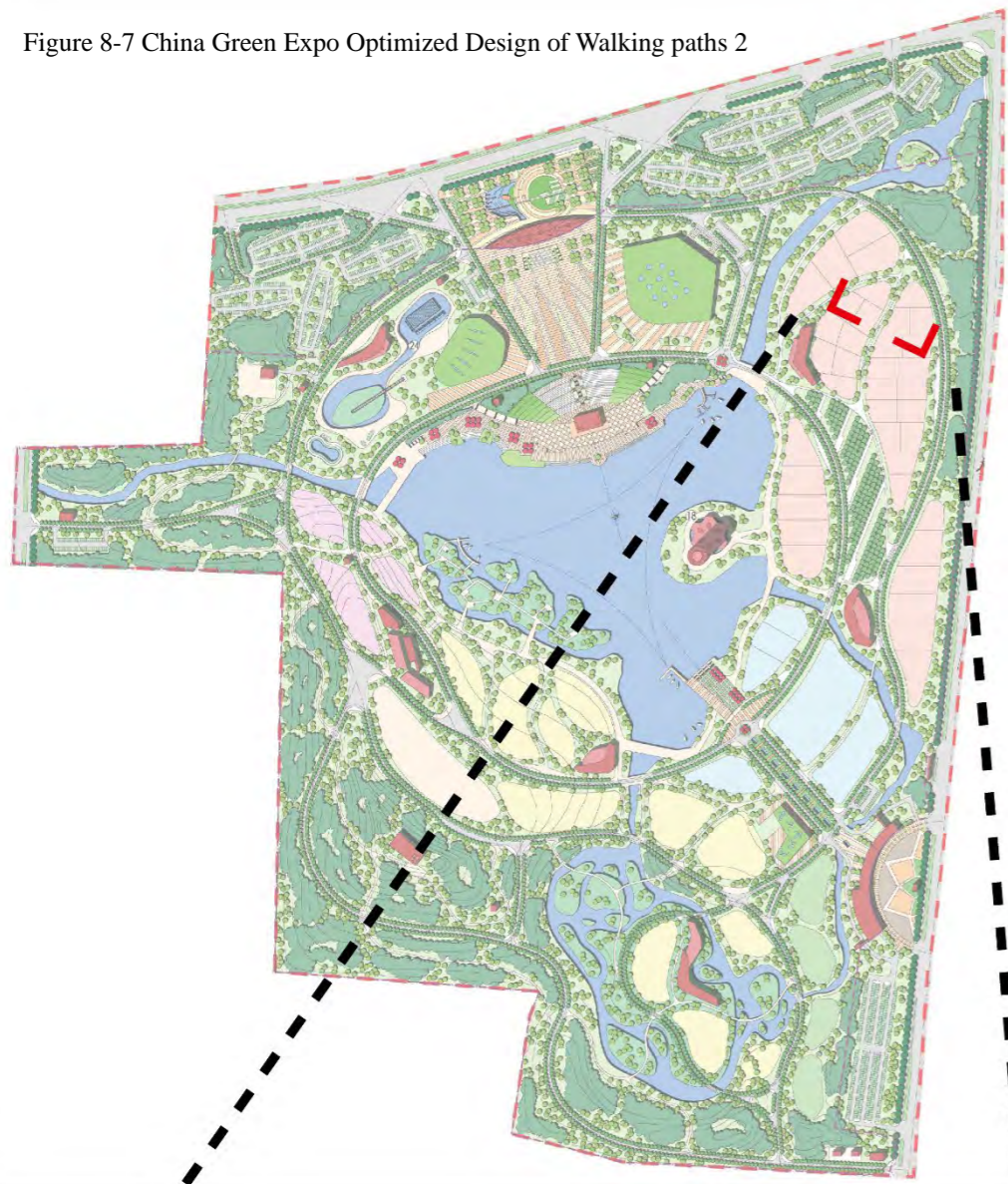
6 m

Figure 8-6 China Green Expo Optimized Design of Walking paths 1



The secondary roads are designed for visitors to stroll in peaceful resting areas, and the plantings along these roads can be more flexible and diverse. Planting trees on one side of the road can provide both shading and floral displays. Therefore, tree species from **1** and **8** are suitable choices.

Figure 8-7 China Green Expo Optimized Design of Walking paths 2



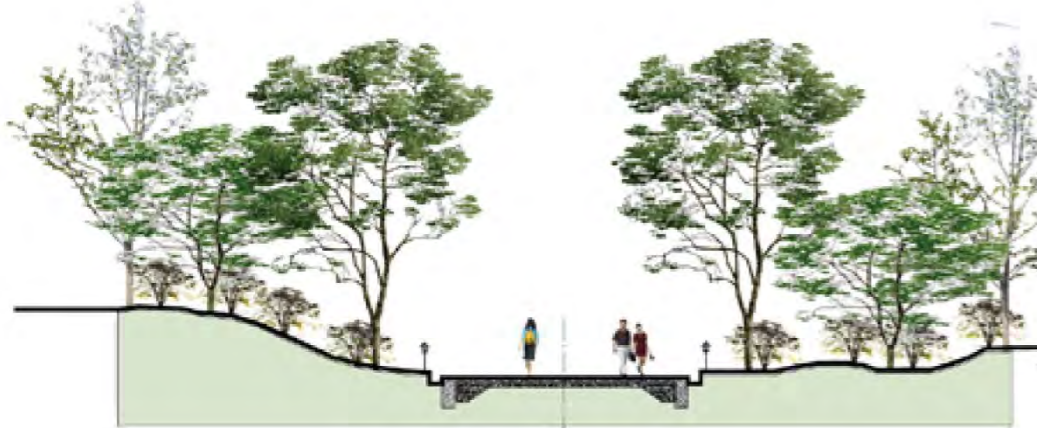
Pinus tabulaeformis



Syringa - pectinifera



Ulmus pumila



3M

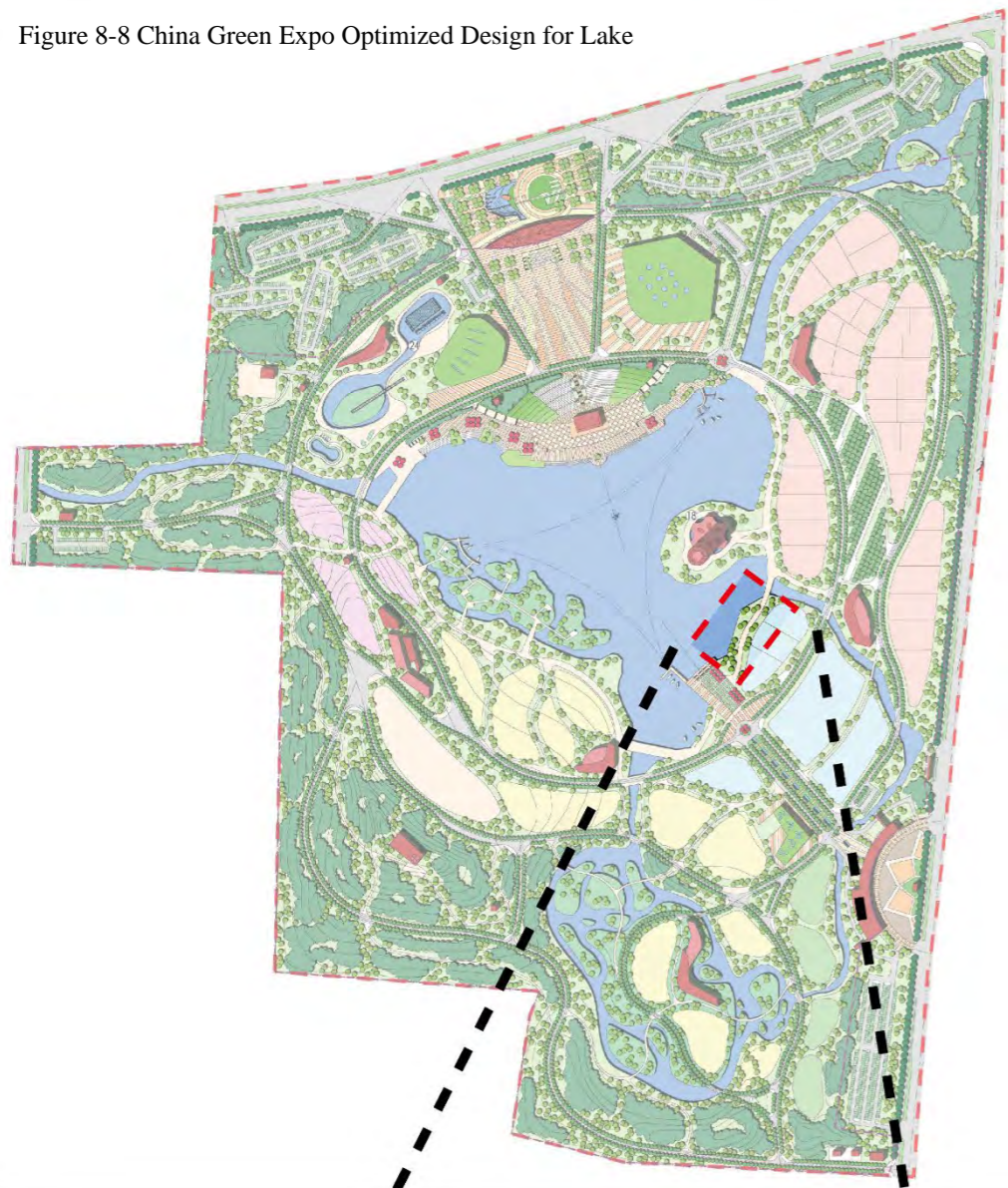
D-D

The secondary roads are designed for visitors to stroll in peaceful resting areas, and the plantings along these roads can be more flexible and diverse. Planting trees on one side of the road can provide both shading and floral displays. Therefore, tree species from **1** and **8** are suitable choices.



3 m

Figure 8-8 China Green Expo Optimized Design for Lake



Planting in groups is often used to create a large area of plant landscape around the lake. Tree species with strong carbon sequestration ability, larger diameter at breast height, and faster growth rate can be selected.

Suitable tree species can be selected from



and



Tamarix chinensis



Prunus serrulata



Toona sinensis



Rhododendron simsii



Pinus tabuliformis

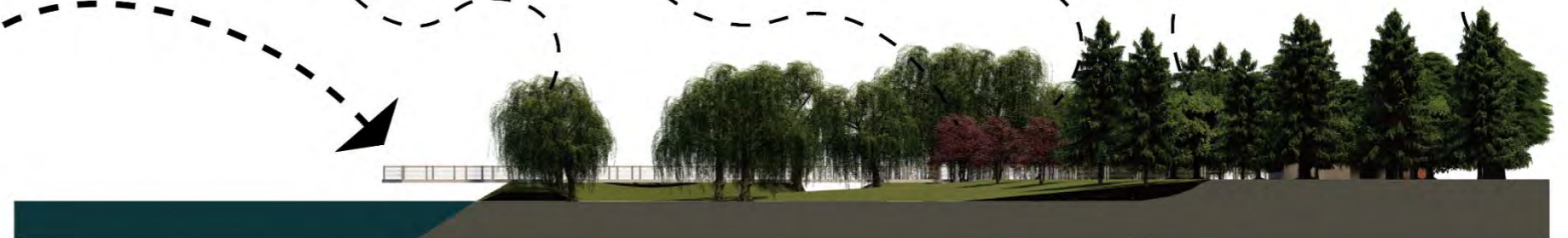
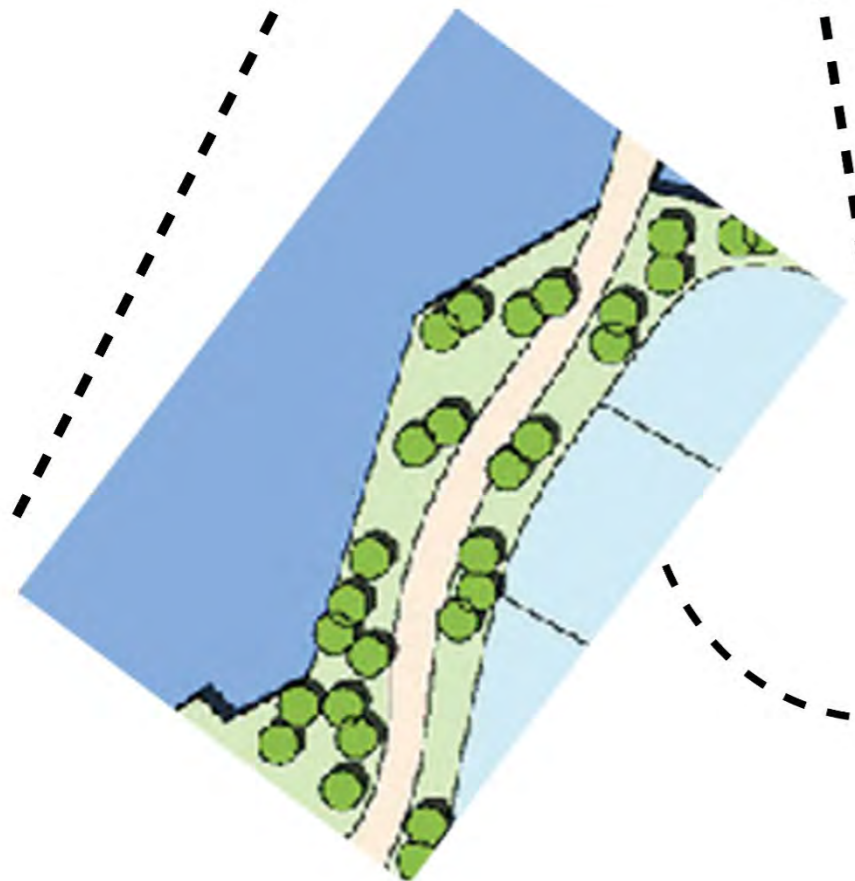
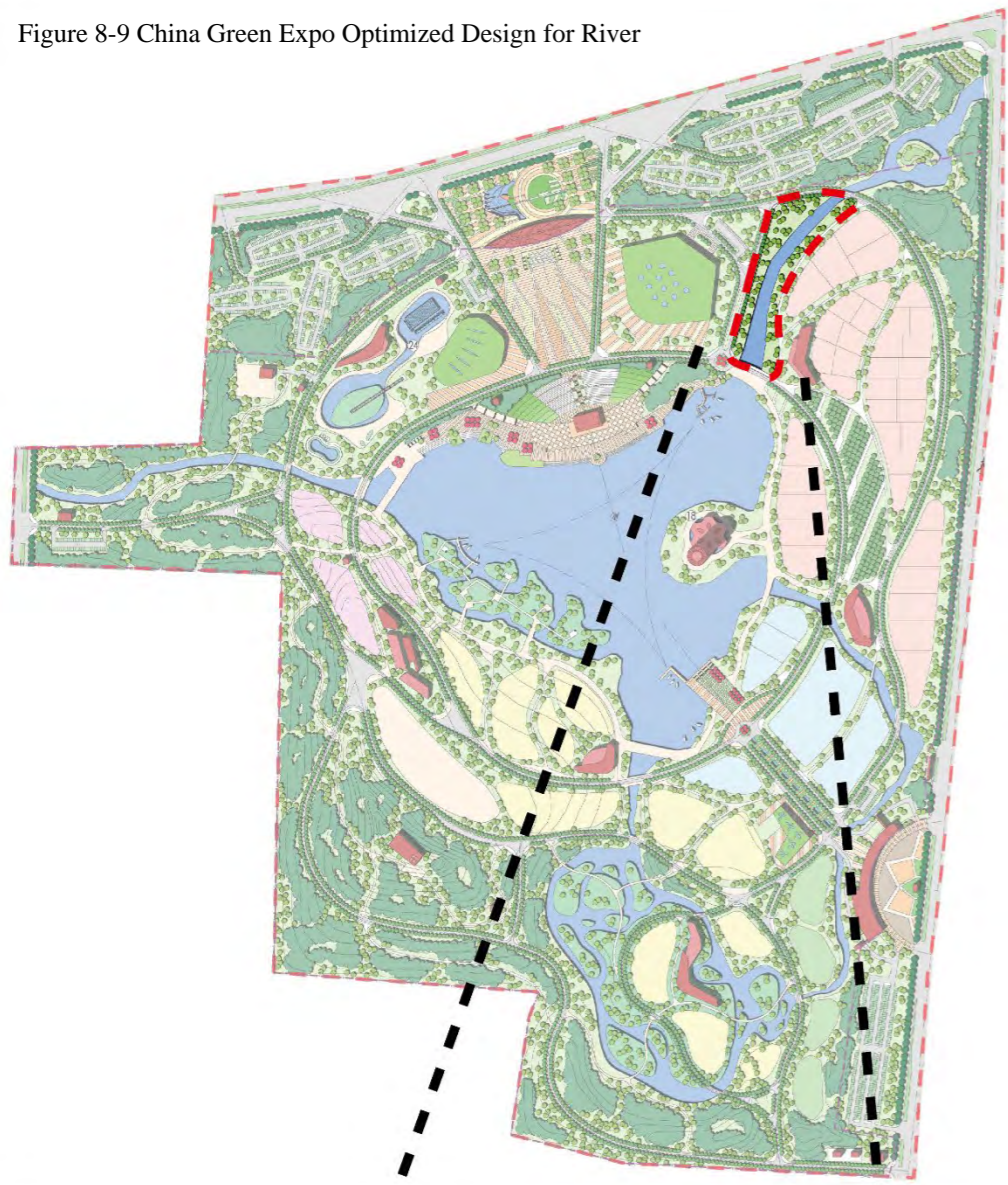


Figure 8-9 China Green Expo Optimized Design for River



In the treatment of river landscapes, tall trees are often planted on both sides. In some formal gardens, a regular canal is also often used, with tall trees planted on both sides. Therefore, fast-growing large deciduous trees can be selected for river landscapes.

Suitable tree species can be selected from

5 and 6 .



Robinia pseudoacacia



Populus tomentosa



Styrax japonicus



Prunus serrulata



Acer negundo



Ailanthus altissima



Taxodium distichum

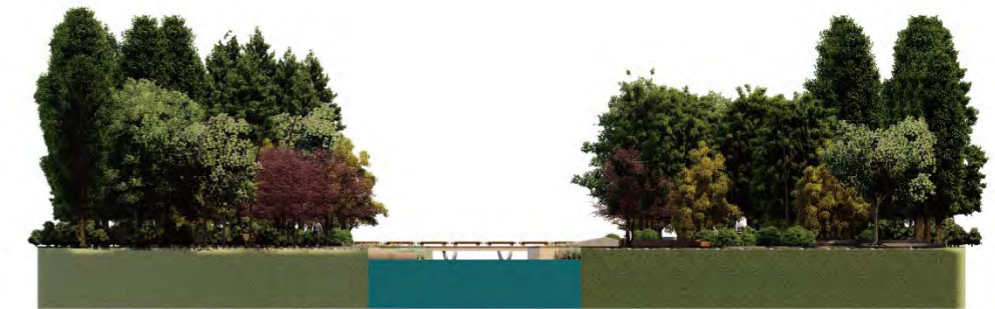
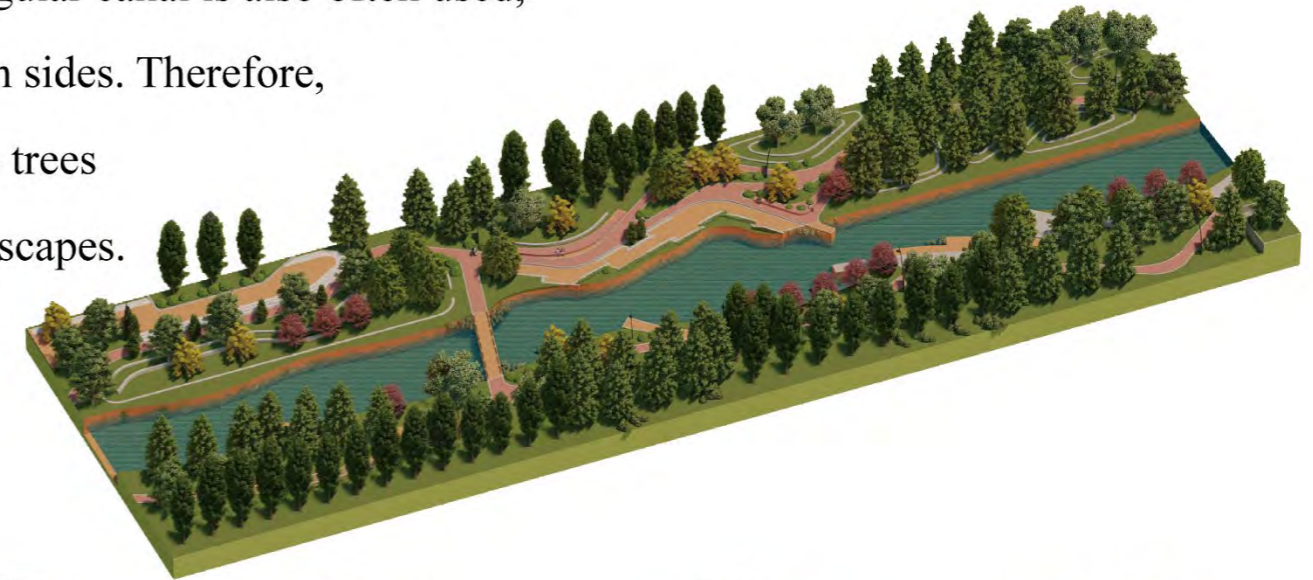
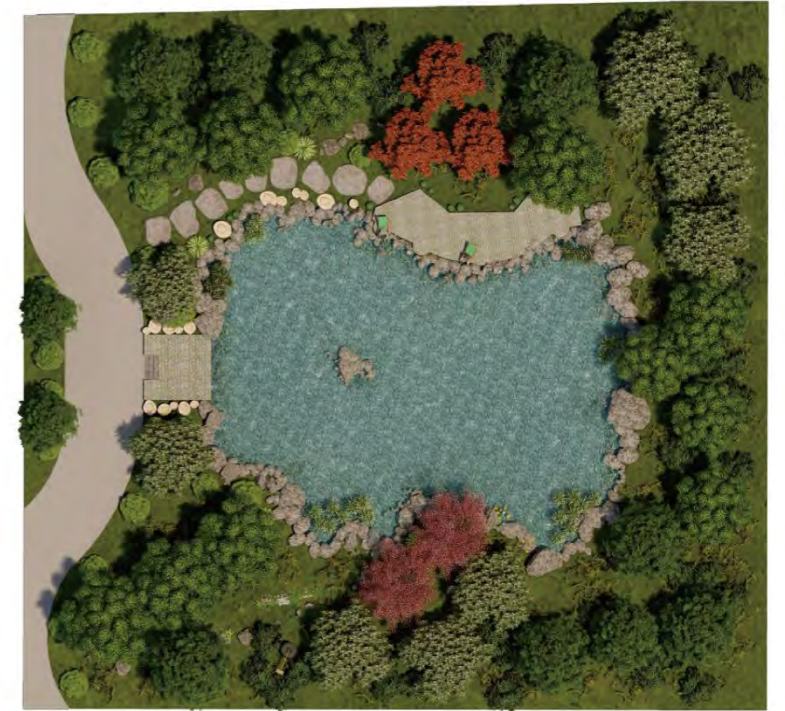
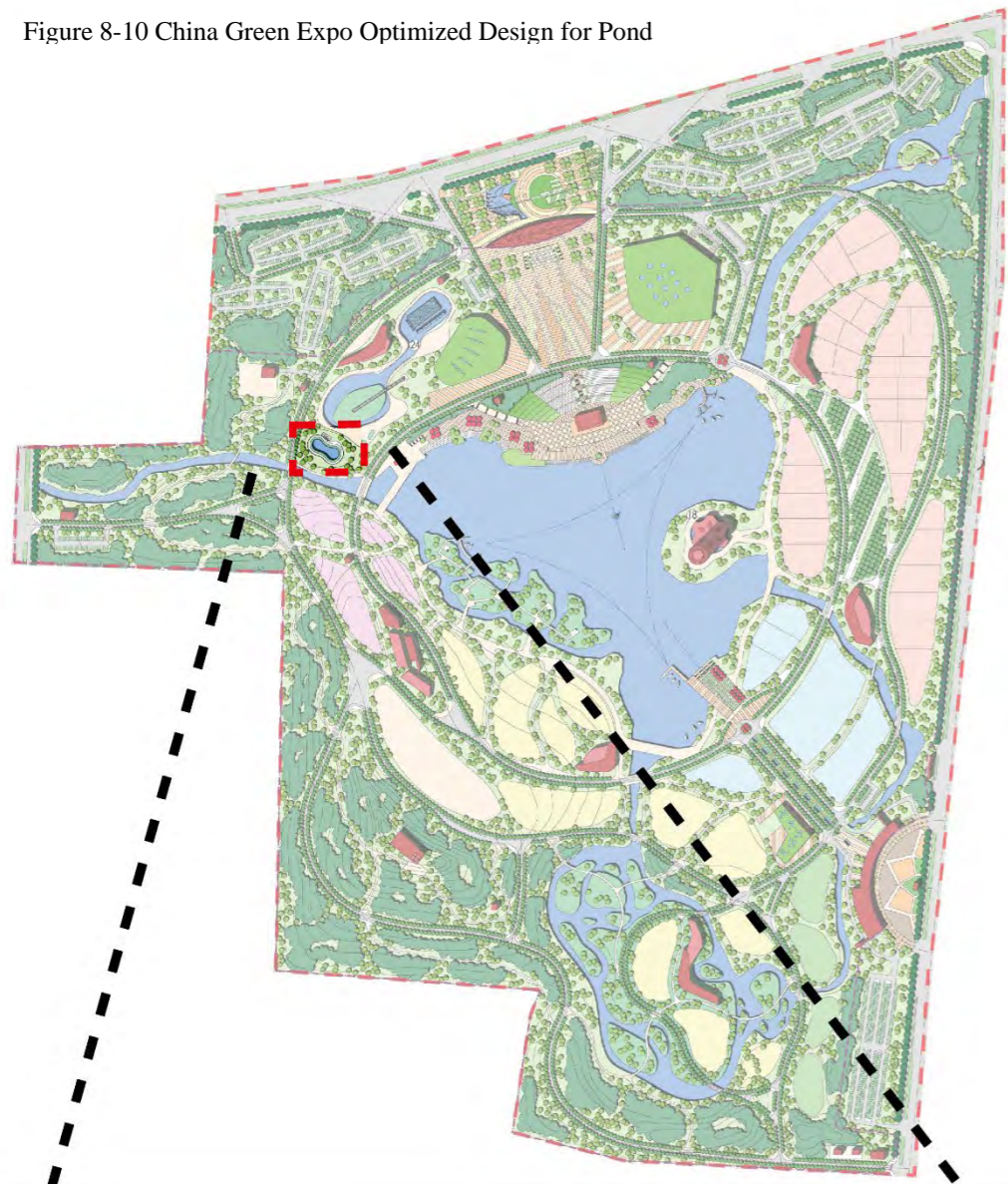


Figure 8-10 China Green Expo Optimized Design for Pond



Euonymus hamiltonianus



Acer pentaphyllum



Ligustrum lucidum



Liquidambar styraciflua



Acer rubrum



Prunus serrulata

In smaller gardens, ponds are often used as the main form of water body. In order to create a "delicate and interesting" effect, the arrangement of plants often emphasizes their individual characteristics, or divides the water surface space through the distribution of plants to increase the sense of hierarchy in the landscape. Suitable tree species can be selected from



and



9 Reference

- [1] National Bureau of Statistics of China[EB/OL][<http://www.stats.gov.cn/was5/web/search?channelid=288041&andsen>]. [2022-09-02].
<http://www.stats.gov.cn/was5/web/search?channelid=288041&andsen=%E5%9F%8E%E9%95%87%E5%8C%96%E7%8E%87>.
- [2] ZHANG C, LIN Y. Panel estimation for urbanization, energy consumption and CO₂ emissions: A regional analysis in China[J/OL]. *Energy Policy*, 2012, 49: 488-498. <https://doi.org/10.1016/j.enpol.2012.06.048>.
- [3] World Population Prospects 2022: Summary of Results | Population Division [EB/OL]. [2022-08-13]. <https://www.un.org/development/desa/pd/content/World-Population-Prospects-2022>.
- [4] LI W, CAO Q, LANG K, etc. Linking potential heat source and sink to urban heat island: Heterogeneous effects of landscape pattern on land surface temperature[J/OL]. *Science of The Total Environment*, 2017, 586: 457-465. <https://doi.org/10.1016/j.scitotenv.2017.01.191>.
- [5] CERVERO R, DAY J. Suburbanization and transit-oriented development in China[J/OL]. *Transport Policy*, 2008, 15(5): 315-323. <https://doi.org/10.1016/j.tranpol.2008.12.011>.
- [6] Lamia Kamal-Chaoui. OECD.pdf[M]//Competitive Cities and Climate Change. Milan, Italy, 2008: 29[2020-10-05].
- [7] SETO K C, DHAKAL S, BIGIO A, etc. Human Settlements, Infrastructure, and Spatial Planning[J]. *Human Settlements*: 78.
- [8] CHURKINA G. The Role of Urbanization in the Global Carbon Cycle[J/OL]. *Frontiers in Ecology and Evolution*, 2016, 3[2022-10-05]. <http://journal.frontiersin.org/Article/10.3389/fevo.2015.00144/abstract>.
- [9] MEEHL G A, TEBALDI C. More Intense, More Frequent, and Longer Lasting Heat Waves in the 21st Century[J/OL]. *Science*, 2004, 305(5686): 994-997. <https://doi.org/10.1126/science.1098704>.
- [10] LIU L, ZHANG Y. Urban Heat Island Analysis Using the Landsat TM Data and ASTER Data: A Case Study in Hong Kong[J/OL]. *Remote Sensing*, 2011, 3(7): 1535-1552. <https://doi.org/10.3390/rs3071535>.
- [11] ZHOU H, SHI P, WANG J, etc. Rapid Urbanization and Implications for River Ecological Services Restoration: Case Study in Shenzhen, China[J/OL]. *Journal of Urban Planning and Development*, 2011, 137(2): 121-132. [https://doi.org/10.1061/\(ASCE\)UP.1943-5444.0000051](https://doi.org/10.1061/(ASCE)UP.1943-5444.0000051).
- [12] DIMOUDI A, NIKOLOPOULOU M. Vegetation in the urban environment: microclimatic analysis and benefits[J]. *Energy and Buildings*, 2003: 8.
- [13] HONU Y A K, CHANDY S, GIBSON D J. Occurrence of Non-Native Species Deep in Natural Areas of the Shawnee National Forest, Southern Illinois, U.S.A.[J/OL]. *Natural Areas Journal*, 2009, 29(2): 177-187. <https://doi.org/10.3375/043.029.0210>.
- [14] FULLER R A, GASTON K J. The scaling of green space coverage in European cities[J/OL]. *Biology Letters*, 2009, 5(3): 352-355. <https://doi.org/10.1098/rsbl.2009.0010>.
- [15] SHAHMOHAMADI P, CHE-ANI A I, MAULUD K N A, etc. The Impact of Anthropogenic Heat on Formation of Urban Heat Island and Energy Consumption Balance[J/OL]. *Urban Studies Research*, 2011, 2011: 1-9. <https://doi.org/10.1155/2011/497524>.
- [16] GOLDEMBERG J, UNITED NATIONS DEVELOPMENT PROGRAMME, UNITED NATIONS, etc. World energy assessment: energy and the challenge of sustainability[M]. New York, NY: United

- Nations Development Programme, 2000.
- [17] HUANG G, ZHOU W, CADENASSO M L. Is everyone hot in the city? Spatial pattern of land surface temperatures, land cover and neighborhood socioeconomic characteristics in Baltimore, MD[J/OL]. *Journal of Environmental Management*, 2011, 92(7): 1753-1759. <https://doi.org/10.1016/j.jenvman.2011.02.006>.
- [18] RASTANDEH A, JARCHOW M. Urbanization and biodiversity loss in the post-COVID-19 era: complex challenges and possible solutions[J/OL]. *Cities & Health*, 2021, 5(sup1): S37-S40. <https://doi.org/10.1080/23748834.2020.1788322>.
- [19] EL-FADEL M, FINDIKAKIS A N, LECKIE J O. Environmental Impacts of Solid Waste Landfilling[J/OL]. *Journal of Environmental Management*, 1997, 50(1): 1-25. <https://doi.org/10.1006/jema.1995.0131>.
- [20] COHEN P, POTCHTER O, MATZARAKIS A. Daily and seasonal climatic conditions of green urban open spaces in the Mediterranean climate and their impact on human comfort[J/OL]. *Building and Environment*, 2012, 51: 285-295. <https://doi.org/10.1016/j.buildenv.2011.11.020>.
- [21] SRIVANIT M, HOKAO K. Evaluating the cooling effects of greening for improving the outdoor thermal environment at an institutional campus in the summer[J/OL]. *Building and Environment*, 2013, 66: 158-172. <https://doi.org/10.1016/j.buildenv.2013.04.012>.
- [22] YU C, HIEN W N. Thermal benefits of city parks[J/OL]. *Energy and Buildings*, 2006, 38(2): 105-120. <https://doi.org/10.1016/j.enbuild.2005.04.003>.
- [23] Urban green space classification standards: CNKI: SUN: ZGYL.0.1999-06-023[M].
- [24] KONDO M, FLUEHR J, MCKEON T, etc. Urban Green Space and Its Impact on Human Health[J/OL]. *International Journal of Environmental Research and Public Health*, 2018, 15(3): 445. <https://doi.org/10.3390/ijerph15030445>.
- [25] TAMOSIUNAS A, GRAZULEVICIENE R, LUKSIENE D, etc. Accessibility and use of urban green spaces, and cardiovascular health: findings from a Kaunas cohort study[J/OL]. *Environmental Health*, 2014, 13(1): 20. <https://doi.org/10.1186/1476-069X-13-20>.
- [26] HARTIG T, MITCHELL R, DE VRIES S, etc. Nature and Health[J/OL]. *Annual Review of Public Health*, 2014, 35(1): 207-228. <https://doi.org/10.1146/annurev-publhealth-032013-182443>.
- [27] GASCON M, TRIGUERO-MAS M, MARTÍNEZ D, etc. Residential green spaces and mortality: A systematic review[J/OL]. *Environment International*, 2016, 86: 60-67. <https://doi.org/10.1016/j.envint.2015.10.013>.
- [28] SANDSTRÖM U G, ANGELSTAM P, KHAKKEE A. Urban comprehensive planning – identifying barriers for the maintenance of functional habitat networks[J/OL]. *Landscape and Urban Planning*, 2006, 75(1-2): 43-57. <https://doi.org/10.1016/j.landurbplan.2004.11.016>.
- [29] KABISCH N, STROHBACH M, HAASE D, etc. Urban green space availability in European cities[J/OL]. *Ecological Indicators*, 2016, 70: 586-596. <https://doi.org/10.1016/j.ecolind.2016.02.029>.
- [30] FAM D. Irrigation of urban green spaces: a review of the environmental, social and economic benefits[M]. Darling Heights, Qld.: Cooperative Research Centre for Irrigation Futures, 2008.
- [31] World | Total including LUCF | Greenhouse Gas (GHG) Emissions | Climate Watch[EB/OL]. [2022-10-06]. <https://www.climatewatchdata.org/>.
- [32] CHURKINA G, BROWN D, KEOLEIAN G. Carbon Stored in Human Settlements: the Conterminous US[C]//AGU Fall Meeting Abstracts: 2008. 2008: B41D-04.
- [33] ZHAO S, ZHU C, ZHOU D, etc. Organic Carbon Storage in China's Urban Areas[J/OL]. *PLoS ONE*, 2013, 8(8): e71975. <https://doi.org/10.1371/journal.pone.0071975>.
- [34] PATAKI D E, ALIG R J, FUNG A S, etc. Urban ecosystems and the North American carbon cycle: URBAN ECOSYSTEMS AND THE NORTH AMERICAN CARBON CYCLE[J/OL]. *Global*

- Change Biology, 2006, 12(11): 2092-2102. <https://doi.org/10.1111/j.1365-2486.2006.01242.x>.
- [35] HUTYRA L R, DUREN R, GURNEY K R, etc. Urbanization and the carbon cycle: Current capabilities and research outlook from the natural sciences perspective[J/OL]. *Earth's Future*, 2014, 2(10): 473-495. <https://doi.org/10.1002/2014EF000255>.
- [36] SCHETKE S, HAASE D, KÖTTER T. Innovative urban land development—A new methodological design for implementing ecological targets into strategic planning of the City of Essen, Germany[J]. *Environmental Impact Assessment Review*, 2012, 32: 195-210.
- [37] SWANWICK C, DUNNETT N, WOOLLEY H. Nature, role and value of green space in towns and cities: An overview[J]. *Built Environment (1978-)*, 2003: 94-106.
- [38] IPCC. Meeting report of the intergovernmental panel on climate change expert meeting on mitigation, sustainability and climate stabilization scenarios[M]//IPCC Working Group III technical support unit. Imperial College London, 2017.
- [39] NG E, REN C. China's adaptation to climate & urban climatic changes: A critical review[J/OL]. *Urban Climate*, 2018, 23: 352-372. <https://doi.org/10.1016/j.uclim.2017.07.006>.
- [40] KHANIAN M, MARSHALL N, ZAKERHAGHIGHI K, etc. Transforming agriculture to climate change in Famenin County, West Iran through a focus on environmental, economic and social factors[J/OL]. *Weather and Climate Extremes*, 2018, 21: 52-64. <https://doi.org/10.1016/j.wace.2018.05.006>.
- [41] Global Warming of 1.5 °C —[EB/OL]. [2022-10-08]. <https://www.ipcc.ch/sr15/>.
- [42] National Development and Reform Commission [EB/OL]. [2022-10-08]. https://www.ndrc.gov.cn/wsdwhfz/202111/t20211111_1303691_ext.html.
- [43] The Paris Agreement | UNFCCC[EB/OL]. [2022-10-08]. <https://unfccc.int/process-and-meetings/the-paris-agreement/the-paris-agreement>.
- [44] www.gov.cn[EB/OL]. [2022-10-08]. http://www.gov.cn/zhengce/zhengceku/2022-01/14/content_5668177.htm.
- [45] GRIMM N B, FAETH S H, GOLUBIEWSKI N E, etc. Global Change and the Ecology of Cities[J/OL]. *Science*, 2008, 319(5864): 756-760. <https://doi.org/10.1126/science.1150195>.
- [46] HUTYRA L R, YOON B, ALBERTI M. Terrestrial carbon stocks across a gradient of urbanization: a study of the Seattle, WA region: URBAN TERRESTRIAL CARBON STOCKS[J/OL]. *Global Change Biology*, 2011, 17(2): 783-797. <https://doi.org/10.1111/j.1365-2486.2010.02238.x>.
- [47] NOWAK D J. Atmospheric Carbon Reduction by Urban Trees[J/OL]. *Journal of Environmental Management*, 1993, 37(3): 207-217. <https://doi.org/10.1006/jema.1993.1017>.
- [48] NOWAK D J, CRANE D E. Carbon storage and sequestration by urban trees in the USA[J/OL]. *Environmental Pollution*, 2002, 116(3): 381-389. [https://doi.org/10.1016/S0269-7491\(01\)00214-7](https://doi.org/10.1016/S0269-7491(01)00214-7).
- [49] NOWAK D J, GREENFIELD E J, HOEHN R E, etc. Carbon storage and sequestration by trees in urban and community areas of the United States[J/OL]. *Environmental Pollution*, 2013, 178: 229-236. <https://doi.org/10.1016/j.envpol.2013.03.019>.
- [50] FRASER L H, PITHER J, JENTSCH A, etc. Worldwide evidence of a unimodal relationship between productivity and plant species richness[J/OL]. *Science*, 2015, 349(6245): 302-305. <https://doi.org/10.1126/science.aab3916>.
- [51] PAQUETTE A, MESSIER C. The effect of biodiversity on tree productivity: from temperate to boreal forests: The effect of biodiversity on the productivity[J/OL]. *Global Ecology and Biogeography*, 2011, 20(1): 170-180. <https://doi.org/10.1111/j.1466-8238.2010.00592.x>.
- [52] HOOPER D U, ADAIR E C, CARDINALE B J, etc. A global synthesis reveals biodiversity loss as a major driver of ecosystem change[J/OL]. *Nature*, 2012, 486(7401): 105-108. <https://doi.org/10.1038/nature11118>.

- [53] KANOWSKI J, CATTERALL C P, WARDELL-JOHNSON G W. Consequences of broadscale timber plantations for biodiversity in cleared rainforest landscapes of tropical and subtropical Australia[J/OL]. *Forest Ecology and Management*, 2005, 208(1-3): 359-372. <https://doi.org/10.1016/j.foreco.2005.01.018>.
- [54] HUNGATE B A, BARBIER E B, ANDO A W, etc. The economic value of grassland species for carbon storage[J/OL]. *Science Advances*, 2017, 3(4): e1601880. <https://doi.org/10.1126/sciadv.1601880>.
- [55] ROSENZWEIG M L, ABRAMSKY Z. How are diversity and productivity related?[J]. *Journal of Environmental Sciences*, 1993: 52-65.
- [56] VAN DER SANDE M T, POORTER L, KOOISTRA L, etc. Biodiversity in species, traits, and structure determines carbon stocks and uptake in tropical forests[J/OL]. *Biotropica*, 2017, 49(5): 593-603. <https://doi.org/10.1111/btp.12453>.
- [57] LUO W, LIANG J, CAZZOLLA GATTI R, etc. Parameterization of biodiversity-productivity relationship and its scale dependency using georeferenced tree-level data[J/OL]. *Journal of Ecology*, 2019, 107(3): 1106-1119. <https://doi.org/10.1111/1365-2745.13129>.
- [58] GUIGAN A, GRAHAM C H, ELITH J, etc. Sensitivity of predictive species distribution models to change in grain size[J/OL]. *Diversity and Distributions*, 2007, 13(3): 332-340. <https://doi.org/10.1111/j.1472-4642.2007.00342.x>.
- [59] THULLER W, POLLOCK L J, GUEGUEN M, etc. From species distributions to meta-communities[J/OL]. *Ecology Letters*, 2015, 18(12): 1321-1328. <https://doi.org/10.1111/ele.12526>.
- [60] TJØRVE E, TURNER W R. The importance of samples and isolates for species-area relationships[J/OL]. *Ecography*, 2009, 32(3): 391-400. <https://doi.org/10.1111/j.1600-0587.2008.05515.x>.
- [61] KESSLER M, HERTEL D, JUNGKUNST H F, etc. Can Joint Carbon and Biodiversity Management in Tropical Agroforestry Landscapes Be Optimized?[J/OL]. *PLoS ONE*, 2012, 7(10): e47192. <https://doi.org/10.1371/journal.pone.0047192>.
- [62] DI MARCO M, WATSON J E M, CURRIE D J, etc. The extent and predictability of the biodiversity-carbon correlation[J/OL]. *Ecology Letters*, 2018, 21(3): 365-375. <https://doi.org/10.1111/ele.12903>.
- [63] GAO T, HEDBLUM M, EMILSSON T, etc. The role of forest stand structure as biodiversity indicator[J/OL]. *Forest Ecology and Management*, 2014, 330: 82-93. <https://doi.org/10.1016/j.foreco.2014.07.007>.
- [64] LINDENMAYER D B, FRANKLIN J F, FISCHER J. General management principles and a checklist of strategies to guide forest biodiversity conservation[J/OL]. *Biological Conservation*, 2006, 131(3): 433-445. <https://doi.org/10.1016/j.biocon.2006.02.019>.
- [65] LECINA-DIAZ J, ALVAREZ A, REGOS A, etc. The positive carbon stocks-biodiversity relationship in forests: co-occurrence and drivers across five subclimates [J/OL]. *Ecological Applications*, 2018, 28(6): 1481-1493. <https://doi.org/10.1002/eap.1749>.
- [66] ZHANG G, GANGULY S, NEMANI R R, etc. Estimation of forest aboveground biomass in California using canopy height and leaf area index estimated from satellite data[J/OL]. *Remote Sensing of Environment*, 2014, 151: 44-56. <https://doi.org/10.1016/j.rse.2014.01.025>.
- [67] RUNNING S W, NEMANI R, HEINSCH F A, etc. A Continuous Satellite-Derived Measure of Global Terrestrial Primary Production[J/OL]. *BioScience*, 2004, 54(6): 547. [https://doi.org/10.1641/0006-3568\(2004\)054\[0547:ACSMOG\]2.0.CO;2](https://doi.org/10.1641/0006-3568(2004)054[0547:ACSMOG]2.0.CO;2).
- [68] ROUSE W, HAAS R H. MONITORING VEGETATION SYSTEMS IN THE GREAT PLAINS WITH ERTS[J].
- [69] RICHARDSON A J. Distinguishing Vegetation from Soil Background Information[J].

- [70] KAUTH R J, THOMAS G S. The Tasselled Cap -- A Graphic Description of the Spectral-Temporal Development of Agricultural Crops as Seen by LANDSAT[J].
- [71] SARKER L R, NICHOL J E. Improved forest biomass estimates using ALOS AVNIR-2 texture indices[J/OL]. *Remote Sensing of Environment*, 2011, 115(4): 968-977. <https://doi.org/10.1016/j.rse.2010.11.010>.
- [72] LU D. Aboveground biomass estimation using Landsat TM data in the Brazilian Amazon[J/OL]. *International Journal of Remote Sensing*, 2005, 26(12): 2509-2525. <https://doi.org/10.1080/01431160500142145>.
- [73] ECKERT S. Improved Forest Biomass and Carbon Estimations Using Texture Measures from WorldView-2 Satellite Data[J/OL]. *Remote Sensing*, 2012, 4(4): 810-829. <https://doi.org/10.3390/rs4040810>.
- [74] BOYD D S, DANSON F M. Satellite remote sensing of forest resources: three decades of research development[J/OL]. *Progress in Physical Geography: Earth and Environment*, 2005, 29(1): 1-26. <https://doi.org/10.1191/0309133305pp432ra>.
- [75] HARALICK R M, SHANMUGAM K, DINSTEN I. Textural Features for Image Classification[J/OL]. *IEEE Transactions on Systems, Man, and Cybernetics*, 1973, SMC-3(6): 610-621. <https://doi.org/10.1109/TSMC.1973.4309314>.
- [76] KUPLICH T M, CURRAN P J, ATKINSON P M. Relating SAR image texture to the biomass of regenerating tropical forests[J/OL]. *International Journal of Remote Sensing*, 2005, 26(21): 4829-4854. <https://doi.org/10.1080/01431160500239107>.
- [77] KELSEY K, NEFF J. Estimates of Aboveground Biomass from Texture Analysis of Landsat Imagery[J/OL]. *Remote Sensing*, 2014, 6(7): 6407-6422. <https://doi.org/10.3390/rs6076407>.
- [78] VAN DER SANDEN J J, HOEKMAN D H. Review of relationships between grey-tone co-occurrence, semivariance, and autocorrelation based image texture analysis approaches[J/OL]. *Canadian Journal of Remote Sensing*, 2005, 31(3): 207-213. <https://doi.org/10.5589/m05-008>.
- [79] FRANKLIN S E, WULDER M A, GERYLO G R. Texture analysis of IKONOS panchromatic data for Douglas-fir forest age class separability in British Columbia[J/OL]. *International Journal of Remote Sensing*, 2001, 22(13): 2627-2632. <https://doi.org/10.1080/01431160120769>.
- [80] CHEN* D, STOW D A, GONG P. Examining the effect of spatial resolution and texture window size on classification accuracy: an urban environment case[J/OL]. *International Journal of Remote Sensing*, 2004, 25(11): 2177-2192. <https://doi.org/10.1080/01431160310001618464>.
- [81] FUCHS H, MAGDON P, KLEINN C, etc. Estimating aboveground carbon in a catchment of the Siberian forest tundra: Combining satellite imagery and field inventory[J/OL]. *Remote Sensing of Environment*, 2009, 113(3): 518-531. <https://doi.org/10.1016/j.rse.2008.07.017>.
- [82] GUO X, COOPS N C, TOMPALSKI P, etc. Regional mapping of vegetation structure for biodiversity monitoring using airborne lidar data[J/OL]. *Ecological Informatics*, 2017, 38: 50-61. <https://doi.org/10.1016/j.ecoinf.2017.01.005>.
- [83] ZHANG Y, SHAO Z. Assessing of Urban Vegetation Biomass in Combination with LiDAR and High-resolution Remote Sensing Images[J/OL]. *International Journal of Remote Sensing*, 2021, 42(3): 964-985. <https://doi.org/10.1080/01431161.2020.1820618>.
- [84] DUBAYAH R O, DRAKE J B. 1 Lidar Remote Sensing for Forestry Applications[J]. 10.
- [85] GAUTAM B R, TOKOLA T, HAMALAINEN J, etc. Integration of airborne LiDAR, satellite imagery, and field measurements using a two-phase sampling method for forest biomass estimation in tropical forests[J]. 7.
- [86] MEANS J. Use of Large-Footprint Scanning Airborne Lidar To Estimate Forest Stand Characteristics in the Western Cascades of Oregon[J/OL]. *Remote Sensing of Environment*, 1999, 67(3): 298-308.

- [https://doi.org/10.1016/S0034-4257\(98\)00091-1](https://doi.org/10.1016/S0034-4257(98)00091-1).
- [87] NI-MEISTER W, LEE S, STRAHLER A H, etc. Assessing general relationships between aboveground biomass and vegetation structure parameters for improved carbon estimate from lidar remote sensing: ABOVEGROUND BIOMASS ESTIMATE FROM LIDAR[J/OL]. *Journal of Geophysical Research: Biogeosciences*, 2010, 115(G2): n/a-n/a. <https://doi.org/10.1029/2009JG000936>.
- [88] HALL S A, BURKE I C, BOX D O, etc. Estimating stand structure using discrete-return lidar: an example from low density, fire prone ponderosa pine forests[J/OL]. *Forest Ecology and Management*, 2005, 208(1-3): 189-209. <https://doi.org/10.1016/j.foreco.2004.12.001>.
- [89] LI W, GUO Q, JAKUBOWSKI M K, etc. A New Method for Segmenting Individual Trees from the Lidar Point Cloud[J/OL]. *Photogrammetric Engineering & Remote Sensing*, 2012, 78(1): 75-84. <https://doi.org/10.14358/PERS.78.1.75>.
- [90] KANKARE V, VASTARANTA M, HOLOPAINEN M, etc. Retrieval of Forest Aboveground Biomass and Stem Volume with Airborne Scanning LiDAR[J/OL]. *Remote Sensing*, 2013, 5(5): 2257-2274. <https://doi.org/10.3390/rs5052257>.
- [91] ZHANG F, TIAN X, ZHANG H, etc. Estimation of Aboveground Carbon Density of Forests Using Deep Learning and Multisource Remote Sensing[J/OL]. *Remote Sensing*, 2022, 14(13): 3022. <https://doi.org/10.3390/rs14133022>.
- [92] CHAVE J, ANDALO C, BROWN S, etc. Tree allometry and improved estimation of carbon stocks and balance in tropical forests[J/OL]. *Oecologia*, 2005, 145(1): 87-99. <https://doi.org/10.1007/s00442-005-0100-x>.
- [93] CIAIS P, SABINE C, BALA G, etc. Carbon and other biogeochemical cycles[M]//Climate change 2013: the physical science basis. Contribution of Working Group I to the Fifth Assessment Report of the Intergovernmental Panel on Climate Change. Cambridge University Press, 2014: 465-570.
- [94] DEVRIES B, VERBESSELT J, KOOISTRA L, etc. Robust monitoring of small-scale forest disturbances in a tropical montane forest using Landsat time series[J/OL]. *Remote Sensing of Environment*, 2015, 161: 107-121. <https://doi.org/10.1016/j.rse.2015.02.012>.
- [95] CHEN W, LI J, ZHANG Y, etc. Relating Biomass and Leaf Area Index to Non-destructive Measurements in Order to Monitor Changes in Arctic Vegetation[J/OL]. *ARCTIC*, 2009, 62(3): 281-294. <https://doi.org/10.14430/arctic148>.
- [96] WALKER A P, DE KAUWE M G, BASTOS A, etc. Integrating the evidence for a terrestrial carbon sink caused by increasing atmospheric CO₂[J/OL]. *New Phytologist*, 2021, 229(5): 2413-2445. <https://doi.org/10.1111/nph.16866>.
- [97] ZHANG Z, GAO X, ZHANG S, etc. Urban development enhances soil organic carbon storage through increasing urban vegetation[J/OL]. *Journal of Environmental Management*, 2022, 312: 114922. <https://doi.org/10.1016/j.jenvman.2022.114922>.
- [98] SONTI N F, GROFFMAN P M, NOWAK D J, etc. Urban net primary production: Concepts, field methods, and BALTIMORE, MARYLAND, USA case study[J/OL]. *Ecological Applications*, 2022, 32(4)[2023-01-31]. <https://onlinelibrary.wiley.com/doi/10.1002/eap.2562>.
- [99] VELASCO E, CHEN K W. Carbon storage estimation of tropical urban trees by an improved allometric model for aboveground biomass based on terrestrial laser scanning[J/OL]. *Urban Forestry & Urban Greening*, 2019, 44: 126387. <https://doi.org/10.1016/j.ufug.2019.126387>.
- [100] WILLIAMS L J, CAVENDER-BARES J, TOWNSEND P A, etc. Remote spectral detection of biodiversity effects on forest biomass[J/OL]. *Nature Ecology & Evolution*, 2020, 5(1): 46-54. <https://doi.org/10.1038/s41559-020-01329-4>.
- [101] SHARIFI A. Co-benefits and synergies between urban climate change mitigation and adaptation

- measures: A literature review[J/OL]. *Science of The Total Environment*, 2021, 750: 141642. <https://doi.org/10.1016/j.scitotenv.2020.141642>.
- [102] Shi, Ge and Jin, etc. Advances in carbon sequestration in urban vegetation [J]. *Forestry Science*, 2016, 52(06): 122-129.
- [103] VENTER Z S, SHACKLETON C M, VAN STADEN F, etc. Green Apartheid: Urban green infrastructure remains unequally distributed across income and race geographies in South Africa[J/OL]. *Landscape and Urban Planning*, 2020, 203: 103889. <https://doi.org/10.1016/j.landurbplan.2020.103889>.
- [104] TANG L, CHEN X, CAI X, etc. Disentangling the roles of land-use-related drivers on vegetation greenness across China[J/OL]. *Environmental Research Letters*, 2021, 16(12): 124033. <https://doi.org/10.1088/1748-9326/ac37d2>.
- [105] ARDILA J P, TOLPEKIN V A, BIJKER W, etc. Markov-random-field-based super-resolution mapping for identification of urban trees in VHR images[J/OL]. *ISPRS Journal of Photogrammetry and Remote Sensing*, 2011, 66(6): 762-775. <https://doi.org/10.1016/j.isprsjprs.2011.08.002>.
- [106] TIMILSINA S, ARYAL J, KIRKPATRICK J B. Mapping Urban Tree Cover Changes Using Object-Based Convolution Neural Network (OB-CNN) [J/OL]. *Remote Sensing*, 2020, 12(18): 3017. <https://doi.org/10.3390/rs12183017>.
- [107] ZHAO J, LIU D, CAO Y, etc. An integrated remote sensing and model approach for assessing forest carbon fluxes in China[J/OL]. *Science of The Total Environment*, 2022, 811: 152480. <https://doi.org/10.1016/j.scitotenv.2021.152480>.
- [108] TANG X, ZHAO X, BAI Y, etc. Carbon pools in China's terrestrial ecosystems: New estimates based on an intensive field survey[J/OL]. *Proceedings of the National Academy of Sciences*, 2018, 115(16): 4021-4026. <https://doi.org/10.1073/pnas.1700291115>.
- [109] PENG L, CHEN S, LIU Y, etc. Application of CITY-green model in benefit assessment of Nanjing urban green space in carbon fixation and runoff reduction[J/OL]. *Frontiers of Forestry in China*, 2008, 3(2): 177-182. <https://doi.org/10.1007/s11461-008-0035-6>.
- [110] MA J, LI X, BAOQUAN J, etc. Spatial variation analysis of urban forest vegetation carbon storage and sequestration in built-up areas of Beijing based on i-Tree Eco and Kriging[J/OL]. *Urban Forestry & Urban Greening*, 2021, 66: 127413. <https://doi.org/10.1016/j.ufug.2021.127413>.
- [111] MCHALE M R, BURKE I C, LEFSKY M A, etc. Urban forest biomass estimates: is it important to use allometric relationships developed specifically for urban trees?[J/OL]. *Urban Ecosystems*, 2009, 12(1): 95-113. <https://doi.org/10.1007/s11252-009-0081-3>.
- [112] RAUM S, HAND K L, HALL C, etc. Achieving impact from ecosystem assessment and valuation of urban greenspace: The case of i-Tree Eco in Great Britain[J/OL]. *Landscape and Urban Planning*, 2019, 190: 103590. <https://doi.org/10.1016/j.landurbplan.2019.103590>.
- [113] GONG W, HUANG C, HOUGHTON R A, etc. Carbon fluxes from contemporary forest disturbances in North Carolina evaluated using a grid-based carbon accounting model and fine resolution remote sensing products[J/OL]. *Science of Remote Sensing*, 2022, 5: 100042. <https://doi.org/10.1016/j.srs.2022.100042>.
- [114] ZHUANG Q, SHAO Z, LI D, etc. Unequal weakening of urbanization and soil salinization on vegetation production capacity[J/OL]. *Geoderma*, 2022, 411: 115712. <https://doi.org/10.1016/j.geoderma.2022.115712>.
- [115] HIRABAYASHI S, KROLL C N, NOWAK D J, etc. i-Tree Eco Dry Deposition Model Descriptions[J].
- [116] HAWKER L, UHE P, PAULO L, etc. A 30 m global map of elevation with forests and buildings removed[J/OL]. *Environmental Research Letters*, 2022, 17(2): 024016. <https://doi.org/10.1088/1748->

- 9326/ac4d4f.
- [117] Zhengzhou city[EB/OL]// Baidu. [2023-01-15].
<https://baike.baidu.com/item/%E9%83%91%E5%B7%9E%E5%B8%82/2439317?fr=aladdin>.
- [118] [Henan Province] Provincial Key Protected Plant List Search [EB/OL]. [2023-01-15].
<http://app.gjzfwf.gov.cn/jmopen/webapp/html5/hnszdbhzwmlcxpcd/index.html>.
- [119] National key protection of wild plants list_Forestry_Chinese government website [EB/OL]. [2023-01-15]. http://www.gov.cn/zhengce/zhengceku/2021-09/09/content_5636409.htm.
- [120] Study on the estimation of above-ground carbon storage in urban green space in Xi'an - China Knowledge Network [EB/OL]. [2023-02-07].
<https://kns.cnki.net/kcms2/article/abstract?v=3uoqIhG8C447WN1SO36whLpCgh0R0Z-iv9r0YoQXiId4v9BfOE9rDvw120oAZuqtVUmxF5VJ4WxrdOtEnF-wNx7y7IJCuaAN&uniplatform=NZKPT>.
- [121] Carbon sequestration in temperate grassland ecosystems and the effects of management, climate and elevated CO₂ concentrations - Jones - 2004 - New Phytologist - Wiley Online Library[EB/OL]. [2023-02-07]. <https://nph.onlinelibrary.wiley.com/doi/full/10.1111/j.1469-8137.2004.01201.x>.
- [122] Study on the net carbon stock of urban landscape in Beijing based on biomass measurement - China Knowledge Network [EB/OL]. [2023-02-07].
https://kns.cnki.net/kcms2/article/abstract?v=3uoqIhG8C447WN1SO36whNHQvLEhcOy4v9J5uF5OhrnQEjv_r9SmqVzvuk57R1IbloSpdelj1ahKBhPu2heCiEQH8I5ZZs5&uniplatform=NZKPT.
- [123] SHI-LONG P, JING-YUN F, JIN-SHENG H, etc. SPATIAL DISTRIBUTION OF GRASSLAND BIOMASS IN CHINA[J/OL]. Chinese Journal of Plant Ecology, 2004, 28(4): 491-498.
<https://doi.org/10.17521/cjpe.2004.0067>.
- [124] NEUMANN M, MORENO A, MUES V, etc. Comparison of carbon estimation methods for European forests[J/OL]. Forest Ecology and Management, 2016, 361: 397-420.
<https://doi.org/10.1016/j.foreco.2015.11.016>.
- [125] SUN W, LIU X. Review on carbon storage estimation of forest ecosystem and applications in China[J/OL]. Forest Ecosystems, 2020, 7(1): 4. <https://doi.org/10.1186/s40663-019-0210-2>.
- [126] CONRAD O, BECHTEL B, BOCK M, etc. System for Automated Geoscientific Analyses (SAGA) v. 2.1.4[J/OL]. Geoscientific Model Development, 2015, 8(7): 1991-2007.
<https://doi.org/10.5194/gmd-8-1991-2015>.
- [127] SINGH J S, YADAVA P S. Seasonal Variation in Composition, Plant Biomass, and Net Primary Productivity of a Tropical Grassland at Kurukshetra, India[J/OL]. Ecological Monographs, 1974, 44(3): 351-376. <https://doi.org/10.2307/2937034>.
- [128] CUTLER M E J, BOYD D S, FOODY G M, etc. Estimating tropical forest biomass with a combination of SAR image texture and Landsat TM data: An assessment of predictions between regions[J/OL]. ISPRS Journal of Photogrammetry and Remote Sensing, 2012, 70: 66-77.
<https://doi.org/10.1016/j.isprsjprs.2012.03.011>.
- [129] CLAUSI D A. An analysis of co-occurrence texture statistics as a function of grey level quantization[J]. Canadian Journal of Remote Sensing, 2002, 28(1): 18.
- [130] MYINT S W, GOBER P, BRAZEL A, etc. Per-pixel vs. object-based classification of urban land cover extraction using high spatial resolution imagery[J/OL]. Remote Sensing of Environment, 2011, 115(5): 1145-1161. <https://doi.org/10.1016/j.rse.2010.12.017>.
- [131] QIAN Y, ZHOU W, YU W, etc. Quantifying spatiotemporal pattern of urban greenspace: new insights from high resolution data[J/OL]. Landscape Ecology, 2015, 30(7): 1165-1173.
<https://doi.org/10.1007/s10980-015-0195-3>.
- [132] AHMAD A, QUEGAN S. Analysis of Maximum Likelihood Classification on Multispectral Data[J].

- 12.
- [133] FOODY G M. Status of land cover classification accuracy assessment[J/OL]. *Remote Sensing of Environment*, 2002, 80(1): 185-201. [https://doi.org/10.1016/S0034-4257\(01\)00295-4](https://doi.org/10.1016/S0034-4257(01)00295-4).
- [134] HOCKETT C F, SHANNON C L, WEAVER W. The Mathematical Theory of Communication[J/OL]. *Language*, 1953, 29(1): 69. <https://doi.org/10.2307/410457>.
- [135] SIMPSON E H. Measurement of Diversity[J/OL]. *Nature*, 1949, 163(4148): 688-688. <https://doi.org/10.1038/163688a0>.
- [136] MAGURRAN A E. *Ecological Diversity and Its Measurement*[M]. Princeton University Press, 1988.
- [137] MAECHLER M, ORIGINAL) P R (Fortran, ORIGINAL) A S (S, etc. cluster: “Finding Groups in Data”: Cluster Analysis Extended Rousseeuw et al.[CP/OL]. (2022-08-22)[2023-02-09]. <https://CRAN.R-project.org/package=cluster>.
- [138] COHEN P, COHEN P, WEST S G, etc. *Applied Multiple Regression/Correlation Analysis for the Behavioral Sciences*[M/OL]. New York: Psychology Press, 2014. <https://doi.org/10.4324/9781410606266>.
- [139] KUK A Y C. All subsets regression in a proportional hazards model[J]. 6.
- [140] R: The R Project for Statistical Computing[EB/OL]. [2022-08-16]. <https://www.r-project.org/>.
- [141] BURNHAM K P, ANDERSON D R. Multi-model Inference: Understanding AIC and BIC in Model Selection[J/OL]. *Sociological Methods & Research*, 2004, 33(2): 261-304. <https://doi.org/10.1177/0049124104268644>.
- [142] ULLMAN J B, BENTLER P M. *Structural Equation Modeling*[J]. 30.
- [143] ROSSEEL Y, JORGENSEN T D, ROCKWOOD N, etc. *Lavaan: Latent Variable Analysis*[CP/OL]. (2022-07-04)[2022-08-16]. <https://CRAN.R-project.org/package=lavaan>.
- [144] GRACE J B. *Structural Equation Modeling and Natural Systems*[M]. Cambridge University Press, 2006.
- [145] WALSH C, NALLY R M. hier-part: Hierarchical Partitioning[CP/OL]. (2020-03-03)[2022-08-16]. <https://CRAN.R-project.org/package=hier.part>.
- [146] NALLY R M. Regression and model-building in conservation biology, biogeography and ecology: The distinction between – and reconciliation of – ‘predictive’ and ‘explanatory’ models[J]. 17.
- [147] CHEN W Y. The role of urban green infrastructure in offsetting carbon emissions in 35 major Chinese cities: A nationwide estimate[J/OL]. *Cities*, 2015, 44: 112-120. <https://doi.org/10.1016/j.cities.2015.01.005>.
- [148] SHI Y. *Vegetation structure characteristics and carbon uptake of urban built-up area in China*[J]. Doctor thesis, Zhejiang Univ., Hangzhou, China, 2013.
- [149] SUN Y, XIE S, ZHAO S. Valuing urban green spaces in mitigating climate change: A city-wide estimate of aboveground carbon stored in urban green spaces of China’s Capital[J/OL]. *Global Change Biology*, 2019, 25(5): 1717-1732. <https://doi.org/10.1111/gcb.14566>.
- [150] YANG J, JI X, DEANE D, etc. Spatiotemporal Distribution and Driving Factors of Forest Biomass Carbon Storage in China: 1977–2013[J/OL]. *Forests*, 2017, 8(7): 263. <https://doi.org/10.3390/f8070263>.
- [151] CALLADINE J, JARRETT D, WILSON M, etc. Stand structure and breeding birds in managed Scots pine forests: Some likely long-term implications for continuous cover forestry[J/OL]. *Forest Ecology and Management*, 2017, 397: 174-184. <https://doi.org/10.1016/j.foreco.2017.04.039>.
- [152] VIERLING K T, VIERLING L A, GOULD W A, etc. Lidar: shedding new light on habitat characterization and modeling[J/OL]. *Frontiers in Ecology and the Environment*, 2008, 6(2): 90-98. <https://doi.org/10.1890/070001>.
- [153] CASTRO-IZAGUIRRE N, CHI X, BARUFFOL M, etc. Tree Diversity Enhances Stand Carbon

- Storage but Not Leaf Area in a Subtropical Forest[J/OL]. PLOS ONE, 2016, 11(12): e0167771. <https://doi.org/10.1371/journal.pone.0167771>.
- [154] LASKY J R, URIARTE M, BOUKILI V K, etc. The relationship between tree biodiversity and biomass dynamics changes with tropical forest succession[J/OL]. Ecology Letters, 2014, 17(9): 1158-1167. <https://doi.org/10.1111/ele.12322>.
- [155] DAVIDSON E A, TRUMBORE S E, AMUNDSON R. Soil warming and organic carbon content[J/OL]. Nature, 2000, 408(6814): 789-790. <https://doi.org/10.1038/35048672>.
- [156] GAITÁN J J, OLIVA G E, BRAN D E, etc. Vegetation structure is as important as climate for explaining ecosystem function across Patagonian rangelands[J/OL]. Journal of Ecology, 2014, 102(6): 1419-1428. <https://doi.org/10.1111/1365-2745.12273>.
- [157] FANG B, YU S, WANG Y, etc. Allelopathic effects of Eucalyptus urophylla on ten tree species in south China[J/OL]. Agroforestry Systems, 2009, 76(2): 401-408. <https://doi.org/10.1007/s10457-008-9184-8>.
- [158] ZHANG C, FU S. Allelopathic effects of eucalyptus and the establishment of mixed stands of eucalyptus and native species[J/OL]. Forest Ecology and Management, 2009, 258(7): 1391-1396. <https://doi.org/10.1016/j.foreco.2009.06.045>.
- [159] JIM C Y, CHEN W Y. Ecosystem services and valuation of urban forests in China[J/OL]. Cities, 2009, 26(4): 187-194. <https://doi.org/10.1016/j.cities.2009.03.003>.
- [160] GRIME J P. Benefits of plant diversity to ecosystems: immediate, filter and founder effects[J/OL]. Journal of Ecology, 1998, 86(6): 902-910. <https://doi.org/10.1046/j.1365-2745.1998.00306.x>.
- [161] YAO Z, LIU J, ZHAO X, etc. Spatial dynamics of aboveground carbon stock in urban green space: a case study of Xi'an, China[J/OL]. Journal of Arid Land, 2015, 7(3): 350-360. <https://doi.org/10.1007/s40333-014-0082-9>.
- [162] SHAN Y, GUAN Y, HANG Y, etc. City-level emission peak and drivers in China[J/OL]. Science Bulletin, 2022: S2095927322003838. <https://doi.org/10.1016/j.scib.2022.08.024>.
- [163] CURRIE W S, KIGER S, NASSAUER J I, etc. Multi-scale heterogeneity in vegetation and soil carbon in exurban residential land of southeastern MICHIGAN, USA[J/OL]. Ecological Applications, 2016, 26(5): 1421-1436. <https://doi.org/10.1890/15-0817>.
- [164] TIMILSINA N, STAUDHAMMER C L, ESCOBEDO F J, etc. Tree biomass, wood waste yield, and carbon storage changes in an urban forest[J/OL]. Landscape and Urban Planning, 2014, 127: 18-27. <https://doi.org/10.1016/j.landurbplan.2014.04.003>.
- [165] BROWN M E, PINZON J E, DIDAN K, etc. Evaluation of the consistency of long-term NDVI time series derived from AVHRR, SPOT-vegetation, SeaWiFS, MODIS, and Landsat ETM+ sensors[J/OL]. IEEE Transactions on Geoscience and Remote Sensing, 2006, 44(7): 1787-1793. <https://doi.org/10.1109/TGRS.2005.860205>.
- [166] GARRIGUES S, ALLARD D, BARET F, etc. Influence of landscape spatial heterogeneity on the non-linear estimation of leaf area index from moderate spatial resolution remote sensing data[J/OL]. Remote Sensing of Environment, 2006, 105(4): 286-298. <https://doi.org/10.1016/j.rse.2006.07.013>.
- [167] HUETE A R, HUIQING LIU, VAN LEEUWEN W J D. The use of vegetation indices in forested regions: issues of linearity and saturation[C/OL]/IGARSS'97. 1997 IEEE International Geoscience and Remote Sensing Symposium Proceedings. Remote Sensing - A Scientific Vision for Sustainable Development: Singapore: IEEE, 1997: 1966-1968[2022-08-07]. <http://ieeexplore.ieee.org/document/609169/>.
- [168] HAWBAKER T J, KEULER N S, LESAK A A, etc. Improved estimates of forest vegetation structure and biomass with a LiDAR-optimized sampling design: LIDAR-OPTIMIZED SAMPLING[J/OL]. Journal of Geophysical Research: Biogeosciences, 2009, 114(G2).

- <https://doi.org/10.1029/2008JG000870>.
- [169] ESTES L, ELSEN PR, TREUER T, etc. The spatial and temporal domains of modern ecology[J/OL]. *Nature Ecology & Evolution*, 2018, 2(5): 819-826. <https://doi.org/10.1038/s41559-018-0524-4>.
- [170] HAWKINS B A. Eight (and a half) deadly sins of spatial analysis: Spatial analysis[J/OL]. *Journal of Biogeography*, 2012, 39(1): 1-9. <https://doi.org/10.1111/j.1365-2699.2011.02637.x>.
- [171] MENCUCCINI M, MARTÍNEZ-VILALTA J, VANDERKLEIN D, etc. Size-mediated ageing reduces vigour in trees: Size reduces vigour in tall trees[J/OL]. *Ecology Letters*, 2005, 8(11): 1183-1190. <https://doi.org/10.1111/j.1461-0248.2005.00819.x>.
- [172] KILGORE G. How to Tell How Old a Tree Is (Trick Works Every Time on All Tree Types)[EB/OL]//8 Billion Trees: Carbon Offset Projects & Ecological Footprint Calculators. (2022-07-25)[2023-02-19]. <https://8billiontrees.com/trees/how-to-tell-how-old-a-tree-is/>.
- [173] Pi Can Help You Determine the Age of Your Trees [EB/OL]//HowStuffWorks. (2020-10-05)[2023-02-19]. <https://home.howstuffworks.com/age-of-tree.htm>.
- [174] Tree Age Calculation [EB/OL]. [2023-02-19]. <https://www.friendsofthewildflowergarden.org/pages/photosubpages/photoinfopages/treeagecalculator.html>.
- [175] Tree Age Calculator | Good Calculators[EB/OL]. [2023-02-19]. <https://goodcalculators.com/tree-age-calculator/>.
- [176] Tree Age Calculator - How Old Is a Tree?[EB/OL]. [2023-02-19]. <https://www.omnicalculator.com/biology/tree-age>.
- [177] Welcome[EB/OL]. [2023-02-19]. <https://www.isa-arbor.com/>.
- [178] NAGENDRA H, ROCCHINI D, GHATE R, etc. Assessing Plant Diversity in a Dry Tropical Forest: Comparing the Utility of Landsat and Ikonos Satellite Images[J/OL]. *Remote Sensing*, 2010, 2(2): 478-496. <https://doi.org/10.3390/rs2020478>.
- [179] CAZZOLLA GATTI R. A century of biodiversity: some open questions and some answers[J/OL]. *Biodiversity*, 2017, 18(4): 175-185. <https://doi.org/10.1080/14888386.2017.1407257>.
- [180] MARVIN D C, ASNER G P, KNAPP D E, etc. Amazonian landscapes and the bias in field studies of forest structure and biomass[J/OL]. *Proceedings of the National Academy of Sciences*, 2014, 111(48)[2022-08-30]. <https://pnas.org/doi/full/10.1073/pnas.1412999111>.
- [181] LEVIN S A. The Problem of Pattern and Scale in Ecology: The Robert H. MacArthur Award Lecture[J/OL]. *Ecology*, 1992, 73(6): 1943-1967. <https://doi.org/10.2307/1941447>.
- [182] FALEIRO F V, MACHADO R B, LOYOLA R D. Defining spatial conservation priorities in the face of land-use and climate change[J/OL]. *Biological Conservation*, 2013, 158: 248-257. <https://doi.org/10.1016/j.biocon.2012.09.020>.
- [183] PALMER M W, WHITE P S. Scale Dependence and the Species-Area Relationship[J/OL]. *The American Naturalist*, 1994, 144(5): 717-740. <https://doi.org/10.1086/285704>.
- [184] LIANG J, CROWTHER T W, PICARD N, etc. Positive biodiversity-productivity relationship predominant in global forests[J/OL]. *Science*, 2016, 354(6309): aaf8957. <https://doi.org/10.1126/science.aaf8957>.
- [185] SCHEPASCHENKO D, SHVIDENKO A, USOLTSEV V, etc. A dataset of forest biomass structure for Eurasia[J/OL]. *Scientific Data*, 2017, 4(1): 170070. <https://doi.org/10.1038/sdata.2017.70>.
- [186] CLEVELAND C C, TAYLOR P, CHADWICK K D, etc. A comparison of plot-based satellite and Earth system model estimates of tropical forest net primary production: NPP IN TROPICAL FORESTS[J/OL]. *Global Biogeochemical Cycles*, 2015, 29(5): 626-644. <https://doi.org/10.1002/2014GB005022>.
- [187] SULLIVAN M J P, TALBOT J, LEWIS S L, etc. Diversity and carbon storage across the tropical

- forest biome[J/OL]. *Scientific Reports*, 2017, 7(1): 39102. <https://doi.org/10.1038/srep39102>.
- [188] VILÀ M, VAYREDA J, COMAS L, etc. Species richness and wood production: a positive association in Mediterranean forests[J/OL]. *Ecology Letters*, 2007, 10(3): 241-250. <https://doi.org/10.1111/j.1461-0248.2007.01016.x>.
- [189] YOUNG B, LIANG J, STUART CHAPIN F. Effects of species and tree size diversity on recruitment in the Alaskan boreal forest: A geospatial approach[J/OL]. *Forest Ecology and Management*, 2011, 262(8): 1608-1617. <https://doi.org/10.1016/j.foreco.2011.07.011>.
- [190] KEIL P, STORCH D, JETZ W. On the decline of biodiversity due to area loss[J/OL]. *Nature Communications*, 2015, 6(1): 8837. <https://doi.org/10.1038/ncomms9837>.
- [191] NEKOLA J C, WHITE P S. The distance decay of similarity in biogeography and ecology[J/OL]. *Journal of Biogeography*, 1999, 26(4): 867-878. <https://doi.org/10.1046/j.1365-2699.1999.00305.x>.
- [192] WHITTAKER R J, WILLIS K J, FIELD R. Scale and species richness: towards a general, hierarchical theory of species diversity: Towards a general theory of diversity[J/OL]. *Journal of Biogeography*, 2001, 28(4): 453-470. <https://doi.org/10.1046/j.1365-2699.2001.00563.x>.
- [193] LIU X, TROGISCH S, HE J S, etc. Tree species richness increases ecosystem carbon storage in subtropical forests[J/OL]. *Proceedings of the Royal Society B: Biological Sciences*, 2018, 285(1885): 20181240. <https://doi.org/10.1098/rspb.2018.1240>.
- [194] TILMAN D, LEHMAN C L, THOMSON K T. Plant diversity and ecosystem productivity: Theoretical considerations[J/OL]. *Proceedings of the National Academy of Sciences*, 1997, 94(5): 1857-1861. <https://doi.org/10.1073/pnas.94.5.1857>.
- [195] LOREAU M. Biodiversity and ecosystem functioning: recent theoretical advances[J/OL]. *Oikos*, 2000, 91(1): 3-17. <https://doi.org/10.1034/j.1600-0706.2000.910101.x>.
- [196] PHILLIPS O L, HALL P, GENTRY A H, etc. Dynamics and species richness of tropical rain forests.[J/OL]. *Proceedings of the National Academy of Sciences*, 1994, 91(7): 2805-2809. <https://doi.org/10.1073/pnas.91.7.2805>.
- [197] WIRTH C, GLEIXNER G, HEIMANN M. Old-Growth Forests: Function, Fate and Value: 207 [M/OL]. Berlin, Heidelberg: Springer Berlin Heidelberg, 2009[2023-02-21]. <https://link.springer.com/10.1007/978-3-540-92706-8>.
- [198] BRZOSTEK E R, DRAGONI D, SCHMID H P, etc. Chronic water stress reduces tree growth and the carbon sink of deciduous hardwood forests[J/OL]. *Global Change Biology*, 2014, 20(8): 2531-2539. <https://doi.org/10.1111/gcb.12528>.
- [199] VAN MANTGEM P J, STEPHENSON N L, BYRNE J C, etc. Widespread Increase of Tree Mortality Rates in the Western United States[J/OL]. *Science*, 2009, 323(5913): 521-524. <https://doi.org/10.1126/science.1165000>.
- [200] HARPER K A, MACDONALD S E, BURTON P J, etc. Edge Influence on Forest Structure and Composition in Fragmented Landscapes[J/OL]. *Conservation Biology*, 2005, 19(3): 768-782. <https://doi.org/10.1111/j.1523-1739.2005.00045.x>.
- [201] Analysis of the typology of urban parks and their relationship with their functions: the example of urban parks in Beijing [EB/OL]. [2023-02-22]. <http://www.dlyj.ac.cn/CN/10.11821/dlyj201310018>.

10 Appendix

Table 10-1 Landscape plant use statistics

Latin name	Evergreen/Deciduous	Flowering	Fruiting	Colorful	Trunk observation
<i>Ilex chinensis</i> Sims	Evergreen	√	√		
<i>Prunus persica</i>	Deciduous	√	√		
<i>Lonicera maackii</i> (Rupr.) Maxim.	Deciduous	√	√		
<i>Pyrus spp</i>	Deciduous	√	√		
<i>Lonicera japonica</i>	Evergreen	√			
<i>Gardenia jasminoides</i> Ellis	Evergreen	√			
<i>Amygdalus triloba</i>	Deciduous	√			
<i>Albizia julibrissin</i> Durazz.	Deciduous	√			
<i>Amygdalus persica</i>	Deciduous	√			
<i>Chimonanthus praecox</i>	Deciduous	√			
<i>Prunus × blireana</i> cv. Meiren	Deciduous	√			
<i>Prunus</i> subg. <i>Cerasus</i>	Deciduous	√			
<i>Malus halliana</i>	Deciduous	√			
<i>Photinia serratifolia</i>	Evergreen	√			
<i>Prunus mume</i>	Deciduous	√			
<i>Lagerstroemia indica</i>	Deciduous	√			
<i>Nerium oleander</i>	Evergreen	√			
<i>Rhododendron simsii</i>	Evergreen	√			
<i>Bothrocaryum controversum</i>	Deciduous	√			
<i>Syringa oblata</i>	Deciduous	√			
<i>Prunus serrulata</i> var. <i>lannesiana</i>	Deciduous	√			
<i>Lonicera japonica</i>	Evergreen	√			
<i>Syringa oblata</i>	Deciduous	√			
<i>Chaenomeles cathayensis</i>	Deciduous	√			
<i>Sambucus australasica</i>	Deciduous	√			
<i>Koelreuteria bipinnata</i> var. <i>integrifoliola</i>	Deciduous	√			
<i>Koelreuteria bipinnata</i> 'integrifoliola'	Deciduous	√			
<i>Koelreuteria paniculata</i>	Deciduous	√			
<i>Yulania × soulangeana</i>	Deciduous	√			
<i>Koelreuteria bipinnata</i> Franch.	Deciduous	√			
<i>Magnolia liliflora</i> Desr.	Deciduous	√			
<i>Catalpa bungei</i>	Deciduous	√			
<i>Osmanthus sp.</i>	Evergreen	√			
<i>Viburnum rhytidophyllum</i>	Evergreen	√			
<i>Malus micromalus</i>	Deciduous	√			
<i>Chionanthus retusus</i>	Deciduous	√			
<i>Malus</i> 'American'	Deciduous	√			

<i>Cercis gigantea</i>	Deciduous	√		
<i>Cercis canadensis</i>	Deciduous	√		
<i>Cercis chinensis</i>	Deciduous	√		
<i>Ligustrum lucidum</i>	Evergreen	√		
<i>Tamarix chinensis</i>	Deciduous	√		
<i>Robinia pseudoacacia</i>	Deciduous	√		
<i>Acer negundo</i>	Deciduous	√		
<i>Magnolia grandiflora</i>	Evergreen	√		
<i>Aesculus × carnea</i>	Deciduous	√		
<i>Campsis grandiflora</i>	Deciduous	√		
<i>Radix Aucklandiae</i>	Evergreen	√		
<i>Aesculus chinensis</i>	Deciduous	√		
<i>Yulania biondii (Pamp.)</i>	Deciduous	√		
<i>Robinia pseudoacacia</i>	Deciduous	√		
<i>Yulania denudata</i>	Deciduous	√		
<i>Amorpha fruticosa</i>	Deciduous	√		
<i>Sapindus saponaria</i>	Deciduous		√	√
<i>Acer truncatum</i>	Deciduous		√	√
<i>Diospyros kaki</i>	Deciduous		√	
<i>Prunus armeniaca</i>	Deciduous		√	
<i>Punica granatum</i>	Deciduous		√	
<i>Pseudocydonia sinensis</i>	Deciduous		√	
<i>Crataegus pinnatifida</i>	Deciduous		√	
<i>Euonymus hamiltonianus</i>	Deciduous		√	
<i>Euonymus bungeanus Maxim.</i>	Deciduous		√	
<i>Malus pumila</i>	Deciduous		√	
<i>Eriobotrya japonica</i>	Evergreen		√	
<i>Photinia davidsoniae</i>	Evergreen		√	
<i>Cornus officinalis</i>	Deciduous		√	
<i>Catalpa ovata</i>	Deciduous		√	
<i>Ailanthus altissima 'Qiantou'</i>	Deciduous		√	
<i>Euonymus maackii</i>	Deciduous		√	
<i>Ziziphus jujuba Mill.</i>	Deciduous		√	
<i>Morus alba</i>	Deciduous		√	
<i>Pterocarya stenoptera</i>	Deciduous		√	
<i>Platanus acerifolia</i>	Deciduous		√	
<i>Zanthoxylum bungeanum</i>	Deciduous		√	
<i>Juglans nigra</i>	Deciduous		√	
<i>Ligustrum lucidum</i>	Evergreen			√
<i>Blue Moss Cypress 'Boulevard'</i> (<i>Chamaecyparis pisifera</i>)	Evergreen			√
<i>Triadica sebifera (Linnaeus)</i>	Deciduous			√
<i>Salix matsudana f.pendula</i>	Deciduous			√
<i>Acer negundo</i>	Deciduous			√
<i>Acer rubrum</i>	Deciduous			√
<i>Metasequoia glyptostroboides</i>	Deciduous			√

<i>Salix chaenomeloides</i>	Deciduous	√	
<i>Euonymus alatus</i> (Thunb.)	Evergreen	√	
<i>Rhus typhina</i>	Deciduous	√	
<i>Acer palmatum</i>	Deciduous	√	
<i>Photinia × fraseri</i>	Evergreen	√	
<i>Liquidambar formosana</i>	Deciduous	√	
<i>Cotinus coggygria</i>	Deciduous	√	
<i>Acer palmatum</i> 'Atropurpureum'	Deciduous	√	
<i>Prunus cerasifera</i> 'Atropurpurea'	Deciduous	√	
<i>Prunus cerasifera</i>	Deciduous	√	
<i>Acer calcaratum</i>	Evergreen	√	
<i>Ailanthus altissima</i> 'Hongye'	Deciduous	√	
<i>Acer pictum</i> subsp. <i>mono</i> (Maxim.)	Deciduous	√	
<i>Acer</i> spp.	Deciduous	√	
<i>Sophora japonica</i> 'Golden Stem'	Deciduous	√	
<i>Ginkgo biloba</i>	Deciduous	√	
<i>Sophora japonica</i> cv. <i>jinye</i>	Deciduous	√	
<i>Quercus nuttallii</i>	Deciduous	√	
<i>Acer</i> L.	Deciduous	√	
<i>Acer griseum</i> (Franch.)	Deciduous	√	
<i>Styphnolobium japonicum</i> 'Golden Stem'	Deciduous		√
<i>Sophora japonica</i>	Deciduous		√
<i>Betula platyphylla</i>	Deciduous		√
<i>Fraxinus hupehensis</i>	Deciduous		√
<i>Ficus religiosa</i>	Deciduous		√

Table 10-2 Growth factors of 169 tree species




	Latin name	growth factors (yr/cm)
1	<i>Ilex chinensis</i> Sims	1.18
2	<i>Lonicera japonica</i>	0.39
3	<i>Ligustrum sinense</i>	0.67
4	<i>Euonymus alatus</i>	1.00
5	<i>Gardenia jasminoides</i>	0.38
6	<i>Diospyros kaki</i>	0.52
7	<i>Rhus typhina</i>	0.55
8	<i>Broussonetia papyrifera</i>	0.38
9	<i>Laurus nobilis</i>	0.81
10	<i>Acer palmatum</i>	0.80
11	<i>Amygdalus triloba</i>	0.50
12	<i>Photinia</i> × <i>fraseri</i>	0.56
13	<i>Prunus armeniaca</i>	0.50
14	<i>Pinus bungeana</i> Zucc.	0.83
15	<i>Aesculus chinensis</i> var. <i>wilsonii</i>	0.56
16	<i>hyllostachys sulphurea</i> (Carr.)	0.89
17	<i>Albizia julibrissin</i>	0.39
18	<i>Amygdalus persica</i>	0.36
19	<i>Prunus persica</i>	0.36
20	<i>Chimonanthus praecox</i>	0.52
21	<i>Buxus sinica</i>	0.79
22	<i>Prunus</i> × <i>blireana</i>	0.52
23	<i>Prunus</i> subg. <i>Cerasus</i>	0.52
24	<i>Liquidambar formosana</i>	0.78
25	<i>Cotinus coggygria</i>	0.52
26	<i>Malus halliana</i>	0.52
27	<i>Punica granatum</i>	0.52
28	<i>Gleditsia sinensis</i>	0.52
29	<i>Photinia serratifolia</i>	0.52
30	<i>Prunus mume</i>	0.52
31	<i>Pseudocydonia sinensis</i>	0.39
32	<i>Zelkova serrata</i>	0.39
33	<i>Crataegus pinnatifida</i>	0.52
34	<i>Euonymus hamiltonianus</i>	0.78
35	<i>Euonymus bungeanus</i>	0.52
36	<i>Malus pumila</i>	0.52
37	<i>Eriobotrya japonica</i>	0.52
38	<i>Lonicera maackii</i>	0.39
39	<i>Ilex crenata</i> f. <i>convexa</i>	0.52
40	<i>Acer truncatum</i> Bunge	0.81
41	<i>Prunus salicina</i>	0.52
42	<i>Photinia davidsoniae</i>	0.52
43	<i>Acer palmatum</i> 'Atropurpureum'	0.81
44	<i>Pinus tabuliformis</i>	0.52

45	<i>Lagerstroemia indica</i>	0.52
46	<i>Platyclusus orientalis</i>	0.58
47	<i>Nerium oleander</i>	0.42
48	<i>Acer buergerianum</i>	0.58
49	<i>Cornus officinalis</i>	0.51
50	<i>Prunus cerasifera</i> 'Atropurpurea'	0.51
51	<i>Rhododendron simsii</i>	0.80
52	<i>Pyrus spp</i>	0.54
53	<i>Prunus cerasifera</i> Ehrh.	0.50
54	<i>Pinus thunbergii</i>	0.54
55	<i>Bambusoideae</i>	0.78
56	<i>Acer calcaratum</i>	0.53
57	<i>Bothrocaryum controversum</i>	0.53
58	<i>Syringa oblata</i> Lindl.	0.53
59	<i>Lagerstroemia caudata</i>	0.52
60	<i>Catalpa ovata</i>	0.37
61	<i>Gleditsia triacanthos</i>	0.49
62	<i>Prunus serrulata</i> var. <i>lannesiana</i>	0.49
63	<i>Fraxinus pennsylvanica</i>	0.36
64	<i>Lonicera japonica</i>	0.30
65	<i>Syringa oblata</i> Lindl. var. <i>alba</i>	0.63
66	<i>Ailanthus altissima</i> 'Hongye'	0.40
67	<i>Celtis koraiensis</i>	0.46
68	<i>Bischofia javanica</i>	0.18
69	<i>Cinnamomum camphora</i>	0.43
70	<i>Acer pictum</i> subsp. <i>mono</i>	0.43
71	<i>Salix matsudana</i> Koidz	0.41
72	<i>Ailanthus altissima</i> 'Qiantou'	0.41
73	<i>Chaenomeles cathayensis</i>	0.18
74	<i>Melia azedarach</i>	0.38
75	<i>Tilia tuan</i>	0.14
76	<i>Acer spp.</i>	0.23
77	<i>Fraxinus chinensis</i> 'Aurea'	0.17
78	<i>Ulmus parvifolia</i>	0.19
79	<i>Paulownia fortunei</i> (Seem.)	0.12
80	<i>Firmiana simplex</i> (Linnaeus)	0.21
81	<i>Sambucus australasica</i>	0.22
82	<i>Ulmus pumila</i> L.	0.21
83	<i>Koelreuteria bipinnata</i> var. <i>integrifoliola</i>	0.86
84	<i>Koelreuteria bipinnata</i> 'integrifoliola'	0.83
85	<i>Euonymus maackii</i>	0.84
86	<i>Juniperus formosana</i>	0.85
87	<i>Eucommia ulmoides</i> Oliver	0.84
88	<i>Koelreuteria paniculata</i>	0.81
89	<i>Sophora japonica</i> 'Golden Stem'	0.85
90	<i>Ginkgo biloba</i>	0.85




91	<i>Yulania × soulangeana</i>	0.70
92	<i>Koelreuteria bipinnata</i>	0.62
93	<i>Sophora japonica</i>	0.50
94	<i>Styphnolobium japonicum</i>	0.49
95	<i>Sophora japonica</i>	0.56
96	<i>Styphnolobium japonicum 'Golden Stem'</i>	0.57
97	<i>Sabina squamata</i>	0.51
98	<i>Sophora japonica</i>	0.58
99	<i>Quercus nuttallii</i>	0.60
100	<i>Acer L.</i>	0.78
101	<i>Firmiana platanifolia</i>	0.58
102	<i>Acer griseum (Franch.)</i>	0.56
103	<i>Juniperus chinensis</i>	0.78
104	<i>Picea asperata Mast.</i>	0.64
105	<i>Taxodium 'Zhongshansha'</i>	0.87
106	<i>Magnolia liliflora Desr.</i>	0.57
107	<i>Catalpa bungei C. A. Mey.</i>	1.30
108	<i>Trachycarpus fortunei</i>	1.32
109	<i>Osmanthus sp.</i>	0.92
110	<i>Viburnum rhytidophyllum</i>	0.84
111	<i>Ziziphus jujuba</i>	0.72
112	<i>Celtis julianae</i>	0.79
113	<i>Ligustrum lucidum</i>	0.54
114	<i>Malus micromalus</i>	0.58
115	<i>Blue Moss Cypress 'Boulevard'</i>	0.60
116	<i>Ligustrum lucidum Ait</i>	0.56
117	<i>Chionanthus retusus</i>	0.46
118	<i>Malus 'American'</i>	0.57
119	<i>Celtis sinensis</i>	0.46
120	<i>Salix babylonica</i>	0.56
121	<i>Cercis gigantea</i>	0.57
122	<i>Salix babylonica</i>	0.56
123	<i>Cercis canadensis</i>	0.57
124	<i>Triadica sebifera</i>	0.54
125	<i>Cercis chinensis</i>	0.57
126	<i>Ligustrum lucidum</i>	0.58
127	<i>Tamarix chinensis</i>	0.57
128	<i>Swida walteri</i>	0.56
129	<i>Pinus parviflora</i>	0.56
130	<i>Pistacia chinensis</i>	0.55
131	<i>Salix matsudana f.pendula</i>	0.56
132	<i>Xylosma racemosum</i>	0.58
133	<i>Sapindus saponaria</i>	0.57
134	<i>Morus alba</i>	0.54
135	<i>Castanea mollissima</i>	0.42
136	<i>Fraxinus chinensis</i>	0.42

137	<i>Pterocarya stenoptera</i>	0.44
138	<i>Platanus acerifolia</i>	0.43
139	<i>Betula platyphylla</i>	0.44
140	<i>Cupressus funebris</i>	0.35
141	<i>Acer negundo</i>	0.33
142	<i>Robinia pseudoacacia</i>	0.42
143	<i>Fraxinus hupehensis</i>	0.41
144	<i>Liriodendron chinense</i>	0.42
145	<i>Acer negundo</i>	0.35
146	<i>Magnolia grandiflora</i>	0.38
147	<i>Aesculus × carnea</i>	0.46
148	<i>Acer rubrum</i>	0.31
149	<i>Juglans regia</i>	0.44
150	<i>Zanthoxylum bungeanum</i>	0.36
151	<i>Populus × canadensis</i>	0.44
152	<i>Acer negundo</i> ‘Aurea’	0.36
153	<i>Campsis grandiflora</i>	0.48
154	<i>Sabina chinensis</i>	0.30
155	<i>Podocarpus macrophyllus</i>	0.43
156	<i>Populus tomentosa</i>	0.45
157	<i>Juglans nigra</i>	0.44
158	<i>Radix Aucklandiae</i>	0.46
159	<i>Ficus religiosa</i>	0.30
160	<i>Aesculus chinensis</i>	0.42
161	<i>Acer buergerianum</i>	0.38
162	<i>Metasequoia glyptostroboides</i>	0.38
163	<i>Yulania biondii</i>	0.39
164	<i>Salix chaenomeloides</i>	0.34
165	<i>Robinia pseudoacacia</i>	0.45
166	<i>Cedrus deodara</i>	0.38
167	<i>Populus simonii</i> var. <i>przewalskii</i>	0.33
168	<i>Yulania denudata</i>	0.44
169	<i>Amorpha fruticosa</i>	0.44

Table 10-3 Carbon sequestration capacity of each tree species

Cluster	Tree species
1 	<i>Koelreuteria bipinnata</i> var. <i>integrifoliola</i> <i>Koelreuteria bipinnata</i> 'integrifoliola' <i>Euonymus maackii</i> Rupr. <i>Juniperus formosana</i> Hayata <i>Eucommia ulmoides</i> Oliver <i>Koelreuteria paniculate</i> <i>Sophora japonica</i> 'Golden Stem' <i>Celtis julianae</i>
2 	<i>Ailanthus altissima</i> 'Hongye' <i>Celtis koraiensis</i> Nakai <i>Cinnamomum camphora</i> <i>Acer pictum</i> subsp. <i>mono</i> (Maxim.) <i>Salix matsudana</i> Koidz <i>Ailanthus altissima</i> 'Qiantou' <i>Melia azedarach</i> <i>Ligustrum lucidum</i> <i>Blue Moss Cypress</i> 'Boulevard' <i>Ligustrum lucidum</i> Ait <i>Chionanthus retusus</i> <i>Salix babylonica</i> <i>Cercis gigantea</i> <i>Salix babylonica</i> <i>Cercis canadensis</i> <i>Triadica sebifera</i> (Linnaeus) Small <i>Cercis chinensis</i> <i>Ligustrum lucidum</i> <i>Tamarix chinensis</i> <i>Swida walteri</i> (Wanger.) Sojak <i>Pinus parviflora</i> <i>Pistacia chinensis</i> Bunge <i>Sapindus saponaria</i> Linnaeus <i>Castanea mollissima</i> Blume
3 	<i>Bischofia javanica</i> <i>Chaenomeles cathayensis</i> Schneid. <i>Ziziphus jujuba</i> <i>Malus micromalus</i> <i>Malus</i> 'American' <i>Celtis sinensis</i> Pers. <i>Salix matsudana</i> f. <i>pendula</i> <i>Xylosma racemosum</i> <i>Morus alba</i>

<p>4</p> 	<p><i>Ginkgo biloba</i> <i>Yulania</i> × <i>soulangeana</i> (Soul.-Bod.) <i>Acer</i> <i>Juniperus chinensis</i> <i>Picea asperata</i> <i>Taxodium 'Zhongshansha'</i></p>
<p>5</p> 	<p><i>Sambucus australasica</i> <i>Koelreuteria bipinnata</i> Franch. <i>Sophora japonica</i> <i>Styphnolobium japonicum</i> Schott <i>Sophora japonica</i> cv. <i>jinye</i> <i>Styphnolobium japonicum</i> 'Golden Stem' <i>Sabina squamata</i> Antoine cv. <i>Meyeri</i> <i>Sophora japonica</i> <i>Quercus nuttallii</i> <i>Firmiana platanifolia</i> <i>Acer griseum</i> (Franch.) Pax <i>Magnolia liliflora</i> <i>Fraxinus chinensis</i> <i>Pterocarya stenoptera</i> <i>Platanus acerifolia</i> (Aiton) Willdenow <i>Betula platyphylla</i> <i>Acer negundo</i> <i>Robinia pseudoacacia</i> <i>Fraxinus hupehensis</i> <i>Liriodendron chinense</i> (Hemsl.) <i>Acer negundo</i> <i>Magnolia grandiflora</i> <i>Aesculus</i> × <i>carnea</i> <i>Acer rubrum</i> <i>Juglans regia</i> <i>Populus</i> × <i>canadensis</i> Moench <i>Acer negundo</i> 'Aurea' <i>Campsis grandiflora</i> (Thunb.) Schum. <i>Sabina chinensis</i> (L.) Ant. cv. <i>Kaizuca</i> <i>Podocarpus macrophyllus</i> (Thunb.) <i>Populus tomentosa</i> <i>Juglans nigra</i> <i>Radix Aucklandiae</i> <i>Acer buergerianum</i> <i>Yulania biondii</i> (Pamp.) <i>Robinia pseudoacacia</i> cv. <i>Idaho</i> <i>Cedrus deodara</i> (Roxb.) Don <i>Populus simonii</i> var. <i>przewalskii</i> (Maxim.) <i>Yulania denudata</i></p>

	<i>Amorpha fruticosa</i>
6	<i>Tilia tuan</i>
	<i>Acer spp.</i>
	<i>Fraxinus chinensis 'Aurea'</i>
	<i>Ulmus parvifolia</i>
	<i>Paulownia fortune (Seem.)</i>
	<i>Firmiana simplex (Linnaeus) W. Wight</i>
	<i>Ulmus pumila</i>
	<i>Cupressus funebris</i>
	<i>Zanthoxylum bungeanum</i>
	<i>Ficus religiosa</i>
	<i>Aesculus chinensis Bunge</i>
	<i>Metasequoia glyptostroboides</i>
	<i>Salix chaenomeloides Kimura</i>
7	<i>Ilex chinensis Sims</i>
	<i>Euonymus alatus (Thunb.) Sieb</i>
	<i>Laurus nobilis</i>
	<i>Acer palmatum</i>
	<i>Pinus bungeana Zucc.</i>
	<i>hyllostachys sulphurea (Carr.) A. 'Viridis'</i>
	<i>Buxus sinica (Rehder & E. H. Wilson)</i>
	<i>Liquidambar formosana Hance</i>
	<i>Euonymus hamiltonianus</i>
	<i>Acer truncatum Bunge</i>
	<i>Acer palmatum 'Atropurpureum'</i>
	<i>Rhododendron simsii</i>
	<i>Bambusoideae</i>
	<i>Catalpa bungei</i>
	<i>Trachycarpus fortunei (Hook.)</i>
	<i>Osmanthus sp.</i>
	<i>Viburnum rhytidophyllum</i>
8	<i>Lonicera japonica</i>
	<i>Ligustrum sinense</i>
	<i>Gardenia jasminoides Ellis</i>
	<i>Diospyros kaki</i>
	<i>Broussonetia papyrifera</i>
	<i>Amygdalus triloba</i>
	<i>Photinia × fraseri Dress</i>
	<i>Prunus armeniaca</i>
	<i>Aesculus chinensis var. wilsonii (Rehder)</i>
	<i>Albizia julibrissin</i>
	<i>Prunus persica</i>
	<i>Chimonanthus praecox (L.) Link</i>
	<i>Prunus × blireana cv. Meiren</i>
	<i>Prunus subg. Cerasus sp.</i>
	<i>Cotinus coggygria</i>

Malus halliana Koehne
Punica granatum
Gleditsia sinensis
Photinia serratifolia (Desfontaines) Kalkman
Prunus mume
Pseudocydonia sinensis (Thouin)
Zelkova serrata (Thunb.) Makino
Crataegus pinnatifida
Euonymus bungeanus Maxim.
Malus pumila
Eriobotrya japonica (Thunb.)
Lonicera maackii (Rupr.)
Ilex crenata f. *convexa* (Makino) Rehder
Prunus salicina
Photinia davidsoniae
Pinus tabuliformis
Lagerstroemia indica
Nerium oleander
Acer buergerianum
Cornus officinalis
Prunus cerasifera 'Atropurpurea'
Pyrus spp
Pinus thunbergii
Acer calcaratum
Bothrocaryum controversum
Syringa oblata
Lagerstroemia caudata
Catalpa ovata G. Don
Gleditsia triacanthos
Prunus serrulata var. *lannesiana* (Carri.)
Fraxinus pennsylvanica
Syringa oblata Lindl. var. *alba* Rehder

9



Rhus typhina
Amygdalus persica
Platycladus orientalis (L.) Franco
Prunus cerasifera
Lonicera japonica

DECLARATION

on authenticity and public assess of mater's thesis

Student's name: JiaXiaoli
Student's Neptun ID: F7OQX2
Title of the document: Optimization of carbon sink capacity in parks
Year of publication: 2023
Department: Department of Landscape Protection and Reclamation

I declare that the submitted master's thesis is my own, original individual creation. Any parts taken from an another author's work are clearly marked, and listed in the table of contents.

If the statements above are not true, I acknowledge that the Final examination board excludes me from participation in the final exam, and I am only allowed to take final exam if I submit another master's thesis.

Viewing and printing my submitted work in a PDF format is permitted. However, the modification of my submitted work shall not be permitted.

I acknowledge that the rules on Intellectual Property Management of Hungarian University of Agriculture and Life Sciences shall apply to my work as an intellectulal property.

I acknowledge that the electric version of my work is uploaded to the repository sytem of the Hungarian University of Agriculture and Life Sciences.

Place and date: 2023 year 4 month 28 day

Jia Xiaoli

Student's signature

STATEMENT ON CONSULTATION PRACTICES

As a supervisor of JiaXiaoli (Student's name) F7OQX2 (Student's NEPTUN ID), I here declare that the master's thesis has been reviewed by me, the student was informed about the requirements of literary sources management and its legal and ethical rules.

I recommend the master's thesis to be defended in a final exam.

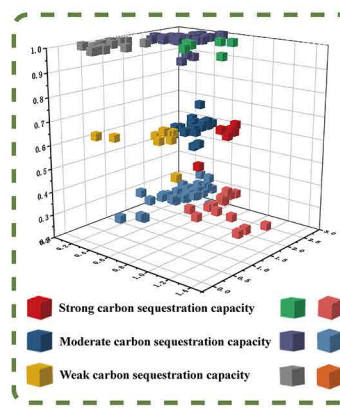
The document contains state secrets or professional secrets: yes no

Place and date: 2023 year 4 month 28 day

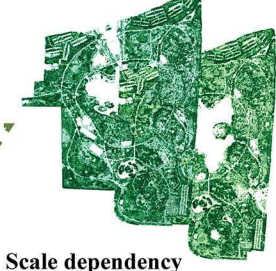


Internal supervisor

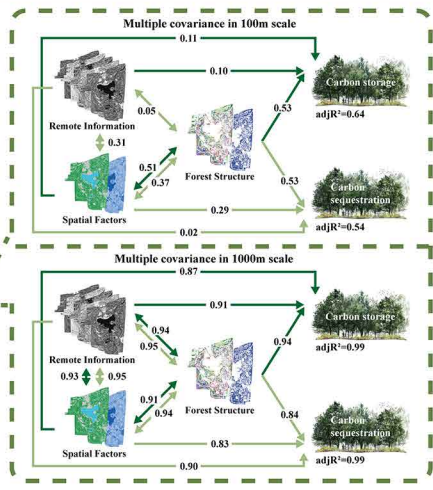
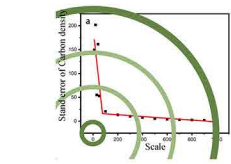
Graphical Abstract



Carbon density

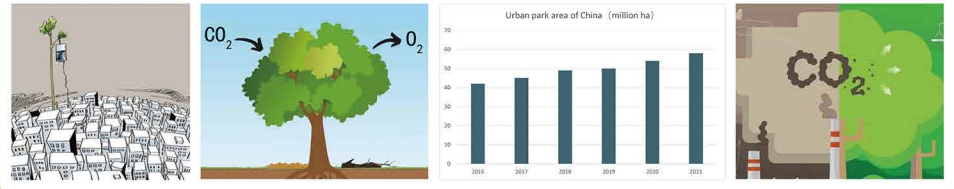


Scale dependency

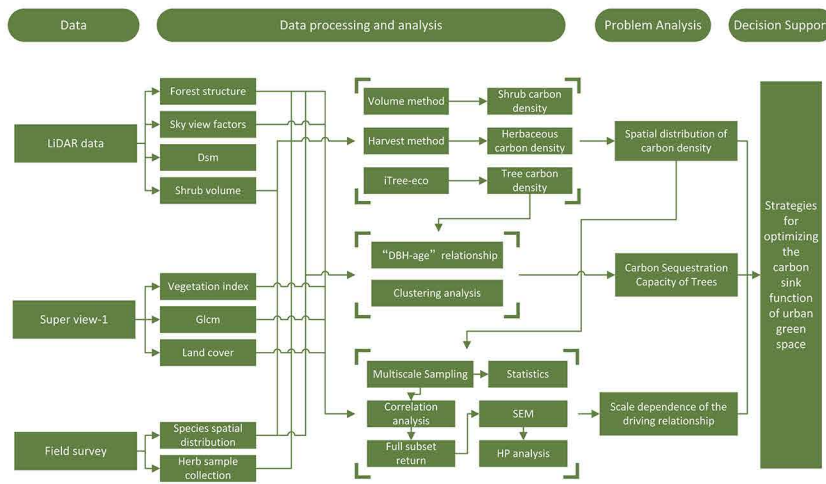


Background

- Rapid urbanization and climate changes issues [1]
- Urban vegetation can absorb large amounts of greenhouse gases [2]
- China's urban green space is increasing rapidly [3]
- China plans to achieve carbon neutrality by 2060 [4]



Methods



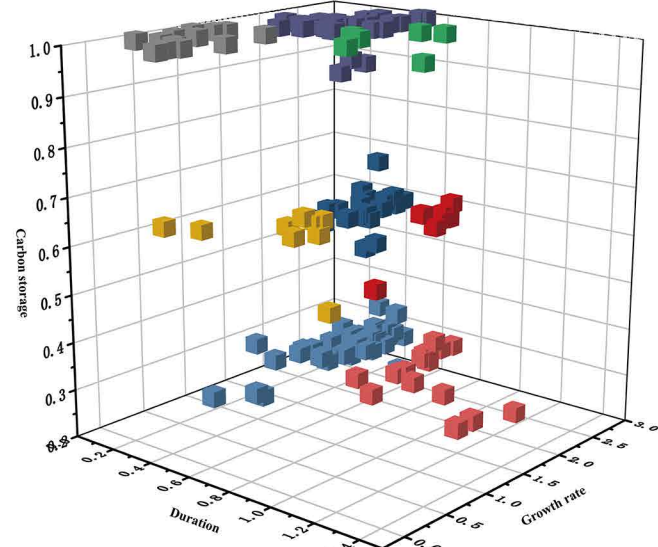
Research Purpose

- Evaluation of the carbon sequestration capacity of each species in combination with the growth indicators of tree species.
- Clarifying the influence of community structure on carbon density in urban park green spaces.
- Combining the current situation of China Green Expo to propose optimization and enhancement strategies.

Results

- (1) The trunk diameter is of medium size. (2) The increase in trunk diameter is slow. (3) With an increase in trunk diameter, carbon sequestration increases significantly.
- (1) The trunk diameter is of medium size. (2) The growth of trunk diameter is moderate. (3) With an increase in trunk diameter, carbon sequestration increases significantly.
- (1) The trunk diameter is of medium size. (2) The growth of trunk diameter is moderate. (3) With an increase in trunk diameter, carbon sequestration increases slightly.
- (1) The trunk diameter is in larger size. (2) The growth rate of trunk diameter is slow. (3) With an increase in trunk diameter, carbon sequestration increases moderately.
- (1) The trunk diameter is in larger size. (2) The growth of trunk diameter is relatively fast. (3) With an increase in trunk diameter, carbon sequestration increases moderately.
- (1) The trunk diameter is in larger size. (2) The growth of trunk diameter is relatively fast. (3) With an increase in trunk diameter, carbon sequestration increases slightly.
- (1) The trunk diameter is in smaller size. (2) The growth of trunk diameter is relatively fast. (3) With an increase in trunk diameter, carbon sequestration increases slightly.
- (1) The trunk diameter is in smaller size. (2) The growth of trunk diameter is slowly. (3) With an increase in trunk diameter, carbon sequestration increases moderately.
- (1) The trunk diameter is in smaller size. (2) The growth of trunk diameter is moderate. (3) With an increase in trunk diameter, carbon sequestration increases significantly.

Clustering analysis results of tree species based on growth characteristic index.



Correlation analysis for carbon sequestration

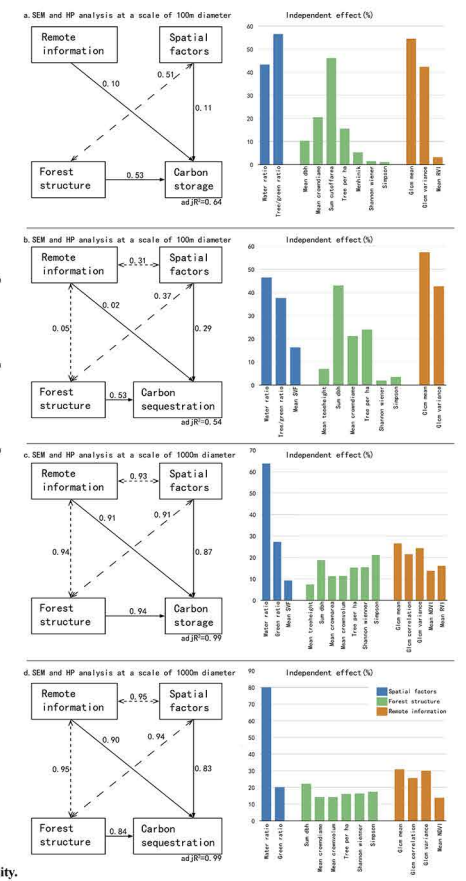
	Mean canopy cover	Green ratio	SVF	Tree/green ratio	Water ratio	Simpson	Shannon wiener	Menhink	Tree per ha	Sum outflow area	Mean crownvolum	Mean crownarea	Mean crown diam	Sum dbh	Mean treeheight	RVI	NDVI	Glm variance	Glm correlation	Glm mean											
Mean canopy cover	0.8700	0.018**	0.021**	0.003**	0.021**	0.185**	0.449**	0.201**																							
Green ratio		0.8700	-0.02**	-0.02**	-0.047**	-0.04**	-0.023**	0.902**	0.071**	0.233**	0.462**	0.603**																			
SVF			0.8700	-0.064**	-0.067**	-0.038**	-0.037**	-0.117**	-0.075**	-0.088**	-0.248**	-0.478**	0.287**																		
Tree/green ratio				0.8700	0.1**	0.029**	0.11**	0.096**	0.354**	0.405**	0.445**	0.454**	0.516**	0.909**																	
Water ratio					0.8700	0.065**	0.084**	0.183**	0.035**	0.08**	0.283**	0.208**	0.121**	0.31**	0.854**																
Simpson						0.8700	-0.038**	-0.005**	-0.051**	-0.05**	-0.131**	-0.236**	-0.205**	-0.534**	-0.574**	-0.814**															
Shannon wiener							0.8700	-0.034**	-0.055**	-0.048**	-0.041**	-0.093**	-0.222**	-0.362**	-0.464**	-0.414**	-0.846**														
Menhink								0.8700	-0.101**	-0.06**	-0.188**	-0.093**	-0.072**	-0.268**	-0.304**	-0.358**	-0.321**	-0.751**													
Tree per ha									0.8700	0.185**	0.072**	0.293**	0.031**	0.091**	0.403**	0.38**	0.36**	0.403**	0.478**	0.803**											
Sum outflow area										0.8700	0.218**	0.112**	0.403**	0.117**	0.131**	0.537**	0.513**	0.493**	0.532**	0.634**	0.833**										
Mean crownvolum											0.8700	-0.024**	-0.023**	-0.21**	-0.06**	-0.077**	-0.30**	-0.438**	-0.457**	-0.386**	-0.72**										
Mean crownarea												0.8700	-0.094**	-0.079**	-0.24**	-0.091**	-0.094**	-0.398**	-0.487**	-0.464**	-0.788**										
Mean crown diam													0.8700	-0.181**	-0.103**	-0.299**	-0.111**	-0.094**	-0.445**	-0.581**	-0.696**										
Sum dbh														0.8700	0.218**	0.105**	0.386**	0.109**	0.123**	0.509**	0.468**	0.443**	0.482**	0.91**	0.86**						
Mean treeheight															0.8700	-0.114**	-0.080**	-0.21**	-0.094**	-0.064**	-0.30**	-0.382**	-0.301**	-0.274**	-0.216**	-0.328**					
RVI																0.8700	-0.054**	-0.036**	-0.048**	0.07**	0.101**	0.231**	0.403**	0.604**	0.804**						
NDVI																	0.8700	-0.02**	-0.024**	-0.023**	-0.031**	-0.411**	-0.441**	-0.493**	-0.404**	-0.283**	-0.198**				
Glm variance																		0.8700	-0.04**	-0.04**	-0.118**	-0.028**	-0.044**	-0.411**	-0.441**	-0.493**	-0.404**	-0.283**	-0.198**		
Glm correlation																			0.8700	-0.04**	-0.04**	-0.118**	-0.028**	-0.044**	-0.411**	-0.441**	-0.493**	-0.404**	-0.283**	-0.198**	
Glm mean																				0.8700	-0.084**	-0.09**	-0.147**	-0.047**	-0.066**	-0.448**	-0.465**	-0.438**	-0.323**	-0.137**	-0.198**

Correlation analysis between influencing factors and carbon density.

- There is a significant correlation between each influencing factor and carbon density.
- Biodiversity has significant impact on carbon density at larger scale, they are negatively correlated.
- Water proportion has significant impact on carbon density at larger scale, they are negatively correlated.
- Tree coverage is positively correlated with carbon density.
- Sky View Factor (SVF) is positively correlated with carbon density at a larger scale.
- Tree density is negatively correlated with carbon density at larger scale.

Regression analysis of influencing factors and carbon density.

- There are scale differences in the driving forces of the influencing factors on carbon density.
- The biodiversity index explains at least 21% of the variation in carbon density.
- The water proportion can explain at least 64% of the variation in carbon density.
- SVF can moderately explain the variation in carbon density, as there is an edge effect in urban vegetation communities.
- The sum of tree diameters at breast height (DBH) can explain at least 22% of the variation in carbon density.



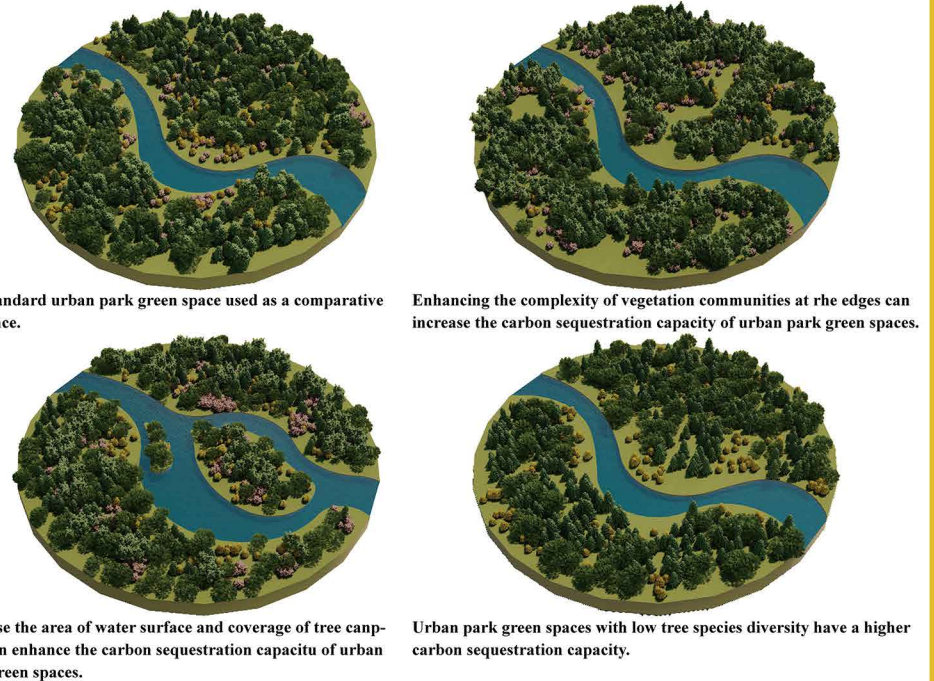
Conclusion

Optimization strategies for landscape tree species.

In urban green space planning, deciduous tree species are categorized as foundational species and common tree species; park roads are divided into main roads and secondary roads; commonly used water features include ponds, rivers, and lakes. Based on research results, we have identified the suitable tree species for each landscape type.

Urban landscape	Recommended tree species	Reasons for recommendation
Foundational tree species	2, 5	The tree species in both of these clusters are characterized by larger trunk diameters, faster growth rates, and stronger carbon sequestration abilities.
Common tree species	1, 9	The tree species in both of these clusters are small trees with high landscape value and strong carbon sequestration abilities.
Parkway	Recommended tree species	Reasons for recommendation
Main roads	5, 6, 7	The quality of the plant configuration on both sides of the main road will directly affect the landscape of urban parks and green spaces. Therefore, fast-growing and strong carbon-sequestering tree species with ornamental value should be selected on both sides of the park road.
Secondary roads	1, 9	The planting design along secondary roads and paths can be more flexible and diverse, and require tree species with moderate size, moderate ornamental value, and strong carbon sequestration capacity.
Water landscape	Recommended tree species	Reasons for recommendation
Ponds	1, 2, 8, 9	The arrangement of plants near a pond often emphasizes their individual characteristics or is used to divide the water surface space through the distribution of plants, thereby enhancing the hierarchical sense of the landscape. It is recommended to select tree species with strong carbon fixation abilities but small size.
Rivers	5, 6	The banks of rivers are often planted with tall trees, so it is recommended to choose large trees that have fast-growing and strong carbon sequestration capabilities to enhance the landscape.
Lakes	4, 5, 6	The surrounding area of a lake often forms a large area of planted vegetation, and it is recommended to select tree species with strong carbon sequestration ability, larger trunk diameter, and faster growth rate through mass planting to form a large plant landscape.

Optimization strategies for vegetation communities.



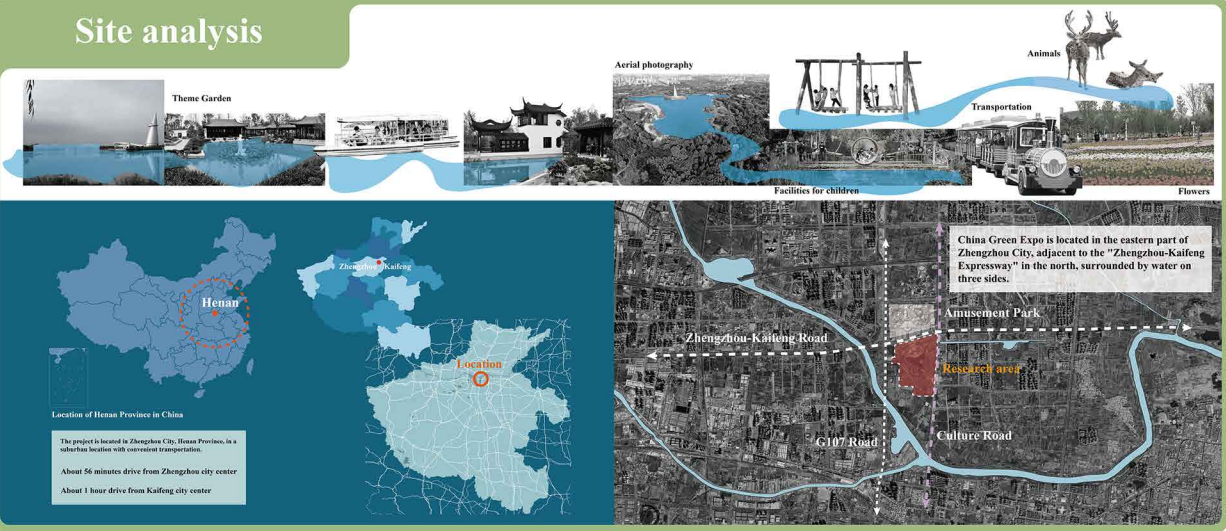
References

- [1] Li W, Cao Q, Lang K, et al. Linking potential heat source and sink to urban heat island: Heterogeneous effects of landscape pattern on land surface temperature[J]. Science of The Total Environment, 2017, 586: 457-465. <https://doi.org/10.1016/j.scitotenv.2017.01.191>
- [2] Rastandeh A, Jarchow M. Urbanization and biodiversity loss in the post-COVID-19 era: complex challenges and possible solutions[J]. Cities & Health, 2021, 5(sup1): S37-S40. <https://doi.org/10.1080/23748834.2020.1788322>
- [3] www.gov.cn[Z]. [2022-10-08]. http://www.gov.cn/zhengce/zhengceku/2022/10/14/content_5668177.htm
- [4] National Development and Reform Commission[M]. [2022-10-08]. https://www.ndrc.gov.cn/wsdwhzf/202211/20221111_1303691_ext.html

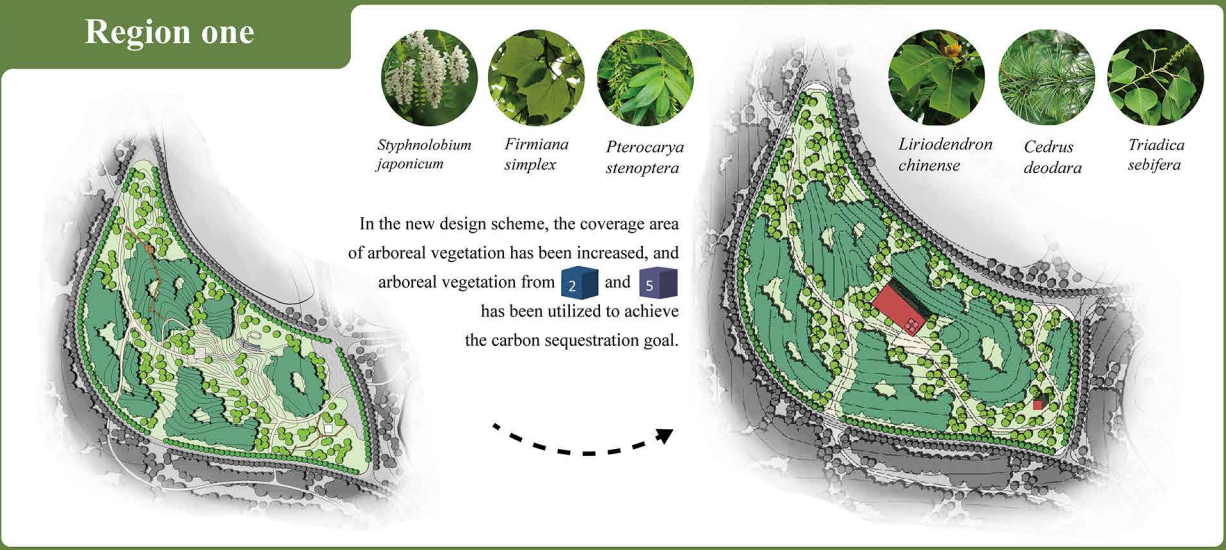
Optimization plan



Site analysis



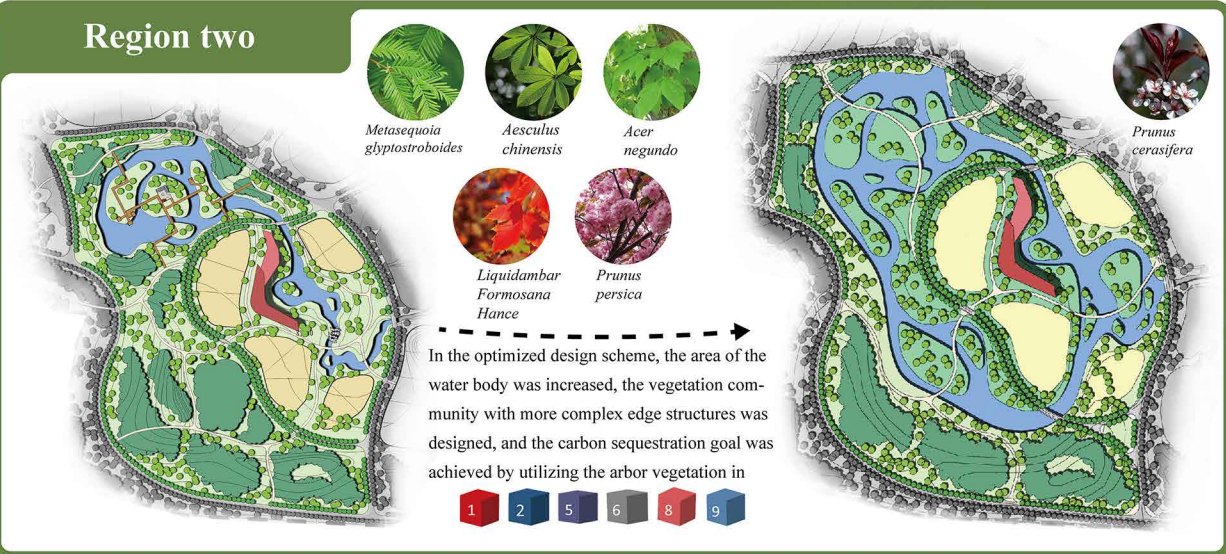
Region one



Visualization

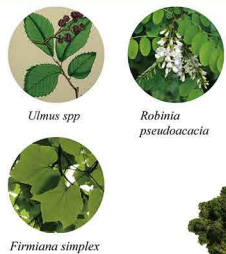


Region two



Parkway

Main roads in the park are present in different areas, and plants on either side significantly impact the park's green spaces. So, we'll use deciduous trees that mature faster and choose them from 5, 6, and 7.



To enhance the park's visual appeal, consider using fast-growing deciduous trees alongside main roads, as well as selecting flowering trees from 5, 6, and 7.



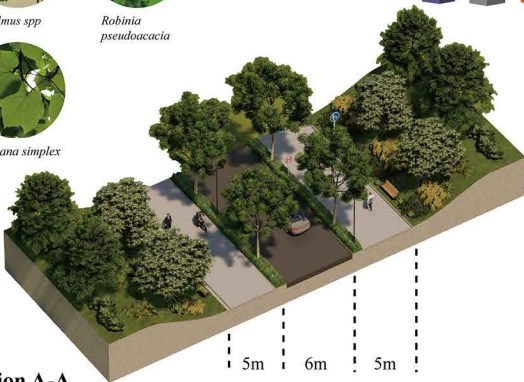
The secondary roads are intended for peaceful strolling, and their plantings can be diverse. Trees planted on one side can offer shade and flowers. Species from 1 and 9 are good options.



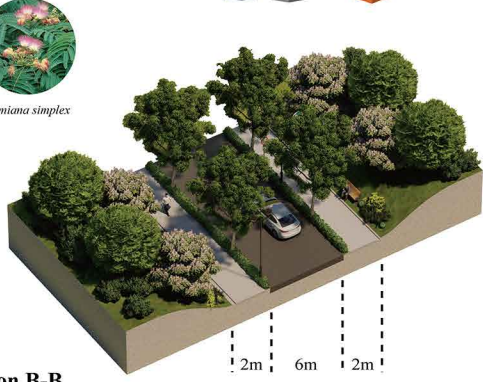
The secondary roads are intended for peaceful strolling, and their plantings can be diverse. Trees planted on one side can offer shade and flowers. Species from 1 and 9 are good options.



Section A-A



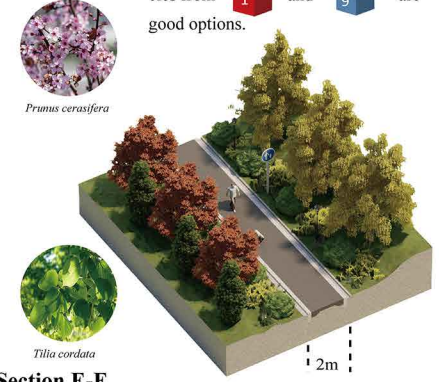
Section B-B



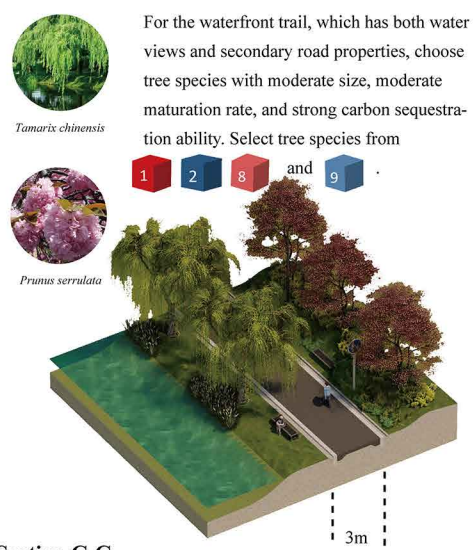
Section D-D



Section E-E



Section C-C



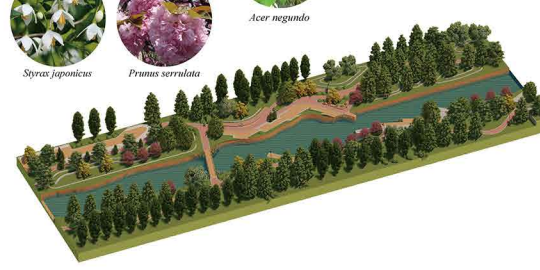
For the waterfront trail, which has both water views and secondary road properties, choose tree species with moderate size, moderate maturation rate, and strong carbon sequestration ability. Select tree species from 1, 2, 8, and 9.

Waterscape

Small gardens often use ponds as their main water feature. To create a "delicate and interesting" effect, plant arrangements highlight individual characteristics or divide the water surface with plants for a hierarchical landscape. Choose suitable tree species from 1, 2, and 8.



Tall trees are often planted on both sides of river landscapes and formal gardens with regular canals. Fast-growing large deciduous trees from 5 and 6 are suitable choices.



Planting in groups can create a large plant landscape around a lake. Choose tree species with strong carbon sequestration, larger diameter, and faster growth rate. 1 and 2, 9 tree species are suitable choices.

